Method Development of a Denuder Based Technique for the Determination of the Partitioning of Nitrophenols

Christine Facca

A Thesis Submitted to the Faculty of Graduate Studies in Partial Fulfilment of the Requirements for the Degree of

Master of Science

Graduate Program in Chemistry
York University
Toronto, Ontario

September 2013

Abstract

The formation of secondary organic matter (SOM), from the photooxidation of aromatic volatile organic compounds is currently quite poorly understood. One class of these secondary organic species are nitrophenols, which are formed in the atmosphere from the hydroxyl radical initiated photooxidation of aromatic hydrocarbons. Due to their semi-volatile nature, nitrophenols exist in the atmosphere in both the gas phase and in particulate matter (PM), which makes understanding their partitioning important in order to gain a better understanding of the formation, yields and processing of SOM. In this work, an application was developed for the IOGAPS (Integrated Organic Gas and Particle Sampler) system to determine concentration measurements for both gas phase and PM for a group of five nitrophenols in the atmosphere. These nitrophenols were found to exist predominately in the gas phase, with their partitioning between the two phases showing only slight dependences on ambient temperature and saturation vapor pressure.

Acknowledgements

I would like to take this opportunity to acknowledge the numerous individuals who have contributed to the successful completion of this thesis.

To my supervisor, Dr. Jochen Rudolph, it has been an honour being a member of your research group. Words cannot begin to describe the sincere gratitude I have for the constant guidance, assistance and support you have provided throughout this work. You have made this a vastly rewarding experience, one which has allowed me to grow both intellectually and personally and one which I will hold dear to my heart forever.

To Dr. Geoffrey Harris who has served as a member of my supervisory committee from the start of this project, thank you for your continuous encouragement as well as for the advice and suggestions you have provided. I would also like to thank the other member of my thesis examination committee, Dr. George Zhu for taking time out of his busy schedule to participate in this final thesis examination.

To the other CAC professors, Dr. Donald Hastie, Dr. Robert McLaren and Dr. Michael Mozurkewich, who I have had the pleasure of getting to know over the duration of this work. Thank you for your willingness to always provide help and support.

To Dr. Douglas Lane who was always willing to offer his advice and expertise and whom I have shared with some valuable scientific discussions. As well, to Environment Canada for providing both instrumentation and laboratory resources which were employed in this work.

To Dr. Anna Kornilova and Marina Saccon who have been the most talented, wonderful and supportive colleagues anyone could wish for. We have shared in many memorable experiences over the duration of this work which will stay with me for the rest of my life, and I am truly honoured to call you both lifelong friends.

To the undergraduate students who have worked in Dr. Rudolph's laboratory throughout the duration of this work: Jana, Menal, Nicholas, Samira and Yasamin, thank you for your dedication and hard work. To the members of CAC who I have gotten to know over the last few years, it has been wonderful sharing this experience with each one of you. To Carol Weldon, not only for all her organizational efforts, but for always providing assistance, no matter how busy her daily schedule. To the "CAC girls": Amanda, Anna, Dana, Kim, Marina, Mehrnaz, Rosalyne, Zena, Zoe and Zoya, I never would have thought that this experience would have allowed me to meet such a group of smart and talented women. The relationships I have built with each one of you and the times we have shared together have made this experience truly memorable.

Lastly, to my family, my parents, Edy and Carmen, my brother Mark and my boyfriend, Stefan. You have been the sources of unconditional love and support throughout this work. The constant encouragement you provided is reflected in this accomplishment, and I would not be the person I am today without you.

Table of Contents

List of Figures

List of Tables

Commonly Used Abbreviations and Special Notations

2-me-4-NP	2-methyl-4-nitrophenol
2,6-dime-4-NP	2,6-dimethyl-4-nitrophenol
3-me-4-NP	3-methyl-4-nitrophenol
4-me-2-NP	4-methyl-2-nitrophenol
4-NP	4-nitrophenol
A	gaseous-associated concentration of compound *i*
ACN	Acetonitrile
ADL	atmospheric detection limit
a_{tsp}	specific surface area of the TSP
AU	arbitrary unit
BSTFA	N,O-Bis(trimethylsilyl)trifluoroacetamide
C	concentration of compound which exits denuder
C/C_o	trapping efficiency
C_o	concentration of compound which enters denuder
C17	Heptadecane
C18	Octadecane
C19	Nonadecane
Cal_{IS}	response of internal standard from calibration curve
Cal_t	response of target compound from calibration curve
C_t	concentration of target compound
D	diffusion coefficient of gas in air
d_1	inside diameter of annuli
d_2	outside diameter of annuli
DCM	Dichloromethane
dimeNP	dimethyl nitrophenol

DL	denuder line
F	particle-associated concentration of compound *i*
$\digamma$	flow rate
f	fraction
f_{OM}	Weight fraction of the TSP
FPL	filter pack line
GC	gas chromatography
GC-MS	gas chromatography – mass spectrometry
Hi-Vol	high volume
HLB	hydrophilic-lipophilic balance
HNO_3	nitric acid
HPLC	high performance liquid chromatography
IOGAPS	integrated organic gas and particle sampler
IS	internal standard
K_p	partitioning coefficient
L_d	coated length of denuder
LDL	lower limit of detection
low vol	low volume
m-	meta position
M_A	molecular weight of air
m_B	blank mass
meNP	methyl nitrophenol
meOH	methanol
M_i	molecular weight of compound *i*
$m_{IS,d}$	mass of derivatized internal standard
MS	mass spectrometry

$MM_{t,d}$	molar mass of an underivatized target compound
$MM_{t,und}$	molar mass of a derivatized target compound
m_t	mass of target compound
MW_{OM}	mean molecular weight of the OM phase
NO_2	nitrogen dioxide
NO_3	nitrate
NP	nitrophenol
N_{Re}	Reynolds number
N_S	surface concentration of adsorption sites
o-	ortho position
o-cresol	2-methylphenol
O_2	oxygen
OH	hydroxyl
OM	organic matter
P	Pressure
p-	para position
p-cresol	4-methylphenol
PAHs	polycyclic aromatic hydrocarbons
PA_{IS}	peak area of internal standard
PA_t	peak area of target compound
p_i	gas phase pressure of compound *i*
PM	particulate matter
$PM_{2.5}$	particulate matter (with diameter smaller than 2.5 μm)
PUF	polyurethane foam
$p^o_{L,i}$	vapor pressure of compound *i* as a liquid
Q	volumetric flow rate

Q_l	enthalpy of desorption from the surface
QA, QB, QC	uncoated quartz filter in filter pack position (A, B or C)
Q_v	enthalpy of vaporization of the sub-cooled liquid
R	gas constant (8.314 J K^{-1} mol^{-1})
R	Radius
SIF	sorbent impregnated filter
SIM	selective ion mode
SOM	secondary organic matter
SPE	solid phase extraction
SVOC	semi-volatile organic compounds
T	Temperature
T	target compound
TIC	total ion chromatogram
TFR	transition flow reactor
TLC	thin layer chromatography
TSP	total suspended particulate
V	sampling volume
V_A	diffusion volume of air
V_i	diffusion volume of compound *i*
VOC	volatile organic compounds
VWD	variable wave detector
XA,XB,XC	XAD-4^{TM} coated SIF in filter pack position (A,B or C)
$X_{i,OM}$	mole fraction of compound *i* in the OM phase
x	distance species travels through the TFR
Δ_a	constant value in denuder efficiency equation
γ	kinematic viscosity of air (0.152 cm^2 s^{-1})

λ	thickness of the stagnant film of air at the wall of the tube
ζ	activity coefficient

1. Introduction

Volatile organic compounds (VOC) are emitted into the Earth's atmosphere from both biogenic and anthropogenic sources. These compounds undergo photochemical processes in the atmosphere to produce secondary products of lower volatility which are then able to partitioning between the gas and particle phases. Nitrophenols are one type of these secondary organic species which are formed in the atmosphere through the photooxidation of aromatic VOC such as benzene, toluene and xylene. They are of interest for ambient monitoring since they have been found to be toxic to both humans (Allen and Allen, 1997) and vegetation (Shäfer and Schönherr, 1985). Many nitrophenols have been classified as semi-volatile organic compounds (SVOC) since they have been found to exist in the atmosphere in both the gas phase and in particulate matter (PM). Vapor pressure measurements of some nitrophenol compounds which have been made by Dr. X. Gong (private communication) showed that most of the nitrophenol species found in the atmosphere indeed fall into the SVOC region, having vapor pressures that lie between 10^{-2} and 10^{-6} Pa.

In order to obtain a better understanding on the formation, yields and processing of these nitrophenols, it is imperative to gain more insight into the partitioning of these compounds, which requires the collection of the gas phase and PM separately. Recent work in Dr. Jochen Rudolph's group has involved using filter-adsorbent techniques with high volume sampling to attempt to measure the two phases separately. Results from

these high volume samples (Busca, 2010; Saccon et al., 2013) have shown that the group of target nitrophenols studied were found to exist predominantly in the gas phase with Busca's work showing that the partitioning between the two phases lacked any significant dependence on vapor pressure. This was an unforeseen result since the vapor pressures for these nitrophenols were found to be orders of magnitude different and therefore if dependences exist, they should be noticeably visible. It is known that results from filter-adsorbent sampling techniques can be biased due to the presence of both positive and negative sampling artifacts (Bidleman et al., 1986; Bidleman, 1988; McDow and Huntzicker, 1990; Pankow and Bidleman, 1991; Volkens and Leith, 2003). Positive sampling artifacts can occur when gas phase species adsorb to filter surfaces due to the large adsorptive capacity of the filter or to particles trapped onto the filter, which lead to an overestimation of the PM measurement. Negative sampling artifacts, which overestimate the gas phase measurement, occur due to the fact that particles that are trapped on the filter surface remain in contact with the airstream, and when gas phase concentrations drop below equilibrium levels, evaporation from these particles can be promoted. The high volume results previously discussed were thought to possibly be biased towards the vapor phase by negative sampling artifacts. Due to the fact that there were still many unanswered questions regarding the partitioning, the thought was to move to a different technique that could possibly eliminate some of the biases due to sampling artifacts and more effectively make measurements on the two phases separately.

A denuder is one type of device typically used to separate gases from aerosols. A denuder-filter-adsorbent technique called the IOGAPS (Integrated Gas and Particle

Sampler) system was employed in this work, in which the gas phase is first removed using a XAD-4™ coated annular diffusion denuder, and the PM fraction remaining in the airstream is collected by a downstream filter pack which contains one uncoated quartz filter followed by two XAD-4™ coated quartz filters. Using a denuder to remove the gas phase first, eliminates the potential for positive particle sampling artifacts while using two XAD-4™ coated filters downstream of the uncoated quartz filter to collect any desorption off particles trapped on the uncoated filter, can eliminate the potential for negative sampling artifacts.

The main purpose of this study was to develop a suitable technique using the IOGAPS system to more accurately separate and collect ambient nitrophenols in the gas phase and in PM. The developed methodology was used to measure atmospheric concentrations of a group of five target nitrophenols over the course of a year. The obtained data set was then used to look at the effectiveness this method through the comparison of results from this denuder-filter based method to relatively simple and well established low volume and high volume filter based techniques which were run in parallel. From the data obtained from the denuder-filter method, insight into the partitioning of these nitrophenols was gained.

Presented in this work in Chapter 2 is background and theory information regarding gas/particle partitoning, formation mechanisms and ambient measurements of nitrophenols as well as collection techniques used for SVOC with emphasis placed on filter-based techniques and denuder-filter based techniques as well as possible caveats of these two methods. The methodology of this work is described in Chapter 3 which

includes detailed descriptions of preparation, sampling, extraction and analysis procedures employed for both filter and denuder samples as well as brief descriptions of tests which were perfomed to validate the method used. Chapter 4 presents results validating the method used as well as results from ambient samples. Chapter 5 comprises the discussion of results obtained for method validation purposes and ambient results. Finally, conclusions and possible future method applications are presented in Chapter 6.

2. Theory

2.1. Gas/Particle Partitioning

Many organic compounds present in the atmosphere are found to exist in both the gas phase and in PM and are therefore referred to as SVOC. These SVOC were defined in published work by Junge (1977) as compounds which have vapor pressures which lie between 10^{-2} and 10^{-6} Pa. Compounds which have vapor pressures above 10^{-2} Pa should be found predominantly in the gas phase whereas compounds which have vapor pressures below 10^{-6} Pa should be found almost entirely in PM. Vapor pressure measurements of some phenols and nitrophenols are shown in Table 2.1, illustrating that many of these species do fall within this intermediate regime, classifying these nitrophenols as SVOC.

Table 2.1. Vapor pressures of phenols and nitrophenols found in the atmosphere.

Target Compound	Vapor Pressure (Pa)
4-methylphenol	1.00×10^{1} [a]
4-methyl-2-nitrophenol	1.11×10^{1} [b]
4-nitrophenol	1.03×10^{-2} [b]
3-methyl-4-nitrophenol	3.13×10^{-3} [b]
2-methyl-4-nitrophenol	8.69×10^{-3} [b]
2,6-dimethyl-4-nitrophenol	6.42×10^{-4} [b]

[a] measured at 294.15 K (CRC Handbook of Chemistry and Physics, 93rd ed.)
[b] measured at 303.15 K (Gong, private communication)

The understanding of the gas/particle phase partitioning of SVOC is imperative in order to determine features such as the formation, yields and processing of these compounds. The partitioning can be dependent on atmospheric conditions such as relative

humidity and ambient temperature as well as particle characteristics such as size distribution and composition. The partitioning can also be dependent on chemical properties such as the equilibrium vapor pressure of the compound according to Rauolt's Law:

$$p_i = X_{i,OM}\, p^o_{L,i} \qquad \text{(Eq. 2.1)}$$

where p_i is the gas phase pressure of compound i, $X_{i,OM}$ is the mole fraction of this compound in the organic material (OM) phase and $p^o_{L,i}$ is the vapor pressure of the compound as a liquid. An activity coefficient (ζ) can be applied to Raoult's Law to correct for deviations from ideal interactions that may occur in the liquid phase between the different molecules, as is shown in Eq. 2.2.

$$p_i = X_{i,OM}\, \zeta_i\, p^o_{L,i} \qquad \text{(Eq. 2.2)}$$

Gas/particle partitioning is generally parameterized by a partitioning constant (K_p) in $m^3\ \mu g^{-1}$ calculated by Eq. 2.3, which is dependent on the concentration of total suspended particulate (TSP) material in $\mu g\ m^{-3}$, the particle-associated concentration of the compound of interest (F) in ng m^{-3} and the gaseous-associated concentration of the compound of interest (A) in ng m^{-3}.

$$K_p = \frac{F/TSP}{A} \qquad \text{(Eq. 2.3)}$$

Early work in gas/particle partitioning (Junge, 1977; Pankow, 1987) made the assumption that particles in the atmosphere were solid and therefore the uptake of SVOC involved physical adsorption to solid particles, or surfaces that are solid-like. When gas/particle partitioning is dominated by adsorption, the partitioning constant (K_p) is given by:

$$K_p = \frac{N_S a_{tsp} T e^{(Q_1 - Q_v)/RT}}{1600 p^o_{L,i}} \quad \text{(Eq. 2.4)}$$

where N_S is the surface concentration of adsorption sites in sites per cm^2, a_{tsp} is the specific surface area of the TSP in $m^2\ g^{-1}$, T is the temperature in K, Q_1 is the enthalpy of desorption from the surface in J mol^{-1}, Q_v is the enthalpy of vaporization of the sub-cooled liquid in J mol^{-1}, and R is the gas constant (8.314 J K^{-1} mol^{-1}).

Since it has been recognized that many atmospheric particles are liquid or have layers that are liquid-like, the uptake of gaseous species can be through absorption onto a liquid particle or a liquid on the surface of a particle. When gas/particle partitioning is dominated by absorption, Pankow (1994) suggested that the partitioning constant is given by:

$$K_p = \frac{f_{OM} 760 RT}{MW_{OM} \zeta p^o_{L,i} 10^6} \quad \text{(Eq. 2.5)}$$

where f_{OM} is the weight fraction of the TSP that makes up the OM phase and MW_{OM} is the mean molecular weight of the OM phase.

In the atmosphere many SVOC can undergo both adsorption and absorption, therefore both mechanisms can contribute to the partition constant as shown in Eq. 2.6.

$$K_p = \frac{N_S a_{tsp} T e^{(Q1-Qv)/RT}}{1600 p^o_{L,i}} + \frac{f_{OM} 760 RT}{MW_{OM} \zeta p^o_{L,i} 10^6} \qquad \text{(Eq. 2.6)}$$

2.2. Formation Mechanisms of Nitrophenols

Nitrophenols are compounds which are primarily formed in the atmosphere from the HO radical initiated photooxidation of aromatic VOC such as benzene, toluene, xylene and phenol, which are emitted predominantly by anthropogenic sources.

Methyl nitrophenols have been found to be the products of the reaction of hydroxyl (HO) radical with toluene (Atkinson, 1994; Forstner et al., 1997). The initial HO radical attack on toluene can follow one of two pathways, either a hydrogen atom abstraction from the methyl group, or a HO addition to the ring structure. The HO addition is the predominant pathway since it has been found to occur 90 % of the time (Atkinson, 1994). The HO addition to the aromatic ring can occur in any of the ortho- (o-), meta- (m-) or para- (p-) positions, with the ortho- position thermodynamically favored (Andino et al., 1996). The methyl hydroxycyclohexadienyl radical produced from this HO addition can react with a number of atmospheric oxidants such as oxygen (O_2)

and nitrogen dioxide (NO_2) to form a methyl phenol (*o*-, *m*- or *p*-cresol) (Atkinson, 1994). This cresol can then react with HO to undergo a hydrogen atom abstraction from the hydroxyl group to form a methyl phenoxy radical (Forstner et al., 1997). The methyl phenoxy radical then undergoes nitration by NO_2 to produce methyl nitrophenols. Since alkyl groups and $^{\bullet}$O-R groups on an aromatic ring tend to be ortho- and para- directing, with $^{\bullet}$O-R being more strongly activating, the NO_2 addition to the ring tends to add to the position ortho- or para- to the oxygen bond (Forstner et al., 1997). The mechanism of methyl nitrophenol formation from toluene, adapted from Forstner et al. (1997), is shown in Fig. 2.1. The formation mechanism of dimethyl nitrophenols, such as 2,6-dimethyl-4-nitrophenol from *m*-xylene as shown in Fig. 2.2, has been found to follow the same reaction pathway as the oxidation of toluene (Zhao et al., 2005) with the HO addition to the *m*-xylene favoring the position ortho- to both methyl groups (Andino et al., 1996).

Nitrophenols are formed by reactions of phenol, which is emitted by anthropogenic sources or through the photooxidation of benzene. The formation mechanism of 4-nitrophenol shown in Fig 2.3(a), illustrates that phenol can undergo a hydrogen abstraction to produce a phenoxy radical, which can then react with NO_2 to form nitrophenol. Bolzacchini et al. (2001) suggested an alternate nitrophenol formation mechanism involving an addition of nitrate (NO_3) to the phenolic carbon followed by the addition of NO_2 to the para- carbon, and a final loss of nitric acid (HNO_3) as is depicted in Fig. 2.3(b). The rates of the reactions of phenol with HO and NO_3 listed in Calvert et al. (2002) are significantly different, 2.7×10^{-11} cm^3 $molecules^{-1}$ s^{-1} and

3.8×10^{-12} cm^3 $molecules^{-1}$ s^{-1} respectively, meaning that the reaction pathway involving the NO_3 addition must be supported by extremely high concentrations of NO_3, which suggests that this reaction is limited to nighttime chemistry since low NO_3 concentrations are observed during the daytime.

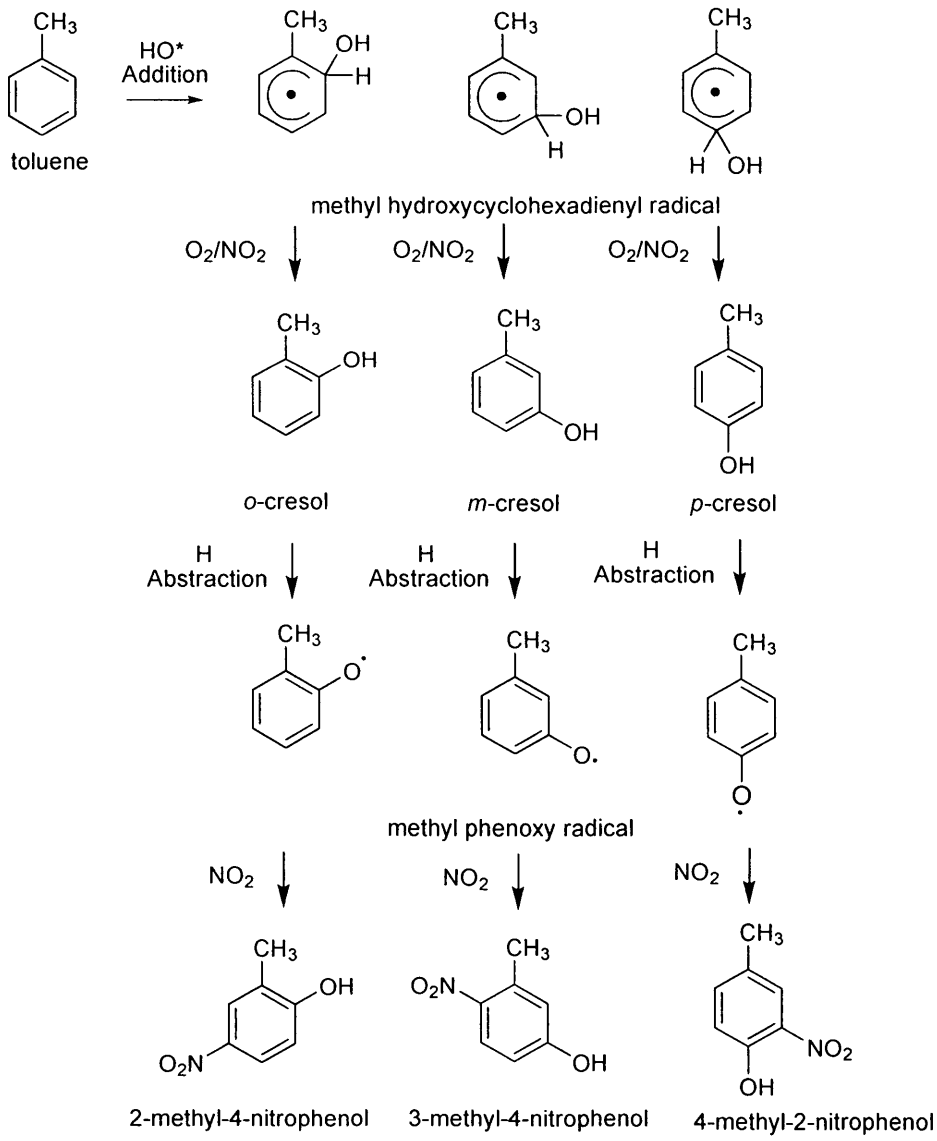

Figure 2.1. Formation mechanisms of methyl nitrophenols from toluene (adapted from Forstner et al. (1997)).

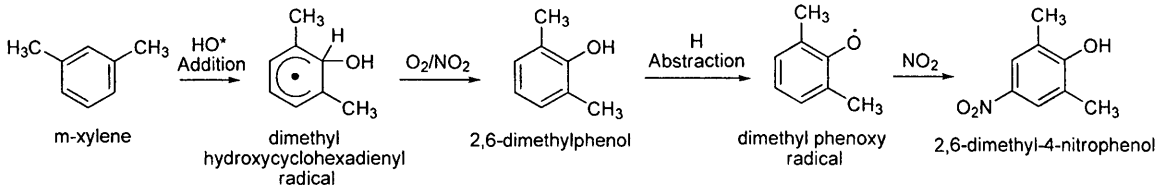

Figure 2.2. Formation mechanism of 2,6-dimethyl-4-nitrophenol from *m*-xylene (adapted from Zhao et al. (2005)).

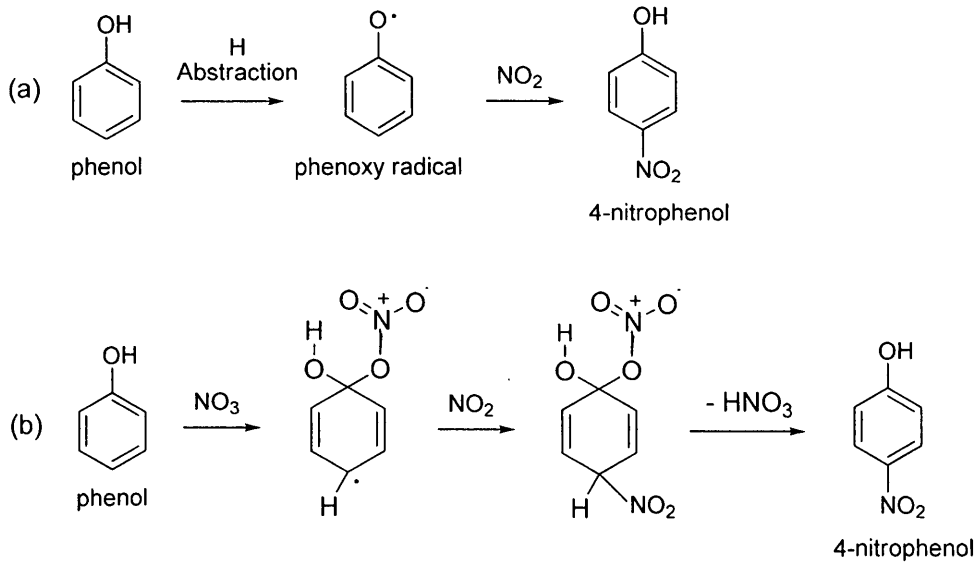

Figure 2.3. Formation mechanism of 4-nitrophenol from reactions of phenol with (a) HO and NO_2 (Atkinson et al., 1992) and (b) NO_3 and NO_2 (Bolzacchini et al., 2001).

2.3. Ambient Measurements of Nitrophenols

Ambient measurements of nitrophenols in literature are limited to work done by a few research groups (Herterich and Herrmann, 1990; Nishioka and Lewtas, 1992; Morville et al., 2004; Cecinato et al., 2005; Delhomme et al., 2010). Measurements of these nitrophenols were conducted in a variety of regions employing a variety of sampling techniques.

Herterich and Herrmann (1990) provided the first reports of ambient nitrophenols, measuring gas phase concentrations at two German hill sites using a column filled with XAD-2^{TM} resin. Nishioka and Lewtas (1992) sampled in the metropolitan area of Boise, Idaho in the 1986/1987 winter using PM_{10} high volume air samplers with PM collection performed using Teflon-impregnated glass fibre filters and gas phase collection using 200 g of XAD-2^{TM} resin. Cecinato et al. (2005) collected twelve samples between February and April 2003 in the downtown region of Rome, Italy sampling gas phase nitrophenols on a KOH coated annular diffusion denuder and PM on Teflon fibre filters. Morville et al. (2004) and Delhomme et al. (2010) both measured gas phase + PM concentrations of phenols and nitrophenols in Strasbourg, France using a high volume air sampler employing glass fibre filters and 20 g of XAD-2^{TM} resin. Morville et al. (2004) sampled at an urban and a suburban site whereas Delhomme et al. (2010) performed five campaigns between spring 2002 and winter 2004 at urban, suburban and rural sites. Total (gas phase + PM) concentration measurements of nitrophenols sampled using $PM_{2.5}$ high volume air samplers employing XAD-4^{TM} resin coated quartz fibre filters were made at

York University by Saccon et al. (2013). The results for gas phase and PM or total (gas phase + PM) concentration measurements from some of these groups are shown in Table 2.2. The measurements of nitrophenols reported in literature and by Saccon et al. (2013) at York University show that the concentration values vary considerably depending on sampling location.

Table 2.2. Ambient phenol/nitrophenol concentrations reported in literature

Compound	Concentration (ng m^{-3})						
	Nishioka and Lewtas (1992)		Morville et al. (2004)	Cecinato et al. (2005)		Delhomme et al. (2010)	Saccon et al. (2013)
	Gas	PM	Gas + PM	Gas	PM	Gas + PM	Gas + PM
Phenol			18.97			10.4[a], 6.5[b], 9.6[c]	
o-cresol			0.36			1.2[a], 1.4[b], 0.9[c]	
m-cresol			0.50			2.2[a], 2.8[b], 2.1[c]	
p-cresol			0.83			2.6[a], 3.0[b], 2.4[c]	
2-NP	0.04-2.40	ND		10.4	3.5		
4-NP	<0.04-0.85	1.90-2.70		3.9	17.8		6.88
3-me-2-NP	<0.04-0.23	ND	0.35			0.5[a], 0.5[b], 0.6[c]	
4-me-2-NP	0.05-1.80	ND	0.58	6.9	2.9	1.6[a], 2.1[b], 2.7[c]	2.78
5-me-2-NP	<0.04-0.59	ND	0.12	4.8	1.7	0.4[a], 0.4[b], 0.6[c]	
6-me-2-NP	<0.04-1.70	ND					
2-me-3-NP			0.09			0.1[a], 0.1[b], 0.04[c]	
2-me-4-NP	<0.04-0.54	0.37-0.77					3.22
3-me-4-NP	0.60-2.70	0.67-1.20	0.69	2.2	7.8	0.4[a], 0.3[b], 0.2[c]	1.09
2,6-dime-4-NP				2.0	5.9		1.06
2,4-diNP			0.65			4.7[a], 5.0[b], 1.1[c]	
2,5-diNP			ND			ND	
2,6-diNP			0.22			0.2[a], 0.4[b], 0.3[c]	

ND: not detected
[a] urban site
[b] suburban site
[c] rural site

2.4. Collection Techniques for Both Phases of SVOC

In order to measure gas/particle distributions for SVOC, techniques must be devised which allow the gas phase and PM to be collected separately. There are a variety of sampling techniques which can be used to attempt to separate and collect gas phase species such as laminar flow separators, transition flow reactors (TFR), scrubbers, filters and denuders. More details regarding filter based sampling techniques and denuder based sampling techniques, both of which were employed in this work, can be found in sections 2.4.1 and 2.4.2, respectively.

Laminar flow separators collect and measure gas phase concentrations by separating gas phase species from PM. Under laminar flow conditions, clean, particle-free air is pushed through the core inlet of the separator and ambient air is drawn into the annular region surrounding the core. The two air masses travel at identical flow velocities through a diffusion zone which is approximately 20 cm in length (Turpin et al., 1993). In this diffusive zone, since gas phase species diffuse orders of magnitude greater than particles, the gas phase species diffuse into the core stream of particle-free air, exiting the separator to be collected downstream by a gas trap, typically a PUF (polyurethane foam) adsorbent. The PM measurement in this technique is performed by subtracting this gas phase concentration determined by the PUF from a total concentration measurement made by a filter-adsorbent sampler run in parallel to the laminar flow separator.

TRF tubes operate at a transition flow regime (2100 < Reynolds number (N_{Re}) < 3500) (Durham et al., 1986). The principle of TFR tubes uses the assumption that there is

a stagnant film of air adjacent to the wall of the tube and a core of turbulent air which passes through the center of the tube. In TFR tubes, only a fraction (f) of the gas, typically only 10 % (Finlayson-Pitts and Pitts, 2000), is trapped on the walls which can be determined by Eq. 2.7

$$f = 1 - e^{\left(-\frac{2\pi r D x}{Q\lambda}\right)} \quad \text{(Eq. 2.7)}$$

where r is the radius of the TFR tube in cm, D is the diffusion coefficient of the gas in air in $cm^2\ s^{-1}$, x is the distance travelled through the TFR tube in cm, Q is the volumetric flow rate in $cm^3\ s^{-1}$ and λ is the thickness of the stagnant film of air at the wall of the tube in cm.

Scrubbers allow for collection of gas phase species from a sample of ambient air by dissolving or absorbing these gas phase species into a liquid (Cofer et al., 1985; Finlayson-Pitts and Pitts, 2000). A mist of water or another aqueous solution is added to the ambient air which enters the chamber and this provides a sufficient interface surface area for mass transfer. The accumulated gas phase analyte in the strongly absorbing liquid can be analyzed for gas phase concentration determination.

2.4.1. Filter Based Sampling Techniques

Filter based sampling techniques have been widely used to collect both gas phase and PM species using both high volume and low volume air sampling systems. Filters of

a variety of materials (quartz fibre, glass fibre and Teflon) are available for use in both types of sampling methods. Uncoated filters collect both liquid and solid particles which collide and deposit onto the surface of a fibre in the filter by five possible mechanisms: diffusion, inertial impaction, interception, electrostatic attraction and gravitational sedimentation (Hinds, 1999). These filters can be coated with an adsorbent resin to produce sorbent impregnated filters (SIFs) which collect both gas phase species and PM.

In this work, quartz fibre filters both uncoated for PM concentration measurement and XAD-4^{TM} resin coated SIFs for measurement of total (gas phase + PM) concentrations were used in both $PM_{2.5}$ high volume and low volume air sampling systems. Typically for sampling with the high volume air sampler set up, one air sampler was equipped with an uncoated quartz fibre filter while a second air sampler was equipped with a SIF. The simple subtraction of the masses found on the uncoated quartz filter from the SIF yielded an estimation of the gas phase mass.

XAD polymeric resins have been widely used as an adsorbent for gas phase nitrophenol collection (Herterich and Herrmann, 1990; Nishioka and Lewtas, 1992; Morville et al., 2004; Delhomme et al., 2010). XAD is a polystyrene-divinylbenzene copolymer resin which is porous, non-polar, hydrophobic and insoluble in water. The XAD-4^{TM} adsorbent used in this work, shown in Fig. 2.4, was chosen for collection of nitrophenols by Busca (2010), due to its higher surface area (780 m^2 g^{-1}) compared to other XAD resins (Kennedy, 1973). Prior to coating, the XAD-4^{TM} resin, which is purchased in the form of small, porous beads, is ground into a fine powder with a

planetary ball mill after being cleaned with various solvents and dried. Grinding the XAD-4™ resin increases the outer surface area of the resin and allows for adhesion to the filter being coated with electrostatic interactions and van der Waals forces (Lane, 1999).

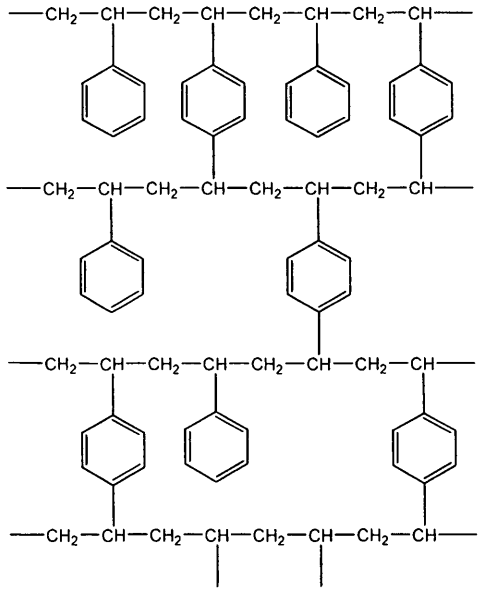

Figure 2.4. Chemical structure of XAD-4™ resin.

2.4.2. Denuder Based Sampling Techniques

The use of an annular or multi-tube denuder (or diffusion denuder) is one technique widely used to remove and collect the gas phase fraction of SVOC (Possanzini et al., 1983; Lane et al., 1988; Sickles et al., 1988). State of the art diffusion denuders are typically composed of one or more adsorbent-coated glass tubes (annuli) with a 2 mm glass rod inserted into the innermost center of the denuder to ensure that the denuder contains only annuli. The principle behind how diffusion denuders operate is

based on the differences in diffusion properties of gases and particles. Under laminar flow conditions PM will travel through the tube due to the low diffusion coefficient of the particles, while the gas phase species will diffuse, come in contact with the walls of the tube and be removed from the air stream. Typically filters are then placed downstream of the denuder to collect the PM fraction which exits the denuder.

For laminar flow conditions to exist, the Reynolds number of each annulus in the denuder must be below 2100. The formula used to calculate the Reynolds number is shown in Eq. 2.8:

$$N_{Re} = \frac{4F}{\gamma\pi(d_1 + d_2)} \qquad \text{(Eq. 2.8)}$$

where F is the flow rate in $cm^3\ s^{-1}$, γ is the kinematic viscosity of air (0.152 $cm^2\ s^{-1}$), and d_1 and d_2 are the inside and outside diameters (cm) of each annulus. The efficiency of a denuder operated under laminar flow conditions is determined by the ratio of the concentration of the compound which exits the denuder (C) over the concentration of the compound entering the denuder (C_o) as is seen in Eq. 2.9 from Possanzini et al. (1983):

$$\frac{C}{C_o} = 0.82 \exp(-22.53\Delta_a) \qquad \text{(Eq. 2.9)}$$

The value Δ_a is calculated using Eq. 2.10:

$$\Delta_a = \frac{\pi D L_d}{4F} \cdot \frac{d_1 + d_2}{d_2 - d_1} \qquad \text{(Eq. 2.10)}$$

where L_d is the coated length of the denuder tube in cm. The diffusion coefficient for a compound *i* in air can be measured or calculated using an expression derived by Fuller et al. (1966) shown in Eq. 2.11:

$$D = \frac{10^{-3}(\frac{T}{K})^{1.75}\sqrt{\left(\frac{1}{M_A}+\frac{1}{M_i}\right)}}{P(V_A^{1/3}+V_i^{1/3})^2} \qquad \text{(Eq. 2.11)}$$

where K is the unit Kelvin, M_A and M_i are the molecular weights of air and compound *i* in g mol^{-1}, P is the pressure in atm and V_A and V_i are diffusion volumes of air and compound *i* as given by Fuller et al. (1966). The diffusion coefficients in air for nitrophenols, methyl nitrophenols and dimethyl nitrophenols have been estimated by Eq. 2.11 to be 0.077 cm^2 s^{-1}, 0.071 cm^2 s^{-1} and 0.066 cm^2 s^{-1}, respectively.

2.5. Caveats for Sampling Techniques

2.5.1. Caveats for Filter Based Sampling Techniques

Filter based sampling techniques are widely used since they potentially allow for sampling of large volumes of air with limited technical effort. There are a number of disadvantages to widely used filter based sampling techniques, such as sampling artifacts. Sampling artifacts can occur when the equilibrium between the gas and

particle phases shifts during the sampling procedure. There are two main types of sampling artifacts that can occur, positive and negative sampling artifacts.

Positive sampling artifacts involve the adsorption of gas phase fractions of SVOC onto filter surfaces due to the large adsorptive capacity of the filter or onto particles trapped onto the filter themselves (McDow and Huntzicker, 1990; Pankow and Bidleman, 1991; Volkens and Leith, 2003). This positive sampling artifact leads to an overestimation of the PM fraction concentration, therefore increasing the partitioning constant defined by Eq. 2.3. The other type of sampling artifact referred to as the negative sampling artifact, overestimate the gas phase concentration and therefore decrease the partitioning constant. Negative sampling artifacts occur due to the fact that particles which are trapped on the filter surface remain in contact with the airstream, and when gas phase concentrations drop below equilibrium levels, evaporation from these particles can be promoted (Bidleman et al., 1986; Bidleman, 1988; Volkens and Leith, 2003). Some other sampling artifacts that can occur are the breakthrough of gas phase species from a coated filter which reduces the gas phase fraction as well as chemical interactions of SVOC with reactive trace gases resulting in either formation or degradation of the target compounds prior to phase separation (Lane, 1999).

The high volume filter based techniques which were discussed in Section 2.4.1 can be biased significantly more by negative sampling artifacts (Lane, 1999). Quantifications of the amount of the negative sampling artifact present in high volume filter samples has been estimated by Busca (2010) and Saccon et al. (2013)

but these values are estimations since both positive and negative artifacts tend to compete (Fitz, 1990). The addition of a denuder to filter based sampling techniques, such as the one used in this work, attempt to significantly reduce the presence of sampling artifacts in filter based techniques (Bidleman, 1988; Lane, 1999). Since the air stream sampled passes through the denuder first, the positive artifact is reduced since the gas phase is removed completely by the denuder. Particles remain in the air stream and are collected on a downstream uncoated quartz fibre filter. Due to the removal of the gas phase from the air stream by the denuder, a shift in equilibrium between the two phases occurs, enhancing the risk for negative artifacts (Lane, 1999). To combat this increase in desorption from particles captured on the uncoated quartz filter, and therefore identify the negative artifact, SIFs are placed downstream of the particle filters.

2.5.2. Caveats for Denuder Based Sampling Techniques

Though it was shown in Section 2.5.1 that adding a denuder to a filter based sampling technique can reduce the positive and negative artifacts attributed to filter based methods, the use of denuders poses some risk for sampling artifacts of its own. Peters et al. (2000) discussed potential sampling artifacts from denuder sampling. The first artifact can be considered as a negative artifact since it overestimates the gas phase measurement. This can occur in two ways: by loss of fine PM to the walls of the denuder or by desorption of SVOC from particles while still in transit through the denuder. The

second artifact which can occur is considered as a positive artifact since the PM fraction is overestimated. This artifact occurs when the denuder wall does not adsorb all of the gas phase and some of the gas phase species travel through the denuder and are collected on downstream filters.

3. Methodology

3.1. Preparation of Filters for Sampling

Quartz fibre filters (Pallflex membrane filters – 2500 QAT – Pall Life Sciences) both rectangular (20.32 x 25.40 cm) and round (47 mm diameter) were baked in a large muffle furnace (Fischer Scientific, Model 550-58) in an atmosphere of synthetic air at a temperature of 1,123 K for 24 hours to remove any organic impurities. These filters were then stored in Pyrex glass containers prior to sampling. Filters used for collecting particle phase species were left untreated after baking, while filters used for gas phase collection were coated with Amberlite XAD-4^{TM} (Sigma Aldrich) adsorbent prior to sampling.

3.1.1 Cleaning and Grinding the XAD-4^{TM} Resin

Extensive cleaning of the XAD-4^{TM} resin was required since the beads were shipped from the supplier as a water-wet product with sodium bicarbonate and sodium chloride salts present to prohibit bacterial growth (Sigma Aldrich Co., 1998). The procedure performed for cleaning of the XAD-4^{TM} resin is based on the method described by Dr. D. A. Lane (Lane, private communication). To clean the resin, 500 g of the XAD-4^{TM} (20-60 mesh) were placed into a 300 mL beaker. Methanol (Reagent grade, Sigma Aldrich) was added to the beaker slowly, under continuous stirring, until the solvent was approximately 1 cm above the adsorbent level. The slurry

of methanol and XAD was sonicated in a 5510R-DTH Bransonic Ultrasonic Cleaner for 35 minutes and then filtered through a 47 mm Nucleopore membrane filter with a 0.45 μm pore size using a vacuum filtration system. The resin was transferred to a clean 300 mL beaker, and the sonication and filtration procedure was repeated twice more using two different solvents, first dichloromethane (Reagent grade, Sigma Aldrich) and then hexane (Reagent grade, Sigma Aldrich). The dichloromethane was used to remove any excess methanol and the hexane was used to remove any excess dichloromethane. The resin was then left to air-dry at room temperature until the hexane had fully evaporated, approximately three weeks in duration.

The grinding of the XAD-4™ resin was performed at Environment Canada (4905 Dufferin Street, Toronto, ON) under the supervision of Dr. D. A. Lane. To grind the resin, two clean agate pots each containing ten agate balls were both filled three-quarters full with the now clean, and dry XAD-4™. The pots were then sealed with a rubber gasket and agate lid and assembled into the Retsch planetary ball mill, which was set to run at a rate of 400 rpm for 34 hours. After grinding, the resin, now in powder form, was transferred into an amber jar fitted with a Teflon cap and stored until usage.

3.1.2 Coating of Quartz Fibre Filters

The coating of the quartz fibre filters performed in this work is based on methods developed by Gundel and Hering (1998) and Galarneau et al. (2006) with modifications made by Busca (2010) and Saccon et al. (2013). In order to coat both 20.32 x 25.40 cm

and 47 mm quartz fibre filters, a slurry with concentration of 10.5 g of XAD-4^{TM} per L of hexane was prepared, and sonicated for 30 minutes. Filters were then coated by separately immersing each filter ten times into the slurry using a stainless steel mesh filter holder. The slurry was sonicated for approximately one minute between each filter coating. After ten coatings, the filters were allowed to dry on a surface covered with clean aluminum foil. The slurry was sonicated for 30 minutes while the filters were left to dry. After the 30 minute sonication had elapsed, the filters were immersed ten times each into the slurry once again, but in the reverse order, to ensure an even and uniform coating. The filters were then allowed to dry overnight. The next day, each of the filters was immersed ten times in hexane in order to remove any excess resin and the filters were then left for approximately three weeks to completely dry. The SIFs were then placed in Pyrex glass containers sealed with Teflon lids until sampling.

For the 20.32 x 25.40 cm filters, a slurry with volume of 2 L was created and placed into a thin layer chromatography (TLC) chamber (Sigma Aldrich) for filter coating. The TLC chamber contained several glass plates to reduce the volume of the slurry required to fill the chamber. Twelve 20.32 x 25.40 cm filters were coated per slurry. For the 47 mm filters a slurry with volume of 275 mL was created and placed in a 300 mL beaker for filter coating. Sixty 47 mm filters were coated per batch of slurry.

3.2 Coating of Annular Diffusion Denuders

In this work, an eight-channel annular denuder measuring 285 mm in length and 52 mm in diameter (URG-2000-30CF, URG Corporation) was used to sample gas phase nitrophenols. The denuder was coated with XAD-4^{TM} resin in procedures developed by Eaton (2003) and Gundel et al. (1995). The XAD-4^{TM} resin used to coat the denuder underwent the same cleaning and grinding procedures as discussed in Sections 3.1.1 and 3.1.2.

3.2.1 Coating an Uncoated Denuder

The procedure for coating annular denuders with XAD-4^{TM} resin was performed based on the method developed by Eaton (2003) with modifications developed by Lane (private communication). A slurry of XAD-4^{TM} and hexane with a concentration of 6.5 g of XAD-4^{TM} per L of hexane was created by weighing approximately 1.8 g of clean, ground XAD-4^{TM} into a 300 mL beaker filled with 275 mL of hexane. The beaker was then covered with aluminum foil and sonicated for 30 minutes. One batch of slurry was used to coat only one denuder. While the slurry underwent sonication, the denuder was rinsed twice with hexane. To perform this rinse, one end cap was placed on one end of the denuder and the denuder was filled half-way full with hexane. The other end cap was then placed on the denuder and the denuder endured a "rolling rinse" technique in which

the capped denuder was rolled back and forth 20 times on a flat lab bench space that was approximately 1 m in length. After the slurry was applied, one end of the denuder was uncapped and the hexane solution was poured into a waste beaker. The denuder was allowed to dry under a low flow of pure nitrogen gas (Grade 5.0, 99.999%, Linde). Another rinse with hexane was performed in the same manner, and the denuder was dried under nitrogen prior to coating.

After the XAD-4^{TM} and hexane slurry had been sonicated for 30 minutes, it was applied to the denuder. This time, one end of the denuder was capped and the denuder was filled three-quarters full with the slurry. The other end of the denuder was then capped and the denuder underwent the "rolling rinse" technique 20 times back and forth as was done with the hexane rinse. The slurry was then decanted back into the original beaker, while rotating the denuder to prevent streaks in the coating. The slurry was topped up to the original 275 mL mark with hexane and the beaker was covered with aluminum foil and underwent another 30 minutes of sonication. During this sonication the denuder was allowed to dry under a soft stream of nitrogen. The slurry was then reapplied to the denuder in the same fashion six more times, with the slurry being sonicated and the denuder being allowed to dry between coatings. After the seven coating steps had been completed, the denuder was allowed to dry overnight and was rinsed twice the following day with hexane in order to remove any excess XAD-4^{TM} particles. The XAD-4^{TM} coating found on the adhesive joints between the annuli was removed by immersing approximately 5 mm of each end of the denuder into a beaker with hexane that

was undergoing sonication, for 15 seconds. The denuder end was allowed to dry before being capped to prevent exposure to ambient air.

3.2.2 Recoating a Previously Coated Denuder

Typically a denuder undergoes recoating when it has lost approximately 5% of its coating (Gundel et al., 1998). According to common recoating procedure, the denuder was extracted twice with the extraction solvent in order to obtain the denuder blank and then a slurry of XAD-4^{TM} and hexane was created as described in Section 3.2.1. The denuder was then coated following the same procedure described in Section 3.2.1, but instead of being coated a total of seven times, the denuder being recoated underwent only five coating steps.

3.3 Ambient Air Sampling

The ambient air sampling described in this work was performed between January 2012 and May 2013 on the roof of the Petrie Science and Engineering building at York University. Both high volume filter based sampling techniques and low volume denuder-filter based sampling techniques were employed to sampling ambient nitrophenols in both the gas phase and in PM. Typically the low volume samples

obtained by the IOGAPS system were sampled in parallel with high volume filter samples. The sampling time for both sampling techniques was always around 24 hours, resulting in typical sampling volumes of approximately 1627 m^3 for the high volume air sampler and approximately 24 m^3 for the low volume air sampler. The IOGAPS system was run at a temperature of 5 K above ambient temperature to prevent condensation from occurring within the denuder. Denuders were extracted immediately after removal from the IOGAPS system while filters (both high volume and low volume) were individually placed into mason jars and stored in a freezer at 253 K until extraction.

3.3.1 High Volume Air Sampling

Two high volume TE-6001 PM_{10} air samplers (Tisch Environmental Inc.) were used for sampling. These air samplers were both retro-fitted with $PM_{2.5}$ heads which employed 40 impactor jets to collect particles with aerodynamic diameters larger than 2.5 μm on an oil-wetted surface (Tisch Environmental). These air samplers were run at a sampling flow rate standard for high volume samplers of 1.13 $m^3\ min^{-1}$. To maintain this flow rate on both samplers, calibrations of the samplers were performed once a month or more frequently if the brushes in the motors required replacement. Due to the fact that only one air sampler was equipped with a flow recorder, a direct calibration of that air sampler and an indirect calibration of the other air sampler were performed. To calibrate the air sampler with a flow recorder, a calibrator orifice (TE-5028A, Tisch Environmental, Inc.) was mounted onto the air sampler and one side of a water

manometer was connected to the orifice with rubber tubing. The flow rate of the air sampler was then adjusted to five different values, and the flow readings at these values obtained by the flow recorder, along with their corresponding monometer readings were recorded. A calibration curve was then constructed with these values, correcting for ambient temperature and pressure, and the equation of the line was used to determine the flow recorder reading which equated to a sampling flow rate of 1.13 m^3 min^{-1}. Once this equated value was set on the sampler with the flow recorder, the manometer reading of this sampler was then used to calibrate the sampler without the flow recorder.

3.3.2 Low Volume Air Sampling – The IOGAPS System

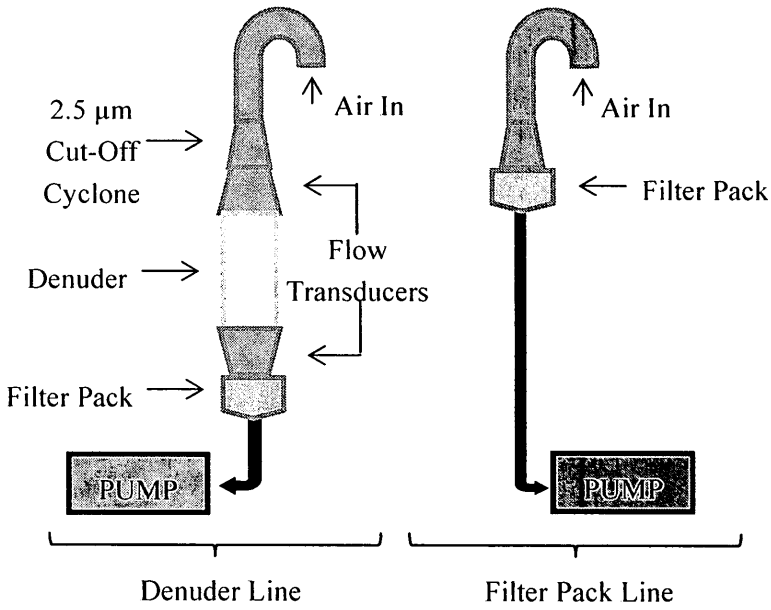

Figure 3.1. Schematic of IOGAPS system with distinction made between the denuder line and the filter pack line.

An IOGAPS system on loan from Environment Canada containing one dual insulated sampling box (URG 2000-01AND, URG Corporation) attached to two computerized sampling pumps (URG 3000-02BB, URG Corporation) were used for sampling. The IOGAPS system was run at the standard sampling flow rate of 1 m^3 hr^{-1}, and the system did not require any calibration due to the fact that both pumps were connected to separate dry gas meters (Gallus 2000) which provided an output of the volume of air sampled. The two sampling lines present in the IOGAPS instrumentation, both used cyclones (URG 2000-30EH, URG Corporation) to remove particles with aerodynamic diameters greater than 2.5 μm. One of the two lines housed in the IOGAPS system, the "denuder line", contained an eight-channel annular diffusion denuder to remove the gas phase fraction upstream of a three-stage filter pack (URG 2000-30FG, URG Corporation) to collect the PM fraction. The other sampling line located in the IOGAPS system, the "filter pack line", contained a three-stage filter pack only, which served to collect a total (gas phase + PM) measurement. The three-stage filter packs employed in both lines were capable of holding up to three 47 mm filters in series, and the filter set-up in both these filter packs for sampling was one uncoated quartz fibre filter upstream of two XAD-4™ coated quartz fibre filters as is depicted in depicted in Fig. 3.2. The sum of the concentrations found on each of the three filters in the filter pack provides a measurement of the PM fraction concentration in the denuder line and a measurement of the total (gas phase + PM) concentration in the filter pack line. This total concentration determined from the sum of the three filters in the filter pack line can then be compared to summation of the concentrations found by two components in the

denuder line of the IOGAPS set-up, the gas phase concentration determined by the denuder and the PM concentration determined by the filter pack.

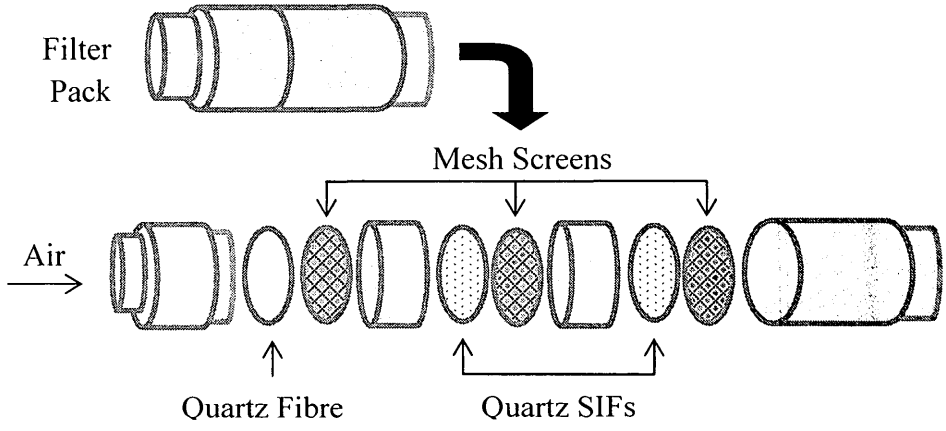

Figure 3.2. Schematic of the filters inside the filter packs located in the IOGAPS system set-up.

3.4 Sample Processing and Analysis

3.4.1 Solvents, Standard Solutions

All solvents and standards used in this work were acquired from Sigma Aldrich or Supelco with purity levels ranging from 97.0 % to 99.8 %. Concentrations of the standard solutions of phenols, nitrophenols and n-alkanes used in this work in calibrations and sample extractions are shown in Table 3.1.

Table 3.1. Concentrations of standard solutions.

Compound	Compound Abbreviation	Standard Concentration (ng μL^{-1})
2-methylphenol	*o*-cresol	104, 100[a]
4-methylphenol	*p*-cresol	101
4-nitrophenol	4-NP	133
4-methyl-2-nitrophenol	4-me-2-NP	101
2-methyl-3-nitrophenol	2-me-3-NP	103
2-methyl-4-nitrophenol	2-me-4-NP	106
2-methyl-5-nitrophenol	2-me-5-NP	103
3-methyl-4-nitrophenol	3-me-4-NP	108
2,6-dimethyl-4-nitrophenol	2,6-dime-4-NP	101
Heptadecane ($C_{17}H_{36}$)	C17	223[b], 228[c]
Octadecane ($C_{18}H_{38}$)	C18	229[b], 213[c]
Nonadecane ($C_{19}H_{40}$)	C19	209[b,c]

[a] standard solution prepared for use in contamination testing
[b] used prior to February 13, 2013
[c] used after February 13, 2013

3.4.2 Extraction and Analysis of 20.32 cm x 25.40 cm Filters

3.4.2.1. Extraction

The extraction procedure used for 20.32 cm x 25.40 cm filters was developed by Moukhtar et al. (2011) with modifications made by Saccon et al. (2013). Prior to extraction the filters were removed from the freezer and allowed to come to room temperature. The filter was then cut into eight pieces using a scalpel and all but one piece of the filter was folded using tweezers and placed into an amber glass jar. The remaining piece of filter was then spiked with approximately 4 μg of each of the two internal

standards used, 2-methyl-3-nitrophenol and 2-methyl-5-nitrophenol. A third internal standard, 2-methylphenol was also spiked in samples extracted prior to April 2012. The spiked piece of filter was added to the amber jar containing the remaining pieces of the filter and approximately 20 mL of acetonitrile (Pestanal Grade, Sigma Aldrich) was added to fully submerge the pieces of filter. A glass rod was then employed to mix the filter pieces in the solution and the jars were then placed in the ultrasonic cleaner to undergo sonication for 15 minutes.

The sonicated filter extract was then filtered through a 20 mL glass syringe (Popper & Sons) equipped with a 0.2 μm PTFE Chromspec syringe filter (Chromatographic Specialties) into a 250 mL round bottom flask. The filter pieces were then sonicated with acetonitrile an additional three times, with filtrations each time added into the same round bottom flask. The combined filter extracts were then evaporated using a Rotavapor R3 rotary evaporator (Buchi) set at 315 K down to volume of approximately 0.5 mL from an approximate volume of 80 mL. The sample was then pipetted into a centrifuge tube and was centrifuged for approximately 5 minutes using a Fisher Scientific Centrific centrifuge (Model 228). After centrifugation, the sample was transferred to a 2 mL conical vial with a stirring bar and evaporated under a soft stream of nitrogen down to an approximate volume of 220 μL. This solution was transferred into a 2 mL vial with a glass insert, for two high-performance liquid chromatography (HPLC) injections. The round bottom flask was then rinsed with 5 mL of acetonitrile three additional times, and each rinse was evaporated using the rotary evaporator and then centrifuged. The three rinses were combined in a conical vial with stirring bar and further

evaporated by nitrogen down to 220 μL. This solution was placed into a separate vial for two additional HPLC injections.

3.4.2.2. HPLC Sample Purification

A Hewlett Packard 1050 HPLC was employed in this work to minimize peak overlap in the filter samples for possible future isotope ratio measurements. The HPLC was equipped with a Supelco Supelcoil LC-18 column (25 cm x 4.6 mm, 5 μm packing size) and a variable wave detector (VWD) which employed a Deuterium lamp and operates at a wavelength of 320 nm. The solvent flow rate of the HPLC was 1 mL min^{-1}, with a gradient elution program employed using acetonitrile and deionized Milli-Q water (18 MΩ) as is shown in Figure 3.3.

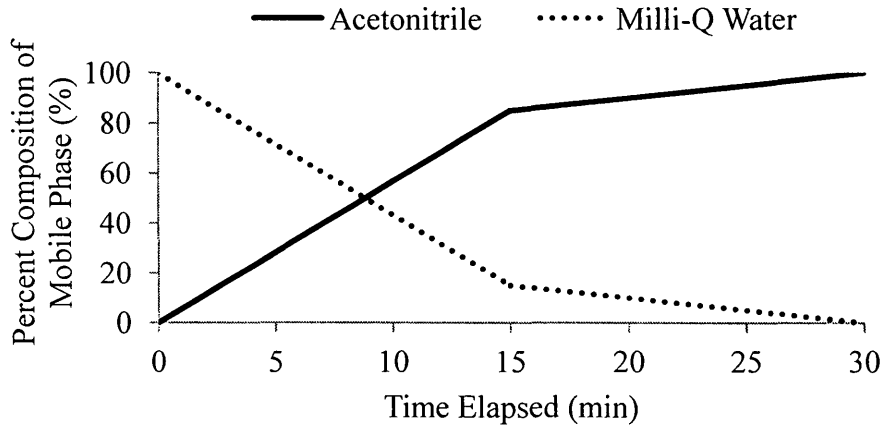

Figure 3.3. Solvent gradient program for HPLC separation.

The effluent of the HPLC was collected during the time in the solvent program when the target compounds eluted, between 10 and 17 minutes. For each of the four HPLC runs, the effluents were collected in the same flask.

3.4.2.3. Evaporation and Solid Phase Extraction

The effluent from the combined HPLC runs from Section 3.4.2.2 contained both water and acetonitrile. In order to remove the acetonitrile, the effluent was evaporated using the rotary evaporator at room temperature for approximately 15 minutes, to reduce the volume of the effluent by a factor of two. The remaining solution was acidified with 3 μL of 0.02 M phosphoric acid to a pH around 5. The solution was then pipetted into an Oasis Hydrophilic-Lipophilic Balance (HLB) extraction cartridge (Waters Corporation) which had been conditioned with acetonitrile and Milli-Q water prior to the addition of the solution, and the solution was allowed to elute out into waste. The HLB cartridge contains polymeric sorbents (N-vinylpyrrolidione and divenylbenzene) which acts as a stationary phase to trap the nitrophenols from the aqueous solution (Waters Corporation, 2008). Once the solution had fully passed through the cartridge, the target nitrophenols were extracted using approximately 10 mL of acetonitrile, which was collected into another flask.

The collected solution was then evaporated by a rotary evaporator to a volume which was approximately 0.5 mL. The solution was transferred to a 2 mL conical vial with a magnetic stir bar, and the flask was rinsed twice with 2 - 3 mL of acetonitrile

which was evaporated and added to the final solution. The solution then underwent further volume reduction under nitrogen to a volume of approximately 50 μL. A 20 μL portion of the mixture of the volumetric standards (C17, C18 and C19) was added to the solution and the vial was covered and allowed to mix. The solution was then divided evenly into two 2 mL vials with 200 μL glass inserts. One of these vials was analyzed by gas chromatography-mass spectrometry (GC-MS) and the other was stored in a freezer at 253 K for possible further analysis.

3.4.2.4. Derivatization by BSTFA

Prior to injection into the GC-MS, the nitrophenols were derivatized in order to increase their thermal stability. The derivatizing agent used in this work was N,O-Bis(trimethylsilyl)trifluoroacetamide (BSTFA). The reaction of BSFTA with 2-methyl-4-nitrophenol shown in Fig.3.4, illustrates the replacement of a labile hydrogen on the nitrophenol by a trimethylsilyl group via a nucleophilic attack. To derivatize the solutions in this work, either 10 or 20 μL of BSTFA (Sigma Aldrich) was added to the final mixture and the solution was allowed to mix for approximately 5 minutes.

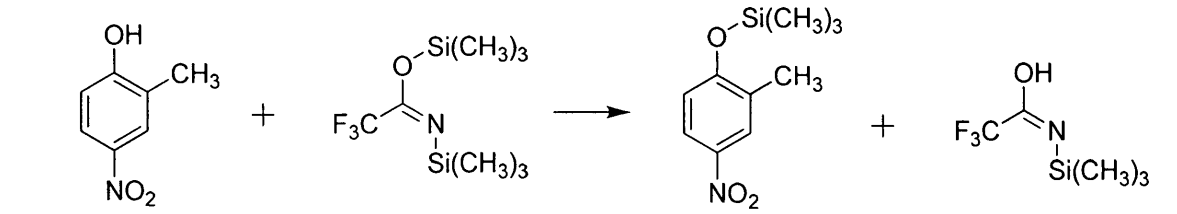

2-methyl-4-nitrophenol BSTFA

Figure 3.4. Derivatization of 2-methyl-4-nitrophenol by BSTFA (Adapted from Knapp, 1979).

3.4.2.5. Analysis by GC-MS

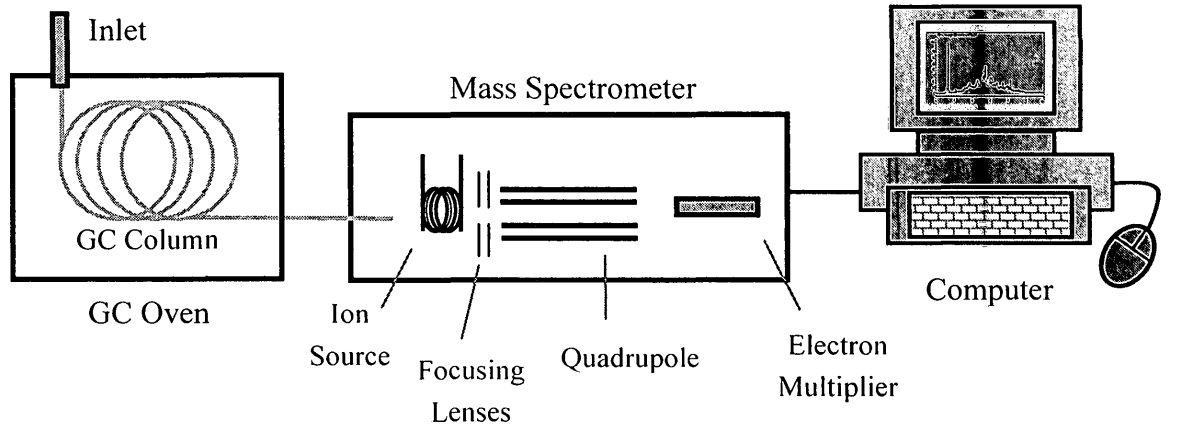

Figure 3.5. Schematic of the GC-MS instrumentation (adapted from Skoog et al., 2007).

A Hewlett Packard 5890 Series II GC equipped with a Hewlett Packard 5972 Series MS detector was used in this work for concentration measurements. After derivatization of the samples, 1 μL splitless injections were performed using a Hewlett Packard 6890 auto sampler. Helium (5.0 Grade, 99.999 %, Linde) was the carrier gas used, at a flow rate of 2 mL min^{-1}. The GC employed either a DB-5MS or SLB-5MS

column (60 m x 0.25 mm i.d. x 1.0 μm film thickness). While the injection port and detector temperature were kept constant at 538 K and 553 K, respectively, the GC separation required a 132 minute long temperature program, as is illustrated in Fig. 3.6. A 125 minutes long temperature program was initially used, but the program was extended to remove low volatility contaminants. Each sample was analyzed twice using selective ion monitoring (SIM) with blank (non-derivatized acetonitrile) runs performed between different samples. The ion masses monitored along with the retention times monitored for each target compound, internal standard and volumetric standard analyzed by GC-MS are shown in Table 3.2.

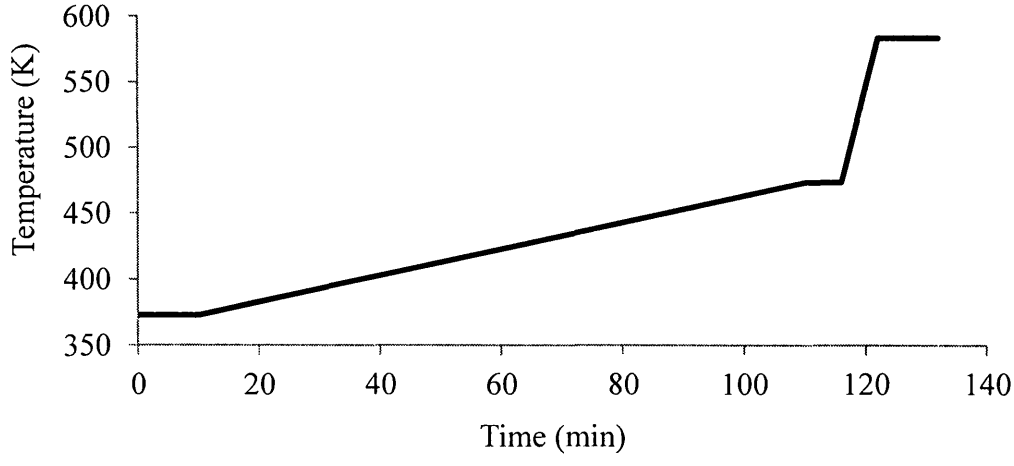

Figure 3.6. Temperature program used for GC separation.

Table 3.2. Ion masses monitored during GC-MS analysis and approximate retention times for compounds of interest in order of increasing retention time.

Compound	Ion Masses Monitored in SIM	Monitoring Time (min)
o-cresol	165, 180	15-55
p-cresol	165, 180	15-55
4-me-2-NP	165, 210, 225	55-90
4-NP	150, 196, 211	55-90
2-me-3-NP	165, 208, 225	55-90
2-me-5-NP	165, 210, 225	55-90
3-me-4-NP	165, 210, 225	55-90
2-me-4-NP	165, 210, 225	55-90
C17	85	90-132
2,6-dime-4-NP	224, 239	90-132
C18	85	90-132
C19	85	90-132

3.4.3. Extraction and Analysis of 47 mm Filters

The extraction procedure used for the 47 mm filters is similar to the procedure outlined in Section 3.4.2. Since these filters were much smaller in size, they were only cut into two pieces, and due to the lower sampling volume, these filters were spiked with only 2 μg of each internal standard. The volume of acetonitrile used was approximately 10 mL per each of the extractions and the syringe filter used for these filters was 10 mL in size. Due to the fact that these samples were collecting less overall material, the clean-up steps employed for the 20.32 cm x 25.40 cm filters, HPLC and solid phase extraction (SPE), were removed for significant time reduction. The four extracts per filter were combined

and reduced by volume reduction, derivatized by BSTFA and analyzed by GC-MS as per Sections 3.4.2.3 - 3.4.2.5.

3.4.4. Extraction and Analysis of Annular Diffusion Denuder

Prior to ambient sampling, newly coated denuders ware extracted twice with approximately 100 mL of acetonitrile following the same rolling rinse technique described in 3.2.1 for the coating procedure. The two extracts then underwent volume reduction, derivatization by BSTFA and analysis by GC-MS as per Sections 3.4.2.3 – 3.4.2.5, to determine blank values.

After ambient sampling, denuders were extracted immediately after being removed from the IOGAPS system with a method adapted from techniques of Gundel et al. (1998), Eaton (2003) and Lane (private communication). One end of the denuders was capped and approximately 100 mL of acetonitrile was added to half-fill the denuder. The denuder then underwent the "rolling-rinse" technique described in Section 3.2.1. This extract was then filtered twice, first using a 47 mm Nucleopore membrane filter (0.45 μm pore size) with a vacuum filtration system and secondly, through a 20 mL glass syringe equipped with a 0.2 μm PTFE Chromspec syringe filter. The filtered extract was then placed into a round bottom flask and 2 μg of each internal standard was added to this filtered solution. The extraction of the denuder was repeated an additional three times with the first three extracts combined into one flask and the fourth extract evaporated and analyzed separately for blank determination. The extracts were volume

reduced with rotary evaporation, derivatized with BSTFA and run through the GC-MS by the methods described in Sections 3.4.2.3 – 3.4.2.5.

3.4.5. Calibration and Target Compound Quantification by GC-MS

GC-MS calibrations were performed once a month by injecting five derivatized standard solutions each, containing all target compounds, internal standards and volumetric standards, with concentrations ranging from 1 to 15 ng μL^{-1}. During the calibrations, each of the five calibration mixtures was run twice, in random order. A typical calibration curve for one compound is shown in Fig. 3.7. Approximately every 20 runs, a single injection of one calibration mixture, typically one in a median concentration level, was run to monitor the GC-MS performance.

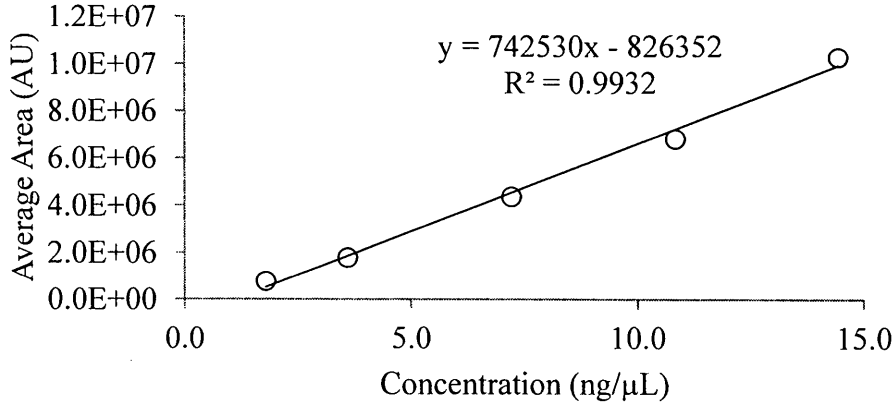

Figure 3.7. Calibration curve for 2-methyl-4-nitrophenol from calibration performed on October 29, 2012.

In order to quantify the target compounds, the summation of the peak areas (in arbitrary units (AU)) for the specific ions monitored, which were shown in Table 3.2, were used to calculate overall peak areas for the target compounds and internal standards in both calibration mixtures and ambient samples. These values were then used to compute the mass of a target compound (m_t) using Eq. 3.1:

$$m_t = \frac{PA_t Cal_{IS}}{Cal_t PA_{IS}} . m_{IS,d} . \frac{MM_{t,und}}{MM_{t,d}} \quad \text{(Eq. 3.1)}$$

Where PA_t and PA_{IS} are the peak areas of the target compound (T) and internal standard (IS), Cal_t and Cal_{IS} are the responses obtained for the target compound and internal standard from the calibration curves, $m_{IS,d}$ is the mass of the derivatized internal standard and $MM_{t,und}$ and $MM_{t,d}$ are the molar masses of the underivatized and derivatized target compound. In order to then determine the atmospheric concentration of the target compound (C_t), the blank mass (m_B) was subtracted from the mass of the target compound (determined by Eq. 3.1), and this blank corrected mass is then divided by the sampling volume (V) as shown in Eq. 3.2 below.

$$C_t = \frac{m_t - m_B}{V} \quad \text{(Eq. 3.2)}$$

For each ambient sample, the average of the two areas determined by each of the replicate runs was used for the PA_T and PA_{IS} values. Since two internal standards were used, this calculation was performed twice for each compound and the average

concentration from the two results was used as long as the individual values agreed within 20 %.

3.5. Description of Tests Conducted

This section describes a number of tests conducted in this work including blank value determination for both denuders and filters as well as a variety of method validation tests including denuder extraction efficiency, denuder collection efficiency and collection efficiency of low volume filters.

3.5.1. Blank Value Determination for Filters and Denuders

To determine blank values for 47 mm quartz fibre filters, both quartz uncoated and XAD-4^{TM} coated SIFs were extracted and analyzed following the same procedure as was described for ambient filters. Three uncoated quartz fibre filters were extracted and analyzed between July and August 2012 and seven XAD-4^{TM} coated SIFs were extracted and analyzed between July 2012 and January 2013. Blanks of XAD-4^{TM} coated SIFs were conducted on every newly coated set of filters, with three conducted in July 2012, three in August 2012 and one conducted in January 2013. Prior to their extraction, filters were handled in the same manner as filters used for ambient sampling.

Blank measurements for XAD-4™ coated denuders were performed prior to each ambient sampling. Denuders were extracted and analyzed for blank values following the same extraction procedure described for ambient samples no more than seven days prior to the sampling date. A number of tests were also conducted in this work to see if there were any significant denuder blank values attributed to other factors involved in the sampling and extraction procedures. To determine if there was any denuder blank value attributed to the transportation of the denuder to and from the sampling site, three tests were conducted where denuders were sampled for ten minute periods and then removed and extracted following the same procedure described for ambient denuder samples. To determine if there was any contributing denuder blank value from the sampling lines located in the IOGAPS instrumentation, which are difficult to clean, three tests were conducted where a 47 mm XAD-4™ coated SIF was placed in front of the IOGAPS inlet in a filter holder. Denuders were then sampled with this set-up for 24 hours and were removed and extracted immediately after sampling following the same procedure described for ambient denuder samples.

3.5.2. Method Validation Tests

To test if the detailed extraction procedure used to clean-up the high volume filter samples could be simplified for the low volume IOGAPS samples, a denuder sampled for 24 hours was extracted, filtered and volume reduced following the procedure for ambient

samples without the HPLC and SPE clean-up steps used in high volume samples and was then run by the GC-MS after derivatization with BSTFA.

Prior to ambient sampling a variety of extractions solvents, listed in Table 3.3, were tested. In order to test the efficiency of these solvents, 4 μg of the two internal standards (2-methyl-3-nitrophenol and 2-methyl-5-nitrophenol) were spiked onto approximately 50 mg of XAD-4™ placed in a 4 mL vial. The internal standards were then extracted from the resin by adding 4 mL of each of the solvents tested to the vial and this extract was then filtered and volume reduced followed by derivatization by BSTFA and analysis by GC-MS. The resin was then extracted another time, following the same procedure. Each solvent was tested in this manner four times.

Table 3.3. Extraction solvents used with sorbent coated devices in literature.

Work	Sorbent Coated Device Used	Extraction Solvent(s) and Ratios Used
Peters et al. (2000)	XAD-4™ coated denuder	Hexane
Fan et al. (2004)	XAD-4™ coated denuder	hexane:DCM:meOH (1:1:1)
Kleindienst et al. (2004)	XAD-4™ coated denuder	hexane:DCM:ACN (1:1:2)
Cecinato et al. (2005)	KOH coated denuder	DCM
Temime et al. (2007)	XAD-4™ coated denuder	meOH:DCM:ACN (0.5:8.5:1)
Saccon et al. (2013)	XAD-4™ coated quartz fibre filters	ACN

DCM: dichloromethane
ACN: acetonitrile
meOH: methanol

To test how the extraction solvent reacted with the sorbent coating on the denuder, a denuder (coated with 0.2534 g of XAD-4™) was repeatedly extracted with approximately 100 mL of acetonitrile a total of 15 times. For each extraction, the sorbent that was removed from denuder was separated from the extract by filtration, allowed to dry and then weighed.

In order to determine the efficiency of the denuder extractions, seven ambient denuder samples from the time period between June 25, 2012 and July 24, 2012, were extracted ten times, with each extract analyzed separately following the extraction procedure described for ambient samples. Amounts of target nitrophenols obtained from each extraction were monitored.

In order to test the efficiency of the denuder itself, three ambient samplings were conducted in August 2012 where two denuders were placed in series.

To determine the collection efficiency of both uncoated quartz and XAD-4™ coated SIFs, filters were places in series in the IOGAPS filter pack. Four tests were conducted in 2012 (June 19, June 20, August 23 and December 13) where three uncoated quartz filters were sampled for 24 hours while placed in series in a filter pack. Three tests were also conducted between May 13 and 15, 2013 where three XAD-4™ coated SIFs were sampled for 24 hours while placed in series in a filter pack. Filters were extracted using the procedures described for ambient filter samples.

4. Results

4.1. Method Evaluation

In this section, results from method evaluation tests are presented which include the determination of blank values and detection limits for both filters and denuders, as well as denuder blank values contributing from denuder transportation and from the sampling lines of the IOGAPS system. A section presenting the discovery of a 2-methylphenol artifact is also included.

4.1.1 Blank Values and Lower Limits of Detection for Filters and Denuders

The blank values for the uncoated filters as well as XAD-4^{TM} coated SIFs are shown in Table 4.1. Average values of all denuder blanks performed in this work are shown in Table 4.2. In order to determine the high volume and low volume blank values for ambient measurements, the average masses of the blank were divided by the average volume of air sampled in 24 hours, 24 m^3 for low volume samples.

Table 4.1. Blank masses, standard deviations and equivalent atmospheric concentrations determined from three uncoated 47 mm quartz fibre filters and seven XAD-4™ coated 47 mm quartz fibre filters.

Compound	Uncoated Quartz Filters			XAD-4™ Coated SIFs		
	Average Mass of Blank (ng)	Standard Deviation of Blank (ng)	High Volume Blank (ng m^{-3})	Average Mass of Blank (ng)	Standard Deviation of Blank (ng)	Low Volume Blank (ng m^{-3})
4-me-2-NP	0.08	0.05	0.003	0.4	0.4	0.02
4-NP	9.2	11.1	0.38	6.1	5.0	0.25
3-me-4-NP	0.2	0.09	0.006	0.4	0.3	0.02
2-me-4-NP	0.2	0.09	0.01	0.6	0.8	0.03
2,6-dime-4-NP	0.08	0.03	0.003	0.2	0.2	0.01

Table 4.2. Blank masses, standard deviations and equivalent atmospheric concentrations determined for XAD-4™ coated denuders. Blank values for denuder transport and IOGAPS sampling lines were each corrected for the blank attributed by the denuder. The total blank values shown are the sum of the three contributions.

Compound	Average Mass of Blank (ng)				TOTAL Low Volume Blank (ng m^{-3})
	Denuder	Denuder Transport	IOGAPS Sampling Line	TOTAL	
4-me-2-NP	1.5 ± 1.0	0.05 ± 0.05	2.9 ± 0.8	4.0 ± 1.3	0.17
4-NP	6.4 ± 8.9	2.6 ± 0.1	6.8 ± 2.9	15.8 ± 9.3	0.66
3-me-4-NP	1.1 ± 2.0	0.2 ± 0.2	1.3 ± 0.9	2.6 ± 2.2	0.11
2-me-4-NP	1.2 ± 1.6	0.3 ± 0.4	5.5 ± 1.2	7.0 ± 2.1	0.29
2,6-dime-4-NP	0.3 ± 0.4	0.2 ± 0.2	3.4 ± 0.6	1.7 ± 0.7	0.07

Lower limits of detection and atmospheric detection limits were determined using three times the blank standard deviation values determined for both 47 mm quartz uncoated and XAD-4™ coated SIFs as well as for XAD-4™ coated denuders and these values are shown in Table 4.3. The atmospheric detection limits were found by dividing the calculated lower limits of detection by the average volume of air sampled in 24 hours.

Table 4.3. Lower limit of detection (LDL) and atmospheric detection limits (ADL) for 47 mm uncoated quartz and XAD-4™ coated SIFs and XAD-4™ coated denuders.

Compound	Uncoated Quartz Filters		XAD-4™ Coated SIFs		XAD-4™ Coated Denuders	
	LDL (ng)	ADL (ng m^{-3})	LDL (ng)	ADL (ng m^{-3})	LDL (ng)	ADL (ng m^{-3})
4-me-2-NP	0.2	0.01	1.1	0.04	3.9	0.16
4-NP	33.4	1.39	15.0	0.63	27.9	1.16
3-me-4-NP	0.3	0.01	0.8	0.04	6.6	0.28
2-me-4-NP	0.3	0.01	2.3	0.10	6.3	0.26
2,6-dime-4-NP	0.1	0.003	0.5	0.02	2.1	0.09

4.1.2 Artifacts

An artifact of 2-methyl-4-nitrophenol was observed when beginning to analyze ambient samples. Figure 4.1 shows the masses of 2-methyl-4-nitrophenol obtained from ten separate extractions of a denuder which was sampled for 24 hours on January 25, 2012.

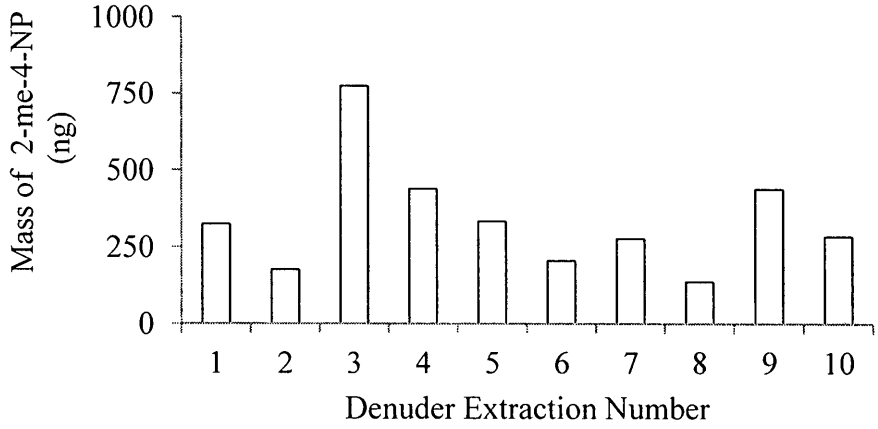

Figure 4.1. Mass of 2-methyl-4-nitrophenol found on each of ten denuder extractions of a denuder sampled for 24 hours on January 25, 2012.

A summary of all tests performed to determine the source of this artifact are found in Table 4.4. All tests listed were performed in triplicate and the volumes used in the tests emulated the volumes used in a typical denuder extraction, therefore approximately 125 mL of acetonitrile was reduced to approximately 50 μL prior to derivatization by BSTFA and analysis by GC-MS.

Table 4.4. Tests conducted to determine source of 2-methyl-4-nitrophenol artifact and results obtained. Masses and standard deviations of artifacts (in ng) are shown in parenthesis.

Test Conducted	Result
ACN[a] + 3 IS[b] (2 μg of each)	Artifact present (256 ± 15)
ACN + 3 IS (2 μg of each) – after rotary evaporator cleaning	Artifact present (119 ± 17)
ACN + no IS	Artifact not present
ACN + 2-mePh (2 μg)	Artifact present (99 ± 22)
ACN + 2-me-3-NP (2 μg)	Artifact not present
ACN + 2-me-5-NP (2 μg)	Artifact not present
ACN + 2-me-3-NP + 2-me-5-NP (2 μg of each IS)	Artifact not present
ACN + 2-mePh (2 μg)[c]	Artifact present (41 ± 5)

[a] ACN: acetonitrile
[b] 3 IS are 2-mePh, 2-me-3-NP and 2-me-5-NP
[c] a new standard of 2-methylphenol was purchased and used for this test

The TIC (total ion chromatogram) of one test where acetonitrile was tested with the addition of 2-methylphenol only is shown in Fig. 4.2. Figure 4.3 shows the mass spectrum of the 2-methyl-4-nitrophenol peak found from this test compared to the mass spectrum of a standard 2-methyl-4-nitrophenol injection.

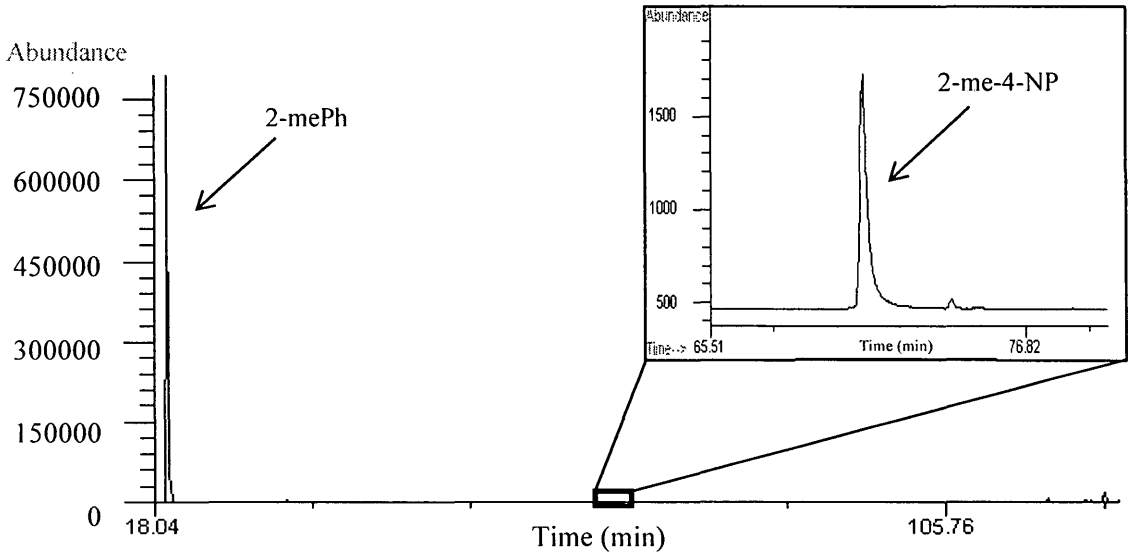

Figure 4.2. The scanning chromatogram showing the presence of 2-methyl-4-nitrophenol in the 2-methylphenol + acetonitrile test. Masses of the 2-methylphenol and 2-methyl-4-nitrophenol peaks are 28.9 ng and 0.8 ng respectively.

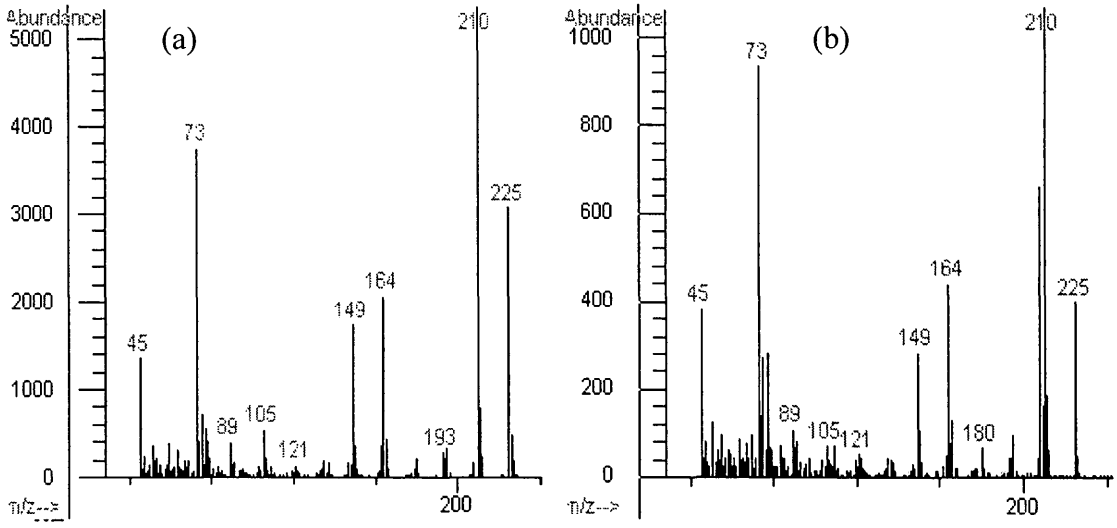

Figure 4.3. Mass spectra of 2-methyl-4-nitrophenol peak present in (a) a standard solution and (b) the 2-methylphenol + acetonitrile test both run in TIC mode.

4.2. Method Validation

In this section, method validation results are presented which include results from modifications made to the extraction procedure for both filters and denuders, efficiency results determined for both denuders and denuder extractions as well as collection efficiency results for denuders and filters.

4.2.1. Modifications to Extraction Procedure

The total ion current for a scanning chromatogram of an extract from an ambient denuder sample without the HPLC and SPE clean-up steps, with compounds of interest labelled, is shown in Fig. 4.4.

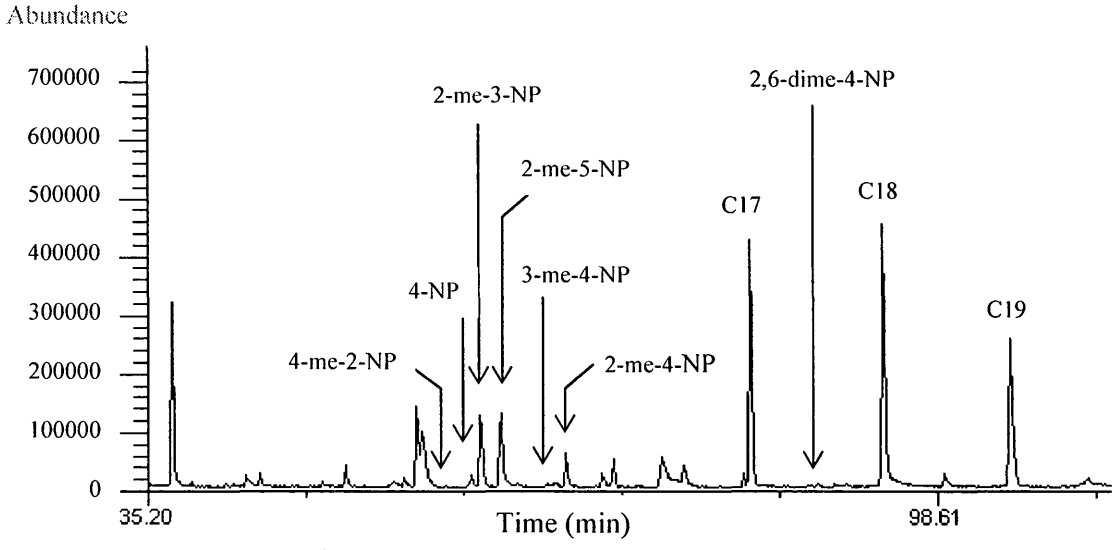

Figure 4.4. The scanning chromatogram for a 24 hour denuder sample extracted without the HPLC and SPE clean-up steps. Labels of target compounds, internal standards and volumetric standards are provided.

4.2.2. Denuder Extraction Solvent Efficiency

Results from recovery tests involving a variety of extraction solvents as well as results from solvent-sorbent interaction tests for acetonitrile and XAD-4™ are presented in this section. The average recoveries and standard deviations of the internal standards, relative to the spiked mass (4 μg) of the internal standards, extracted with a variety of extraction solvents are shown in Table 4.5. The results from the solvent-sorbent tests conducted are illustrated in Table 4.6.

Table 4.5. Internal standard recoveries and standard deviations for a variety of solvent mixtures tested four times.

Extraction Solvent Solution	Extraction Number	Recovery (%)	
		2-me-3-NP	2-me-5-NP
Hexane	1	10 ± 8	10 ± 9
	2	5 ± 2	5 ± 3
DCM[a]	1	14 ± 6	15 ± 8
	2	7 ± 2	5 ± 2
1:1:1 (hexane:DCM:meOH[b])	1	< LDL	< LDL
	2	< LDL	< LDL
1:1:2 (hexane:DCM:ACN[c])	1	40 ± 9	41 ± 7
	2	12 ± 3	12 ± 4
0.5:8.5:1 (meOH:DCM:ACN)	1	31 ± 19	30 ± 20
	2	17 ± 5	13 ± 6
ACN	1	80 ± 6	82 ± 9
	2	9 ± 2	9 ± 2

[a] DCM: dichloromethane
[b] meOH: methanol
[c] ACN: acetonitrile

Table 4.6. Amount of sorbent removed from denuder for a series of extractions with acetonitrile.

Extraction Number	Mass of XAD-4™ Removed (g)	Integrated Mass Loss (g)	Integrated Percentage of Total Coating Loss (%)
1	0.0004	0.0004	0.2
2	0.0014	0.0018	0.7
3	0.0012	0.0030	1.2
4	0.0009	0.0039	1.5
5	0.0009	0.0048	1.9
6	0.0009	0.0057	2.3
7	0.0003	0.0060	2.4
8	0.0001	0.0061	2.4
9 10	0.0001 [a]	0.0062	2.4
11 12	0.0001[a]	0.0063	2.5
13 14 15	0.0001[a]	0.0064	2.5

[a] several extracts were combined for mass determination

4.2.3. Efficiency of Denuder Extractions

The results from seven ambient denuder samples which were extracted ten times, with each extract analyzed separately are illustrated in Table 4.7. as percentage of the target compounds extracted in each extraction, calculated as efficiency as defined by Eq. 4.1,

$$Efficiency = \frac{Mass\ in\ Extraction_i}{Total\ Mass\ in\ all\ Extractions}\ x\ 100\ \% \qquad \text{(Eq. 4.1)}$$

Table 4.7. Efficiency of denuder extractions and standard deviations of the efficiency for extractions 1-4 (extractions 5-10 masses were below DL masses).

Compound	Percentage of Mass Found in Each Extraction (%)			
	Extraction 1	Extraction 2	Extraction 3	Extraction 4
4-me-2-NP	84 ± 11	13 ± 7	3 ± 4	0.3 ± 0.8
4-NP	87 ± 14	10 ± 12	3 ± 4	0.3 ± 0.8
3-me-4-NP	84 ± 7	14 ± 8	2 ± 1	0.4 ± 0.4
2-me-4-NP	88 ± 7	8 ± 4	3 ± 3	0.9 ± 2
2,6-dime-4-NP	93 ± 2	4 ± 1	3 ± 3	0.5 ± 0.4

4.2.4. Collection Efficiency of Denuder

The efficiency of the front denuder for each target compound was calculated for each of the three ambient samplings performed with two denuders placed in series, using Eq. 4.2. The efficiency of the front denuder for each target compound was calculated to see if there were any losses occurring due to inefficient collection of the denuder. The results for these tests are presented in Table 4.8.

$$\text{Efficiency (\%)} = \frac{Mass\ on\ front\ denuder}{(Mass\ on\ front\ denuder) + (Mass\ on\ back\ denuder)}\ x\ 100\% \qquad \text{(Eq. 4.2)}$$

Table 4.8. Average and standard deviation of efficiency of the front denuder for the target nitrophenols from three collection efficiency tests.

Compound	Efficiency (%)			
	01-Aug-12	13-Aug-12	15-Aug-12	Average
4-me-2-NP	95	95	100	97 ± 3
4-NP	94	100	100	98 ± 3
3-me-4-NP	99	99	93	97 ± 3
2-me-4-NP	98	95	100	98 ± 3
2,6-dime-4-NP	100	100	95	98 ± 3

4.2.5. Collection Efficiency of Low Volume Filters

Figures 4.5 and 4.6 depict the percentage of mass of the target nitrophenols found on the second and third filter (over the total mass found on all three filters) for both uncoated quartz filters and XAD-4^{TM} coated SIFs.

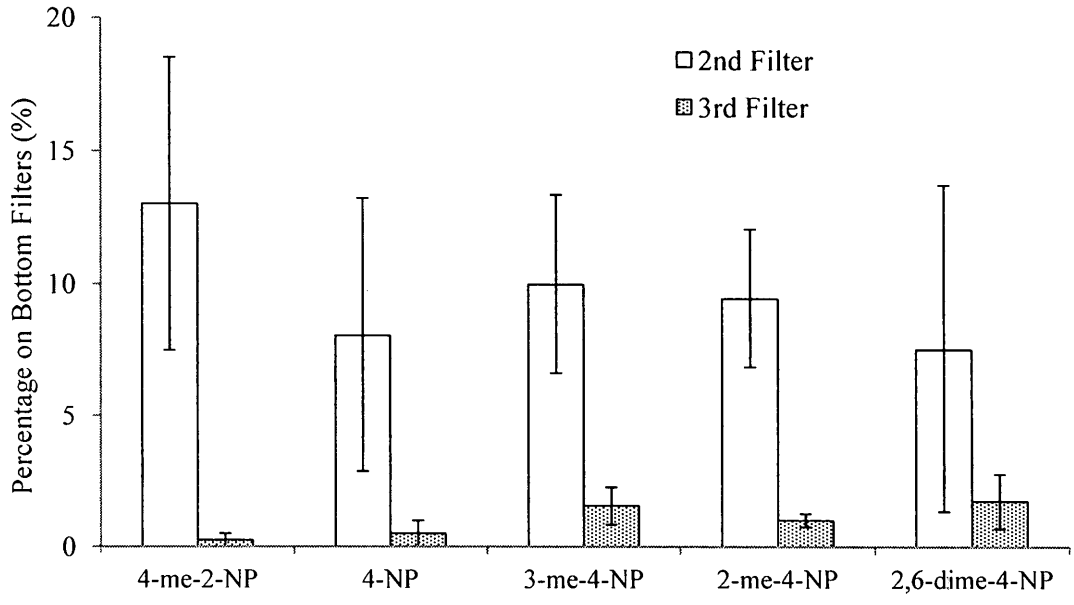

Figure 4.5. Efficiency of second and third uncoated quartz fibre filters when collected in series based on four tests. The error bars represent the error of the mean.

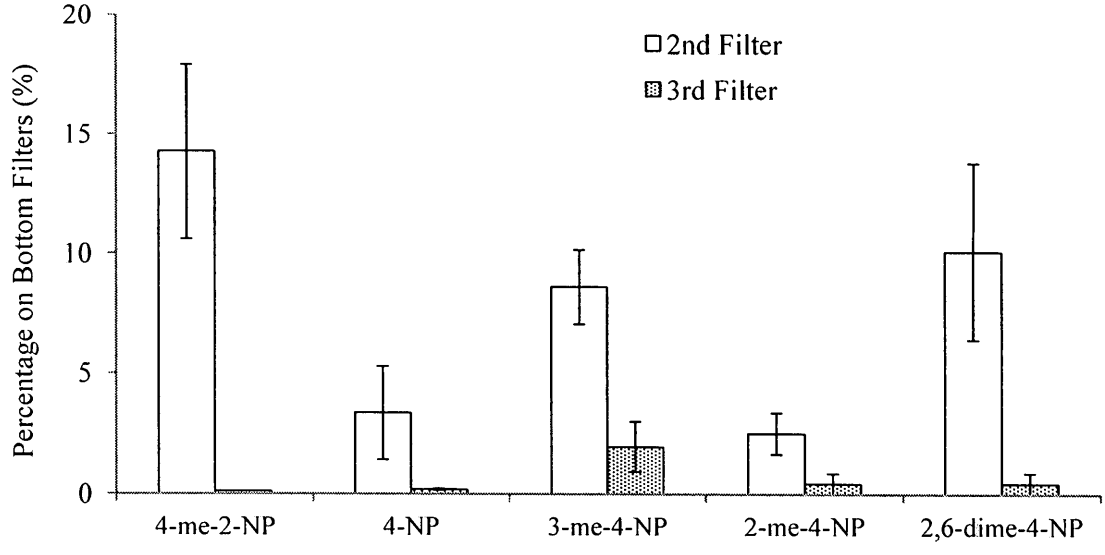

Figure 4.6. Efficiency of second and third XAD-4^{TM} coated SIFs when collected in series based on three tests. The error bars represent the error of the mean.

4.3. Results of Ambient Measurements

A total of 32 ambient samples were collected using the IOGAPS instrumentation between June 25, 2012 and May 2, 2013 with high volume filter samples collected in parallel on 25 of these dates. In this section, ambient results are presented which include filter pack evaluation as well as average concentration values and partitioning data for the target nitrophenols from the IOGAPS instrumentation.

4.3.1. Filter Pack Evaluation

Average masses, standard deviations and error of the mean values found on each of the three filters in both the denuder line filter pack and the filter pack line filter pack for all ambient samples are shown in Table 4.9. The masses found on each of the filters in the filter packs were then converted to average percentages of total mass and were plotted, for comparison, in Figs. 4.7 and 4.8.

Table 4.9. Average blank corrected masses and standard deviations found on each of the three filters in the denuder line (DL) filter pack and the filter pack line (FPL) filter pack. Error of the mean values are given in parenthesis.

Filter Pack	Filter Description[a]	Mass (ng)				
		4-me-2-NP	4-NP	3-me-4-NP	2-me-4-NP	2,6-dime-4-NP
DL	QA	0.8 ± 0.8 (0.1)	7.3 ± 6.2 (1.8)	1.0 ± 0.9 (1.8)	2.1 ± 3.1 (0.6)	0.7 ± 0.8 (0.2)
	XB	1.6 ± 2.4 (0.5)	31.8 ± 59.2 (11.4)	1.0 ± 2.0 (0.4)	3.0 ± 6.2 (1.2)	0.5 ± 0.7 (0.1)
	XC	1.7 ± 2.8 (0.8)	18.8 ± 20.6 (4.9)	0.4 ± 0.5 (0.1)	0.9 ± 1.6 (0.3)	0.2 ± 0.3 (0.1)
FPL	QA	1.3 ± 1.6 (0.3)	19.7 ± 28.2 (5.9)	2.1 ± 2.3 (0.4)	4.6 ± 5.9 (1.0)	1.4 ± 1.6 (0.3)
	XB	5.7 ± 6.7 (1.2)	220.7 ± 251.88 (42.6)	7.5 ± 7.6 (1.3)	43.2 ± 66.8 (11.3)	14.7 ± 16.8 (2.9)
	XC	3.2 ± 4.1 (1.0)	26.8 ± 21.5 (4.5)	1.1 ± 1.3 (0.3)	4.2 ± 4.7 (0.9)	1.8 ± 2.3 (0.5)

[a] For the filter description there are two types of filters Q (uncoated quartz) and X (XAD-4™ coated SIF) and three positions these filters can have inside the filter packs: A (1st filter or most upstream filter), B (2nd filter) and C (3rd filter).

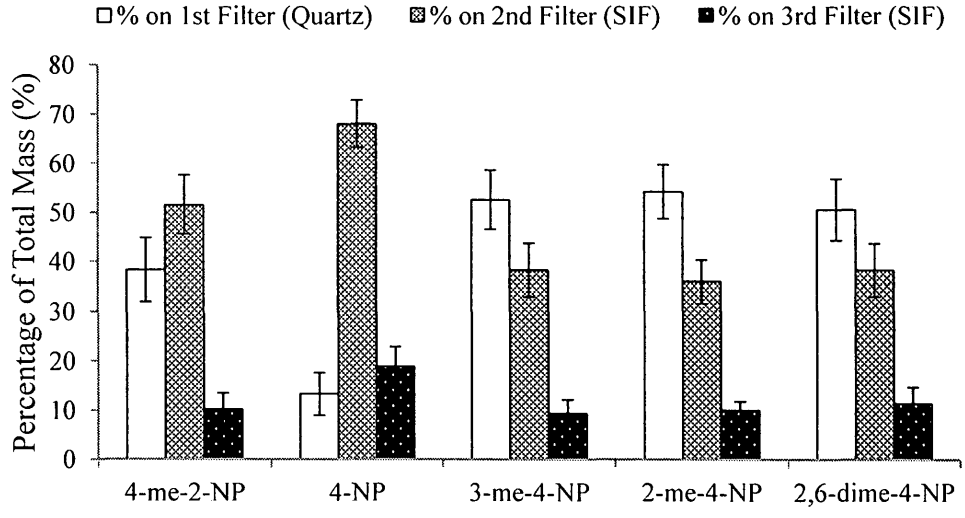

Figure 4.7. Average percentage of total mass of target nitrophenols found on three filters in the denuder line filter pack for all ambient samples. Error bars represent error of the mean.

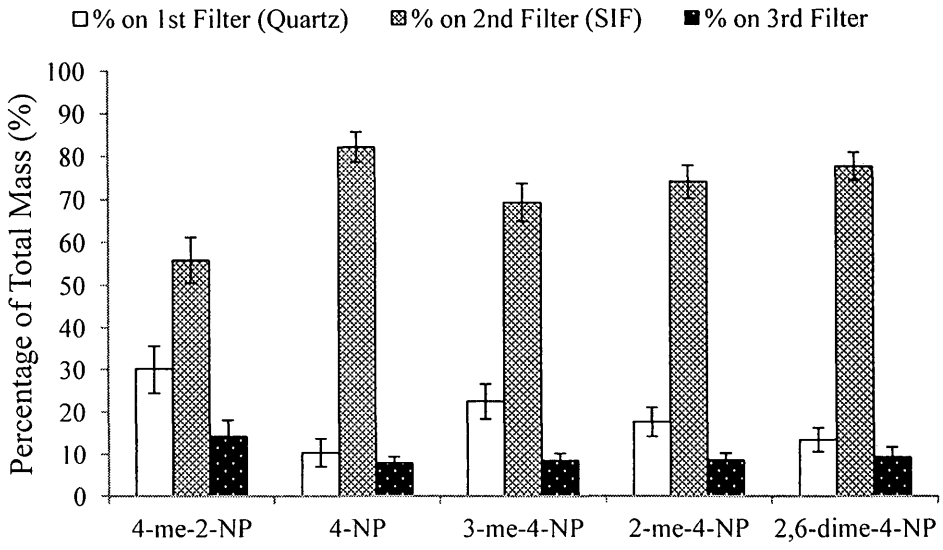

Figure 4.8. Average percentage of total mass of target nitrophenols found on three filters in the parallel filter pack line for all ambient samples. Error bars represent error of the mean.

4.3.2. Average Concentrations of Nitrophenols in Gas Phase and PM

Gas phase and PM concentrations measured by the IOGAPS denuder line (gas phase determined by mass found on denuder and PM determined by mass found on three filters in denuder filter pack) and total (gas phase + PM) concentrations made by the IOGAPS filter pack line (sum of masses found on three filters in filter pack) obtained from ambient measurements for each of the five target compounds are shown in Figs. 4.9 – 4.13. Average concentrations and error of the mean values were calculated from the data obtained from all 32 sampling dates. The masses found on filters and denuders which were used to calculate ambient concentrations were blank corrected, as was previously discussed in Section 3.4.5, using the blank values determined for the

uncoated quartz filters and XAD-4™ coated SIFs as well as the blank values determined for the XAD-4™ coated denuders. Outliers were determined in this work using the z-test, which discards values which are three standard deviations above or below the mean. Table 4.10 illustrates average concentrations and error of the mean values with the inclusion and exclusion of outlying points. Plots illustrating possible dependences of gas, PM and total (gas phase + PM) concentrations on average daily temperature are shown in Figs. 4.14 – 4.16.

Day and night sampling was also conducted over a course of three consecutive days (April 30 - May 2, 2013). During these late spring months daytime was classified as 7:00 a.m. - 7:00 p.m. and nighttime was classified as 7:00 pm - 7:00 am. Average day and night concentrations as well as error of the mean values are shown in Table 4.11.

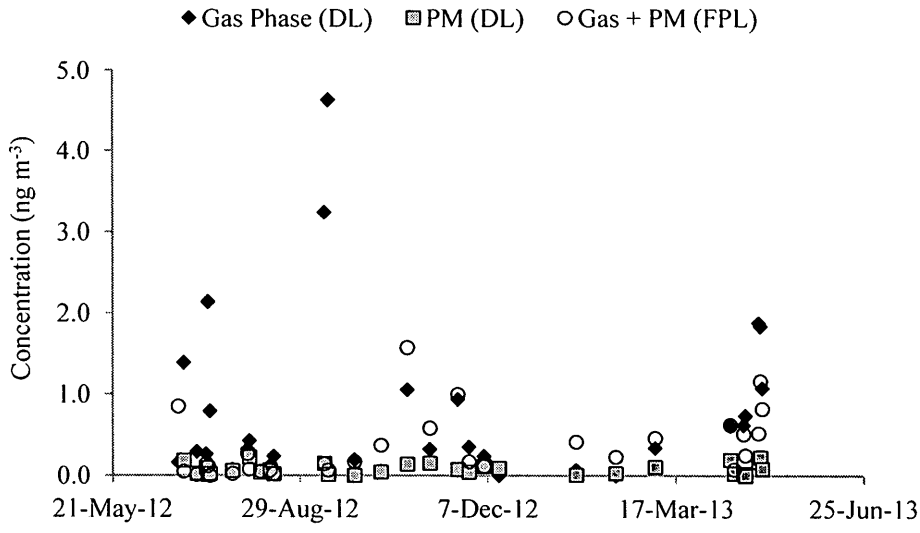

Figure 4.9. Gas phase and PM concentration measurements from denuder line (DL) and gas phase + PM concentration measurements from the filter pack line (FPL) placed in parallel for 4-methyl-2-nitrophenol of all ambient samples.

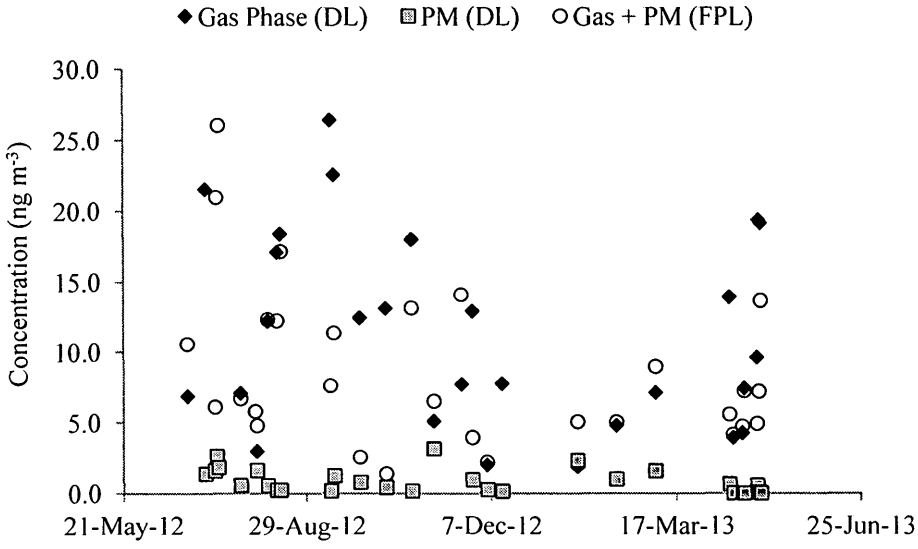

Figure 4.10. Gas phase and PM concentration measurements from DL and gas phase + PM concentration measurements from the FPL placed in parallel for 4-nitrophenol of all ambient samples.

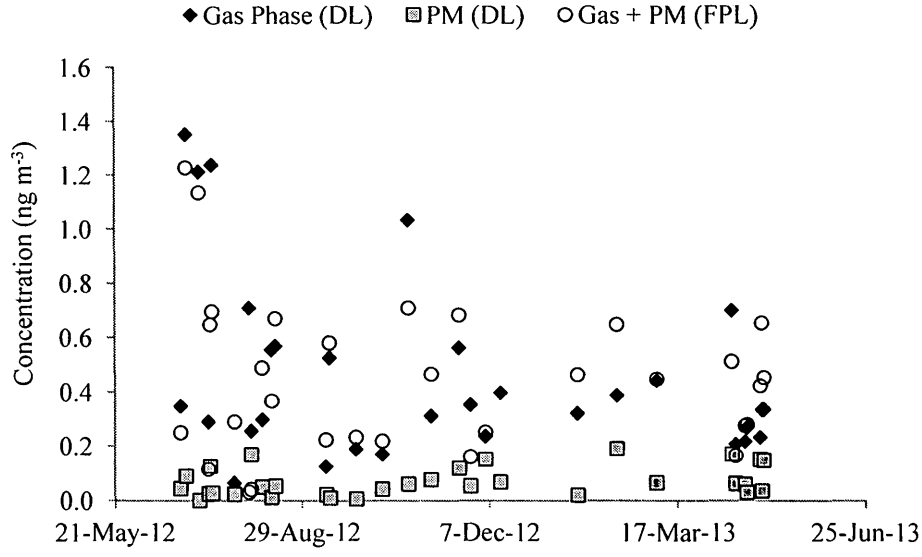

Figure 4.11. Gas phase and PM concentration measurements from DL and gas phase + PM concentration measurements from the FPL placed in parallel for 3-methyl-4-nitrophenol of all ambient samples.

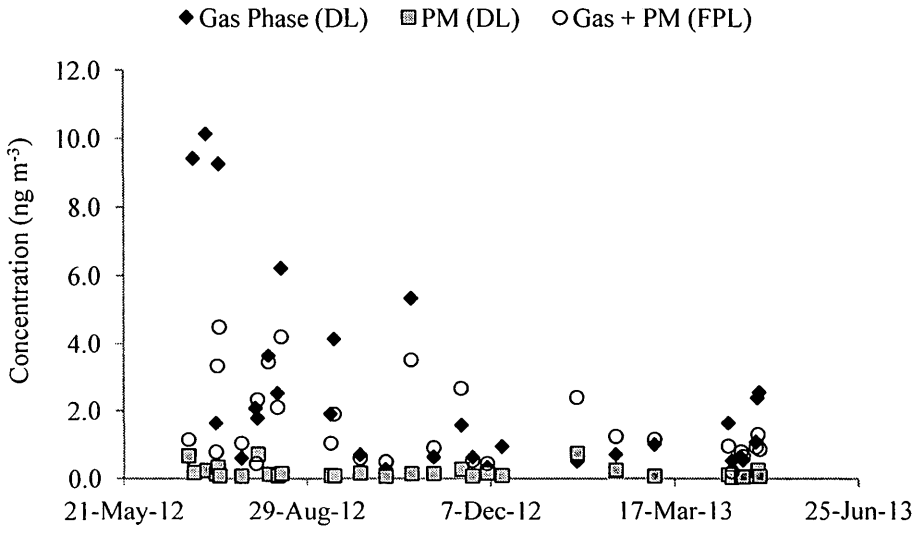

Figure 4.12. Gas phase and PM concentration measurements from DL and gas phase + PM concentration measurements from the FPL placed in parallel for 2-methyl-4-nitrophenol of all ambient samples.

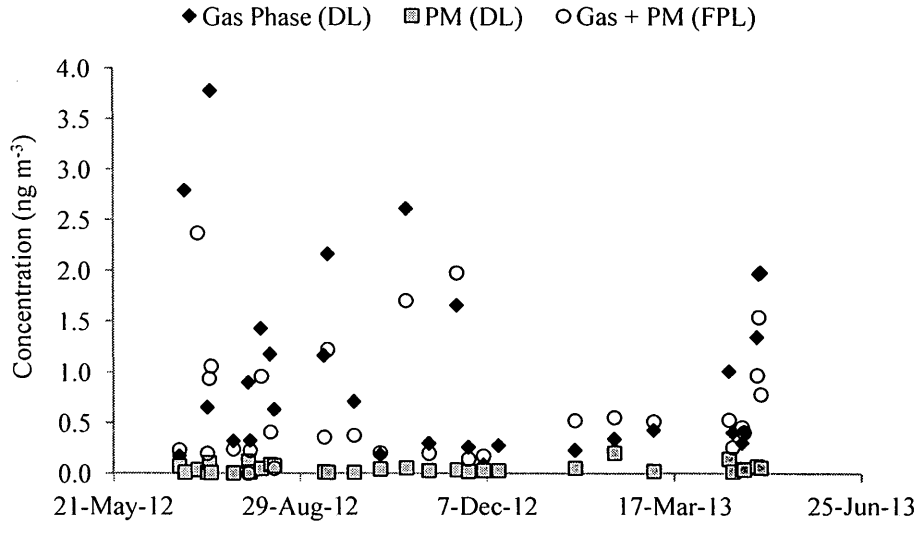

Figure 4.13. Gas phase and PM concentration measurements from DL and gas phase + PM concentration measurements from the FPL placed in parallel for 2,6-dimethyl-4-nitrophenol of all ambient samples.

Table 4.10. Mean of concentration measurements and error of the mean values measured by the IOGAPS denuder line and the IOGAPS filter pack line with and without outlier removal. The number of data points used in outlier corrected means and non-outlier corrected means are also shown. In the cases where no data points were identified as outliers, only one mean value is shown.

Compound	IOGAPS Denuder Line						IOGAPS Filter Pack Line	
	Gas Phase		PM		Total (Gas Phase + PM)		Total (Gas Phase + PM)	
	Concentration ($ng\ m^{-3}$)	Number of Data Points	Concentration ($ng\ m^{-3}$)	Number of Data Points	Concentration ($ng\ m^{-3}$)	Number of Data Points	Concentration ($ng\ m^{-3}$)	Number of Data Points
4-me-2-NP	0.77 ± 0.18	32	0.12 ± 0.03	32	0.89 ± 0.19	30	0.36 ± 0.07	31
			0.08 ± 0.07	30	0.96 ± 0.21	28		
4-NP	29.71 ± 11.12	32	1.51 ± 0.43	32	31.22 ± 11.21	32	10.75 ± 9.75	32
	11.32 ± 1.34	27	0.86 ± 0.16	29	12.36 ± 1.39	25	8.69 ± 1.05	30
3-me-4-NP	0.54 ± 0.10	32	0.08 ± 0.01	32	0.62 ± 0.10	32	0.44 ± 0.28	32
	0.46 ± 0.06	31	0.07 ± 0.01	31	0.52 ± 0.06	30	0.45 ± 0.05	31
2-me-4-NP	3.01 ± 0.74	32	0.22 ± 0.04	32	3.23 ± 0.75	32	2.18 ± 0.47	31
	2.45 ± 0.50	31	0.18 ± 0.03	31	2.64 ± 0.51	31	1.59 ± 0.23	29
2,6-dime-4-NP	1.33 ± 0.29	32	0.06 ± 0.09	32	1.39 ± 0.29	32	0.72 ± 0.13	32
	1.00 ± 0.17	30	0.05 ± 0.01	31	1.01 ± 0.17	29	0.65 ± 0.11	30

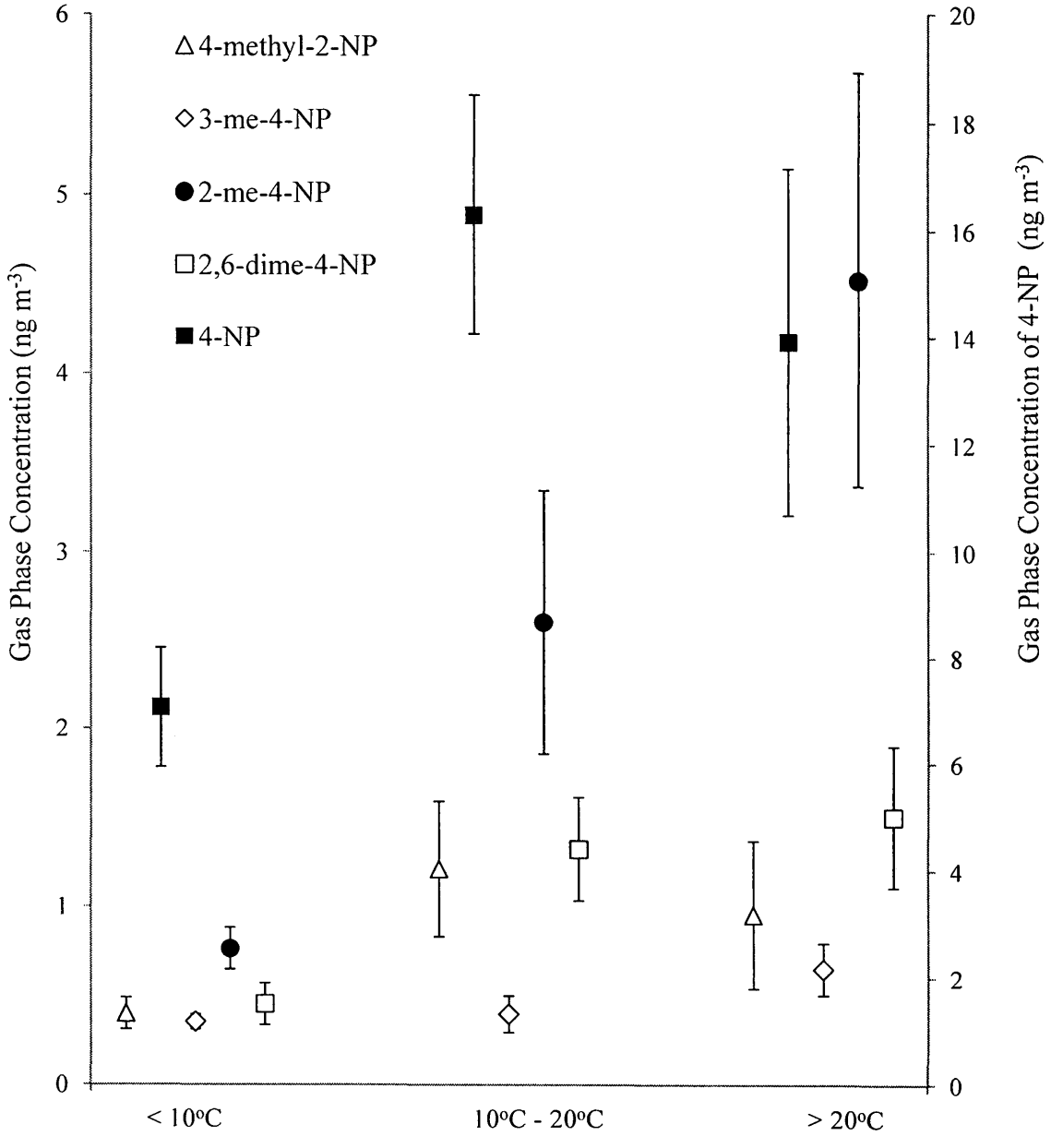

Figure 4.14. Average gas phase concentrations of nitrophenols as a function of temperature. Error bars represent the error of the mean. Number of sampling dates in each bin are: < 10°C (13); 10°C – 20°C (8); > 20°C (11).

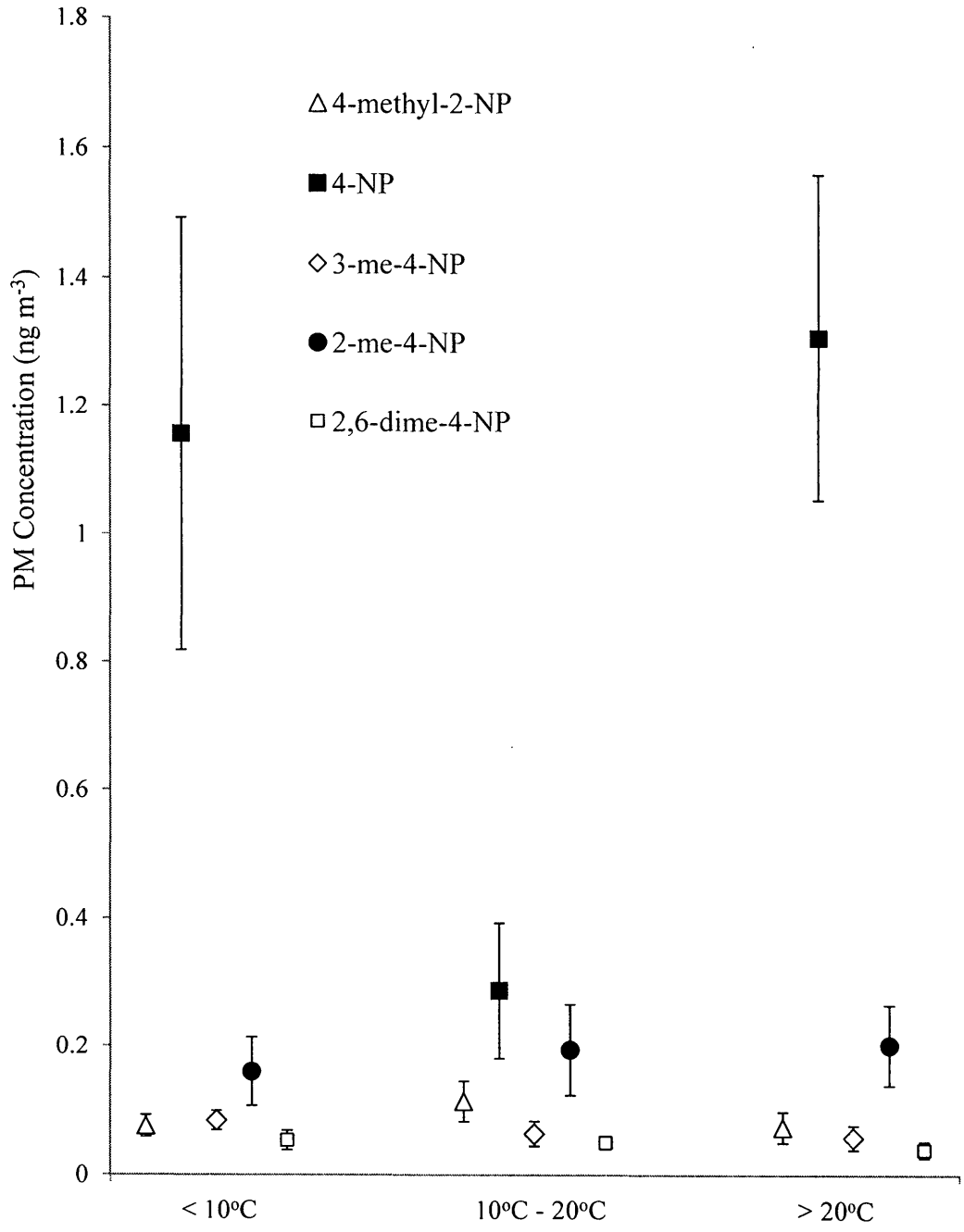

Figure 4.15. Average PM concentrations of nitrophenols as a function of temperature. Error bars represent the error of the mean. Number of sampling dates in each bin are: < 10°C (13); 10°C – 20°C (8); > 20°C (11).

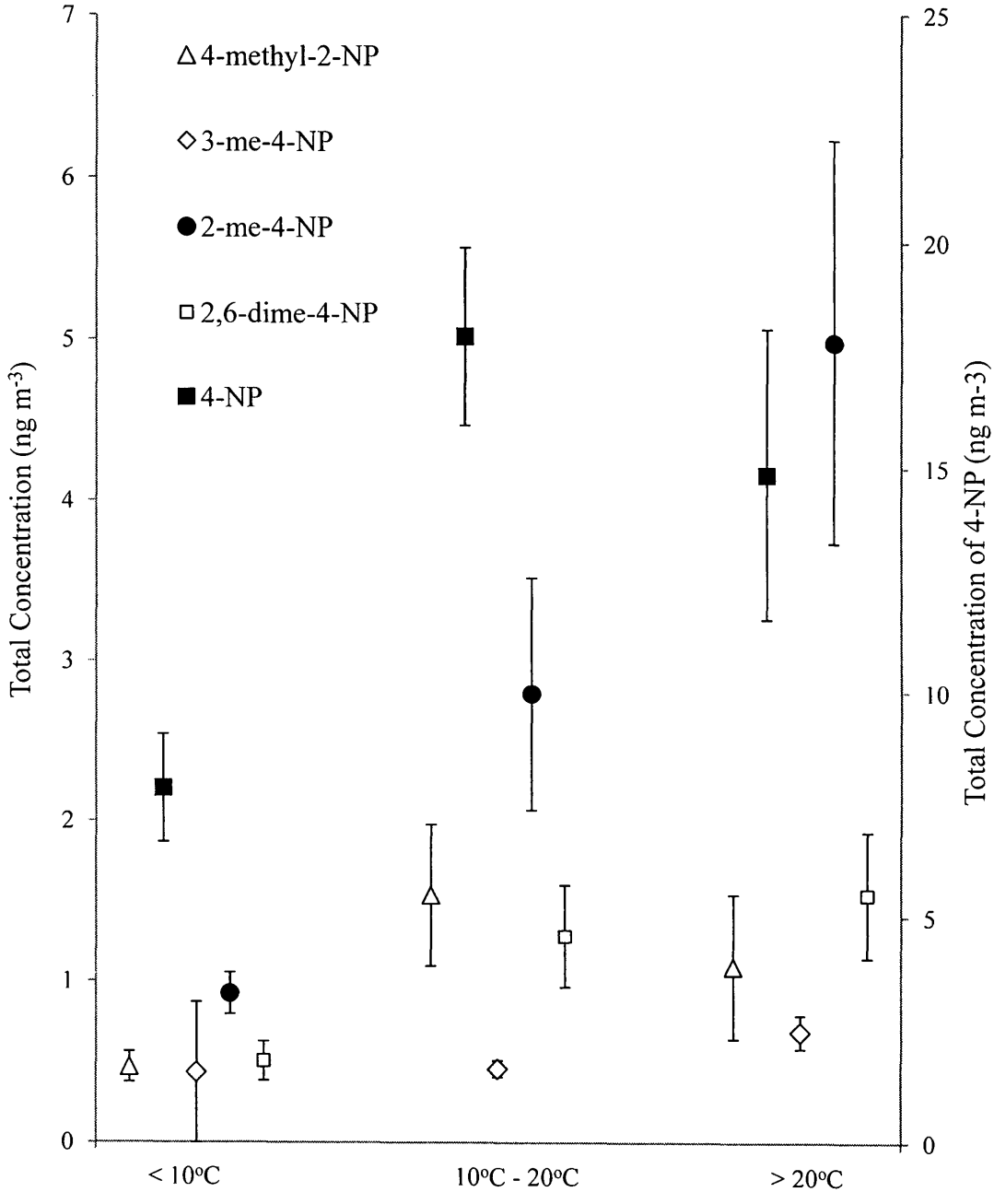

Figure 4.16. Average total (gas phase + PM) phase concentrations of nitrophenols as a function of temperature. Error bars represent the error of the mean. Number of sampling dates in each bin are: < 10°C (13); 10°C – 20°C (8); > 20°C (11).

Table 4.11. Mean of concentration measurements and error of the mean values measured by the IOGAPS denuder line (DL) and the IOGAPS filter pack line (FPL) from three consecutive day and night measurements.

Compound	Time	DL			FPL
		Gas Phase Concentration ($ng\ m^{-3}$)	PM Concentration ($ng\ m^{-3}$)	Total (Gas Phase + PM) Concentration ($ng\ m^{-3}$)	Total (Gas Phase + PM) Concentration ($ng\ m^{-3}$)
4-me-2-NP	Day	1.95 ± 0.16	0.21 ± 0.10	2.16 ± 0.26	0.83 ± 0.30
	Night	1.25 ± 0.49	0.12 ± 0.07	1.36 ± 0.55	0.84 ± 0.26
4-NP	Day	20.26 ± 3.50	0.42 ± 0.33	20.67 ± 3.02	6.48 ± 1.71
	Night	11.83 ± 3.02	< LDL	11.83 ± 0.64	10.64 ± 5.09
3-me-4-NP	Day	0.33 ± 0.09	0.09 ± 0.02	0.43 ± 0.10	0.57 ± 0.15
	Night	0.27 ± 0.03	0.06 ± 0.02	0.32 ± 0.05	0.45 ± 0.01
2-me-4-NP	Day	3.02 ± 1.00	0.21 ± 0.15	3.23 ± 1.05	1.00 ± 0.13
	Night	1.00 ± 0.24	0.08 ± 0.02	1.08 ± 0.23	1.06 ± 0.24
2,6-dime-4-NP	Day	2.82 ± 0.61	0.38 ± 0.33	3.20 ± 0.76	1.23 ± 0.28
	Night	0.71 ± 0.24	0.07 ± 0.01	0.79 ± 0.25	0.97 ± 0.30

4.3.3. Partitioning of Nitrophenols

The fraction of nitrophenols in the gas phase was determined using concentration values obtained from separate gas phase and PM measurements made by the IOGAPS denuder line. The partitioning values shown in Fig. 4.17 are calculated as percentage in the gas phase over total (gas phase + PM).

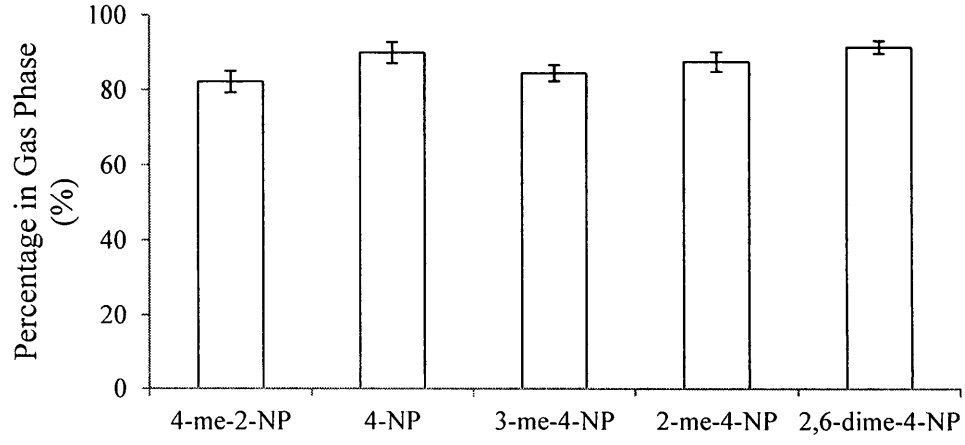

Figure 4.17. Percentage of nitrophenols found in the gas phase determined by IOGAPS denuder line values. Error bars represent the error of the mean.

The partitioning values for the day and night sampling conducted in this work, also calculated as percentage in the gas phase over total (gas phase + PM), are shown in Fig. 4.18.

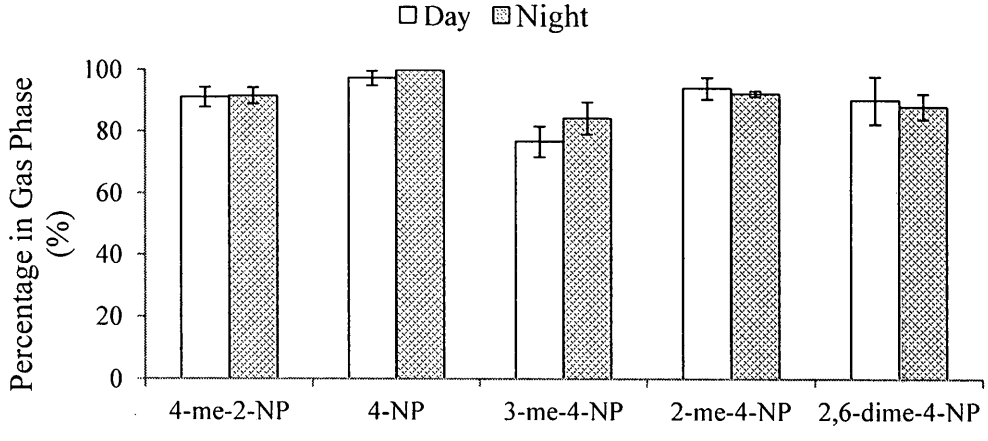

Figure 4.18. Percentage of nitrophenols found in the gas phase determined on three day/night sampling dates from IOGAPS denuder line samples. Error bars represent the error of the mean.

Partitioning coefficients shown in Table. 4.12 were found using the concentration values obtained from separated gas phase and PM measurements made by the IOGAPS denuder line and daily $PM_{2.5}$ measurements obtained from Ontario Ministry of the Environment's North Toronto site, which are listed in Appendix B. The partitioning coefficients were calculated using Eq. 2.3.

Table 4.12. Average partitioning coefficients and error of the mean determined for the nitrophenol compounds.

Compound	Partitioning Coefficient (m^3 μg^{-1})
4-me-2-NP	0.045
4-NP	0.022
3-me-4-NP	0.034
2-me-4-NP	0.044
2,6-dime-4-NP	0.022

5. Discussion

5.1. Blank Values and Atmospheric Detection Limits for Filters and Denuders

Blank values and atmospheric detection limits for both uncoated and XAD-4™ coated 47 mm filters as well as XAD-4™ coated denuders which were determined in this work, are presented in Table 5.1 along with blank values and atmospheric detection limits determined for 20.32 x 25.40 cm uncoated and XAD-4™ coated filters (extracted by Busca (2010), Hassani (private communication) and Saccon (private communication)). The blank values determined in this work were found to be in the sub nanogram range for all of the target nitrophenols but 4-nitrophenol for the filter samples and in the low nanogram region for all target nitrophenols for the denuder samples. 4-nitrophenol was consistently found to have the largest blank value of the target nitrophenols for all filter and denuder samples but it is also the most abundant of the five target nitrophenols in the atmosphere, therefore this compound is least effected by the blank value.

Table 5.1. Blank masses atmospheric detection limits for uncoated and XAD-4™ coated 20.32 x 25.40 cm and 47 mm filters as well as for XAD-4™ coated denuders. Average atmospheric concentrations determined from ambient measurements by the IOGAPS system are also listed.

Compound	Blank Mass (ng)					Atmospheric Detection Limit (ng m^{-3})					Atmospheric Concentration (ng m^{-3})		
	20.32 x 25.40 cm Filters[a]		47 mm Filters		Denuder	20.32 x 25.40 cm Filters[a]		47 mm Filters		Denuder	Gas Phase	PM	Total (Gas Phase + PM)
	Uncoated	SIF	Uncoated	SIF		Uncoated	SIF	Uncoated	SIF				
4-me-2-NP	1.6	3.4	0.1	0.4	4.0	0.003	0.003	0.01	0.04	0.16	0.77	0.08	0.89
4-NP	24.7	9.4	9.2	6.1	15.8	0.06	0.01	1.39	0.63	1.16	11.32	0.86	12.36
3-me-4-NP	1.9	2.8	0.2	0.4	2.6	0.004	0.003	0.01	0.04	0.28	0.46	0.07	0.52
2-me-4-NP	2.2	2.5	0.2	0.6	7.0	0.01	0.001	0.01	0.10	0.26	2.45	0.18	2.64
2,6-dime-4-NP	0.4	1.8	0.1	0.2	1.7	0.001	0.002	0.003	0.02	0.09	1.00	0.05	1.01

[a] 20.32 x 25.40 cm uncoated filter data was based on five measurements made by Saccon et al. (2013) while 20.32 x 25.40 cm SIF data was based on nine measurements made by Saccon et al. (2013) and Hassani (private communication)

Three blank values were determined every time a new batch of SIFs were coated to see if there were any large blank values attributed to that batch which would make the newly coated group of filters considered unusable for ambient studies. As well, blank values were determined in January 2013 for three SIFs coated in August 2012 to see if there was any significant blank value due to filter storage. The blank values obtained from all these standard tests showed that the blank values remained consistent (within 10 %) throughout this work and that there was no increase in blank values due to filter storage.

The blank values reported in Table 5.1 for XAD-4^{TM} coated denuders are total values which include contributions from the denuder itself, from denuder transportation to and from the sampling site and from the sampling lines of the IOGAPS system. Blank values from the denuder itself were determined using denuder extractions performed no more than seven days prior to an ambient sampling. The specific blank values determined for each sampling were subtracted from the masses found on the denuder after that sampling. The average blank values determined from denuder transportation and the IOGAPS sampling lines by tests performed in this work were also subtracted from masses found on the denuder after that sampling. The specific contributions, as percentage of average mass found on a 24 hour denuder sample (Table 5.2), for each of these three blank sources are shown in Fig. 5.1.

Table 5.2. Averages and standard deviations of masses of nitrophenols found on 24 hour denuder samples.

Compound	Average Mass on 24 hour Denuder Sample (ng)
4-me-2-NP	24.1 + 4.3
4-NP	231.7 + 32.0
3-me-4-NP	12.5 + 1.6
2-me-4-NP	69.3 + 13.5
2,6-dime-4-NP	23.5 ± 3.9

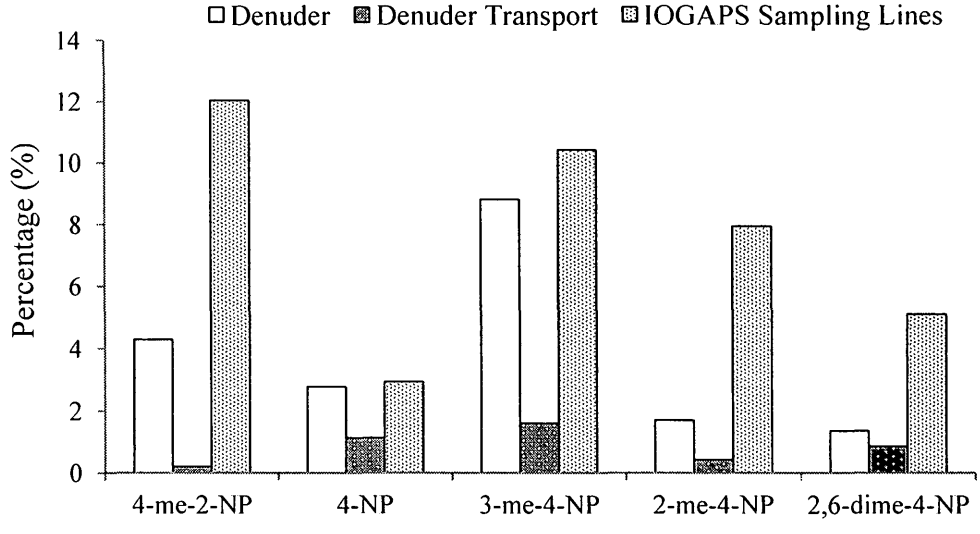

Figure 5.1. Blank masses from denuder, denuder transport and IOGAPS sampling lines as percentages of the average masses found on 24 hour denuder samples. Blank values shown for denuder transport and IOGAPS sampling lines were each blank corrected with the respective blank values determined prior to the sampling and testing of that denuder.

The largest contribution of the denuder blank for all target nitrophenols was found to be coming from the IOGAPS sampling lines, with approximately 10 % of the typical

24 hour denuder sample mass attributed to this source. The contribution to the blank value from the denuder itself was found on average to be approximately 5 % of the typical 24 hour denuder sample mass for all target compounds, while the contribution from denuder transportation was found to be the least significant of the three blank value sources, approximately 2 % for all target compounds. When looking at the blank values as functions of typical masses observed on 24 hour denuder samples, it was found that 4-methyl-2-nitrophenol and 3-methyl-4-nitrophenol were the target compound which showed the largest overall influence from blank values. These two target nitrophenols are always found to be the least atmospherically abundant of the five target nitrophenols, therefore their observation may be biased due to larger relative measurement as well as blank uncertainties which are associated with small concentration measurements.

The atmospheric detection limits determined by this method for both uncoated and XAD-4^{TM} coated 47 mm filters and XAD-4^{TM} coated denuders are compared to atmospheric detection limits determined for both uncoated and XAD-4^{TM} coated 20.32 x 25.40 cm filters (Saccon et al., 2013; Hassani, private communication) as well as average atmospheric concentrations determined from this work were shown in Table 5.1. The atmospheric detection limits were found to be much smaller than the measured atmospheric concentrations in all cases except for 4-nitrophenol in the uncoated 47 mm filters. 4-nitrophenol was also the only compound found in this work to have atmospheric detection limits which were higher than the atmospheric detection limit of 0.28 ng m^{-3} for phenols determined by Cecinato et al. (2005). These higher atmospheric detection limits for 4-nitrophenol are attributed to the higher blank values and variability which were

obtained for this compound. The atmospheric detection limits of the 47 mm filters, both uncoated and XAD-4™ coated, were found to always be larger than the atmospheric detection limit measurements for the 20.32 x 25.40 cm filters due to the fact that determining these atmospheric detection limits involved dividing the detection limit values by the 24 hour sample volumes collected by the sampling methods used for each filter, and the 20.32 x 25.40 cm filters have sampling volumes which are almost 60 times larger than the sampling volumes for the 47 mm filters (1627.2 m^3 versus 24 m^3). The consequence of this is that blank values become more problematic when dealing with low volume sampling methods as opposed to high volume sampling methods. Therefore, in some cases, the detection limits for these low volume filters do exceed the ambient concentrations, especially for PM concentrations of 4-nitrophenol. As seen in Table 5.1, the atmospheric detection limits for XAD-4™ coated denuders were found to be orders of magnitude larger than the atmospheric detection limits determined for any of the filter samples with limits in the sub to low nanogram region for all target nitrophenols. One of the reasons this detection limit and corresponding blank value were thought to be so high was due to the fact that there were so many contributing blank factors.

5.2. Artifact of 2-methyl-4-nitrophenol

While beginning to conduct ambient testing, one of the target compounds, 2-methyl-4-nitrophenol, began appearing in much higher than normal quantities (several hundreds of nanograms compared to the average mass found on 24 hour denuder samples

from Table 5.2 which was 69.3 $\pm$ 13.5 ng). Due to the randomized pattern observed from this contamination, as seen in an ambient denuder sample illustrated in Fig. 4.1, a number of tests were conducted (Table 4.4) which determined two sources for this artifact. Taking apart and cleaning the rotary evaporator was found to reduce the mass of the artifact to approximately half of the original mass found on controlled tests. This cleaning of the rotary evaporator in addition to eliminating one of the internal standards typically used in high volume sampling of nitrophenol studies (Busca, 2010; Saccon et al., 2013), 2-methylphenol, solved the problem of the high 2-methyl-4-nitrophenol blanks observed in this work. The purpose of this internal standard in the high volume nitrophenol studies performed by Busca (2010) and Saccon et al. (2013) was to monitor possible losses attributing from the extraction procedure for a target compound studied in these works, 4-methylphenol. The recovery of the 2-methylphenol standard compared to the recoveries of the other two internal standards, all relative to the spiked mass of the internal standards, were found to be much lower in high volume XAD-4^{TM} coated SIF testing shown in Table 5.3, which was thought to be a consequence of the high volatility of 2-methylphenol. Therefore the results obtained for 4-methylphenol in these works were always considered highly uncertain and therefore no quantitative evaluation of these measurements was attempted for the low volume samples.

Table 5.3. Average and standard deviations for recovery of internal standards from high volume XAD-4™ blank filter extractions where blank filters were spiked with approximately 4 μg of each internal standard (Saccon et al., 2013).

Compound	Average Recovery (%)
2-mePh	13 ± 8
2-me-3-NP	59 ± 11
2-me-5-NP	61 ± 12

5.3. Modification to Extraction Procedure

Since the IOGAPS system samples low volumes, the detailed extraction procedure used to clean up the high volume filter samples was simplified for the low volume filter and denuder samples. Figure 4.4 depicts a chromatogram from one denuder sample which was extracted without the HPLC and SPE clean-up steps used in the high volume filter samples and analyzed in scanning mode with the GC-MS. The chromatogram shows good separation of the target compounds, internal standards and volumetric standards from each other and from other species present in the sample, therefore low volume ambient filter and denuder samples obtained in this work were extracted without the HPLC and SPE clean-up steps.

5.4. Method Validation

5.4.1 Denuder Extraction Efficiency

Prior to ambient sampling, the selection of an appropriate extraction solvent to use to extract the nitrophenols from the denuder was required. An appropriate extraction solvent is thought to be one which satisfies two important requirements: the extraction solvent must provide good recovery of the compounds being collected and as well, must not remove large amounts of the sorbent which is coated on the denuder. After testing the six extraction solvents which were listed in Table 3.3, the results, as shown in Table 4.5, illustrated that the only extraction solvent solution that had high recoveries of the internal standards (90 % extracted after two extractions) was acetonitrile. This result was not surprising since acetonitrile has been previously employed for nitrophenol analysis with XAD-4^{TM} coated quartz fibre filter samples (Busca, 2010; Saccon et al., 2013). Due to the fact that acetonitrile was not found to be used as an extraction solvent in literature with XAD-4^{TM} coated denuders, the effect acetonitrile had on removal of the sorbent from the denuder was required to be tested since if the solvent was removing large amounts of the sorbent, denuder recoating would be required much more frequently. From the results of this test, as shown in Table 4.6, it was observed that the amount of sorbent removed from the denuder by acetonitrile was minimal and the trend that was observed was that less and less sorbent was removed with increasing denuder extractions. It was established that after 15 consecutive denuder extractions with acetonitrile, only

2.5 % of the coating was removed. Since denuders are typically recoated after 5 % of the coating is removed (Lane, private communication), it was concluded that newly coated denuders could be easily extracted 40 times before recoating was deemed necessary.

Once the appropriate extraction solvent was chosen, another important aspect that needed to be studied was how many extractions were required to effectively extract all, or almost all, of the target nitrophenols from the sorbent coated denuder. The results from seven ambient tests which looked at the amounts of the nitrophenols extracted from each of ten consecutive denuder extractions, found in Table 4.7, concluded that approximately 100% of the target nitrophenols are extracted from the denuder within four extractions, with the first, second, third and fourth extractions containing approximately 87 %, 9 %, 3 % and 1 % of the nitrophenols, respectively. For ambient sampling performed after these tests were conducted (from September 2012 and onwards), denuders were extracted a total of four times after sampling. The first three extracts were combined and analyzed as one sample and the fourth extraction was analyzed separately in order for this extraction to also be used as a blank value for the next ambient sampling performed with this denuder as long as the sampling was within seven days from the date of this extraction.

5.4.2. Collection Efficiency of Denuder

Using the formulas presented in Section 2.4.2, the theoretical trapping efficiency, or C/C_o, of the denuder used in this work was calculated for each annulus as shown in Table 5.4. This C/C_o value represents the fraction of the target compounds which exit the denuder compared to the fraction which enters the denuder, therefore a smaller C/C_o value translates to a more efficient denuder. From the calculated values, annulus G was found to theoretically be the least efficient at collecting the target nitrophenols, but this annulus should still collect 99.997 %, 99.42 % and 99.40 % of the target nitrophenols, methyl nitrophenols and dimethyl nitrophenols, respectively.

Table 5.4. Physical dimensions and calculated Reynolds number and trapping efficiency (C/C_o) for each of the denuder annuli.

Annulus	Inside Diameter (cm)	Outside Diameter (cm)	Annular Width (cm)	Flow[a] ($cm^3\ s^{-1}$)	N_{Re}	C/C_o (NP)[b]	C/C_o (meNP)[c]	C/C_o (dimeNP)[d]
A	0.6	0.8	0.10	7.6	45.7	2.5E-16	7.4E-03	1.0E-02
B	1.0	1.2	0.10	12.0	45.7	2.5E-16	4.1E-02	5.0E-02
C	1.4	1.6	0.12	16.4	45.7	2.6E-16	9.1E-02	1.1E-01
D	2.0	2.2	0.10	22.9	45.7	2.6E-16	1.7E-01	1.9E-01
E	2.6	2.8	0.10	29.4	45.7	2.5E-16	2.4E-01	2.6E-01
F	3.2	3.4	0.10	36.0	45.7	2.5E-16	3.0E-01	3.2E-01
G	3.6	4.1	0.14	105.0	114.2	2.7E-03	5.8E-01	6.0E-01
H	4.4	4.6	0.12	49.0	45.7	2.6E-16	3.9E-01	4.1E-01

[a] the sum of the individual flows is the total flow of 278.33 $cm^3\ s^{-1}$ (16.7 L min^{-1})
[b] NP : nitrophenols
[c] meNP : methyl nitrophenols
[d] dimeNP : dimethyl nitrophenols

The trapping efficiency of the denuder was estimated from three experimental tests, which are shown in Table 4.8, they were found to be approximately 98 $\pm$ 7 % effective on average for all target nitrophenols. For individual compounds the experimentally determined 97 % or better efficiency is within their 3% uncertainty, compatible with the calculated efficiency. Nevertheless, the finding that all measured efficiencies are slightly below the theoretical values suggests that the efficiency of the denuders is slightly lower than theoretically predicted. However, the average difference is less than 3 % and therefore much lower than the uncertainty of the measurements. Therefore no corrections for denuder efficiency were made. The method used here to determine trapping efficiency, provided estimations on denuder efficiency. To truly test the efficiency of the denuder, it would be affective to run an airstream with known concentrations of target compound through the two denuders and then the amount collected could be converted to a true measurement of efficiency. This experiment was not attempted in this work due to the difficulty of instrumentation set up and the fear of introducing large contaminants into the denuder.

5.4.3. Collection Efficiency of Low Volume Filters

A summary of the collection efficiency results for the low volume filter tests where three uncoated quartz filters and three XAD-4^{TM} coated SIFs were placed in series conducted in this work is found in Table 5.5.

Table 5.5. Average percentages and standard deviations of target nitrophenols found on each of three filters for both tests where three uncoated filters were placed in series and where three XAD-4™ coated SIFs were placed in series.

Compound	Uncoated Quartz Filters			XAD-4™ coated SIFs		
	% on 1st Filter	% on 2nd Filter	% on 3rd Filter	% on 1st Filter	% on 2nd Filter	% on 3rd Filter
4-me-2-NP	87 ± 3	13 ± 2	0.5 ± 0.5	86 ± 4	14 ± 3	0.1 ± 0.003
4-NP	91 ± 1	8 ± 1	0.5 ± 1	96 ± 2	4 ± 3	0.2 ± 0.1
3-me-4-NP	88 ± 7	10 ± 3	2 ± 1	89 ± 4	9 ± 3	2 ± 1.8
2-me-4-NP	90 ± 6	10 ± 2	1 ± 0.5	97 ± 1	3 ± 2	0.4 ± 0.7
2,6-dime-4-NP	91 ± 4	8 ± 1	2 ± 2	89 ± 6	10 ± 6	0.4 ± 0.8
AVERAGE	89 ± 10	10 ± 5	1 ± 3	91 ± 8	8 ± 11	1 ± 2

The results from low volume filter tests where three uncoated quartz filters were placed in series (Fig 4.5), showed that the collection efficiency for low volume uncoated quartz filters was found to be found to be 89 % on average for the five target compounds, with an average of 10 % and 1% of the total mass collected found on the second and third filters placed in series, respectively. Collection efficiencies of suspended particles on filters regardless of particle size or flow rate was found in literature to be 99 % (Chow, 1995), therefore inefficient particle collection by the quartz filter is unlikely causing this discrepancy. The masses found on the second and third uncoated quartz filters were thought to possibly be attributed to the inefficient collection of very small particles (low nanometer range).

Results obtained for low volume filter tests where three XAD-4™ coated SIFs were placed in series, as seen in Fig. 4.6, showed that the collection efficiency of these

filters was found to be found to be 91 % on average for the five target compounds, with an average of 8 % and 1 % of the total mass collected found on the second and third XAD-4^{TM} coated SIFs placed in series, respectively. This collection efficiency was coincidentally found to be almost identical to the low volume uncoated filter efficiency and was thought to be likely due to incomplete adsorption of gas phase species onto to XAD-4^{TM} resin or possible desorption of the gas phase from the resin.

Since the results from the filter in series tests determined that on average for the target nitrophenols particle losses of 11 % were expected for uncoated quartz filters and 9 % gas phase losses due to inefficient collection by the XAD-4^{TM} resin were expected for the SIFs, it was effective to look at results from the percentages found on ambient filters to see if this is what was actually being observed in ambient filter measurements. The results from Figs. 4.7 and 4.8 which presented the percentages found on the three filters placed in the denuder line filter pack and the filter pack line filter pack respectively have been summarized in Table 5.6.

Table 5.6. Average percentages and standard deviations of target nitrophenols found on each of three filters (quartz in position A (Q-A) which is upstream of SIF in position B (X-B) which is upstream of SIF in position C (X-C)) for 32 denuder line (DL) filter pack samples and 31 filter pack line (FPL) filter pack samples.

Compound	DL			FPL		
	% on Q-A	% on X-B	% on X-C	% on Q-A	% on X-B	% on X-C
4-me-2-NP	38 ± 34	52 ± 32	10 ± 17	30 ± 29	56 ± 28	14 ± 21
4-NP	13 ± 22	68 ± 24	19 ± 20	11 ± 17	88 ± 35	9 ± 13
3-me-4-NP	52 ± 32	38 ± 28	9 ± 15	26 ± 28	80 ± 58	12 ± 24
2-me-4-NP	54 ± 30	36 ± 23	10 ± 10	18 ± 19	75 ± 20	9 ± 11
2,6-dime-4-NP	50 ± 34	38 ± 29	11 ± 18	14 ± 15	81 ± 16	14 ± 35
AVERAGE	42 ± 34	46 ± 30	12 ± 16	20 ± 23	76 ± 36	12 ± 22

The denuder line filter pack is always placed downstream of a denuder therefore this filter pack should only be collecting the remaining PM fraction in the airstream. The results showed that for the target compounds 3-methyl-4-nitrophenol, 2-methyl-4-nitrophenol and 2,6-dimethyl-4-nitrophenol, the majority of the total mass found in the filter pack was located on the uncoated quartz filter which is what was to be expected. The other two target compounds, 4-methyl-2-nitrophenol and 4-nitrophenol, had the majority of the total mass found to be located on the XAD-4™ coated SIF downstream on the uncoated quartz. The discrepancy observed with 4-nitrophenol is most likely attributed to the large blank value observed with uncoated quartz filters which would cause the PM mass found on the filter to become significantly reduced after blank correction. The discrepancy observed with the 4-methyl-2-nitrophenol compound may be

due to the combination of the fact that this target nitrophenol had the most inefficient collection on uncoated quartz filters (Table 5.5) and the fact that it is one of the least abundant of the nitrophenols. The amount of the target nitrophenols found on the XAD-4^{TM} coated SIFs placed downstream of the uncoated quartz was quite significant, with 46 % of the total mass on average for all target compounds found on this filter. This larger than anticipated percentage observed on the XAD-4^{TM} coated SIF downstream of the uncoated quartz fibre was a contribution from a few different factors. The first contributing factor to this higher mass being collected on the XAD-4^{TM} coated SIF is due to higher losses of VOC from PM due to the depleted gas phase caused by the denuder. This change in equilibrium observed in the airstream which exits the denuder causes a shift from PM to gas phase in the remaining fraction to attempt to offset this equilibrium imbalance, and this now "gas phase" fraction would be primarily collected on the XAD-4^{TM} coated SIF downstream of the uncoated quartz filter. Another significant contribution to the large percentage of nitrophenols collected by the XAD-4^{TM} coated SIF downstream of the uncoated quartz filter in the denuder pack is the approximately 3% breakthrough of gas phase observed for the denuder. Table 5.7 evaluated the impact this determined denuder inefficiency has on denuder line PM phase measurement, since the target nitrophenols are found to be so much more prevalent in the gas phase. On average it was found that for the target nitrophenols, 3 % of the gas phase equated to approximately 40 % of the average PM mass observed in low volume ambient samples. Since the XAD-4^{TM} coated SIF downstream of the uncoated quartz filter collected on average approximately 46 % of the total mass of nitrophenols collected by the denuder

line filter pack, much of this percentage is likely attributed to the denuder inefficiency. The small percentage observed on the second XAD-4™ coated SIF downstream of the uncoated quartz filter and first XAD-4™ coated SIF may be attributed to the inefficient collection capacity observed by XAD-4™ coated SIFs in this work, but the large uncertainty of these values do not justify firm conclusions.

Table 5.7. Evaluation of impact of denuder inefficiency on denuder line filter pack PM measurement.

Compound	3 % of Average Gas Phase Mass Determined by 24 hour Denuder Samples (ng)	Average PM Mass from 24 hour DL Filter Samples (ng)	Percentage Impact on PM (%)	Percentage of Mass Found on X-B in DL (%)
4-me-2-NP	0.66	2.22	30	52 ± 32
4-NP	9.05	22.42	40	68 ± 24
3-me-4-NP	0.37	1.78	21	38 ± 28
2-me-4-NP	1.99	4.68	43	36 ± 23
2,6-dime-4-NP	0.81	1.26	64	38 ± 29
AVERAGE	N/A	N/A	40 ± 16	46 ± 30

The performance of the filters contained in the filter line filter pack (Fig. 4.8 and Table 5.6) was also analyzed in this work. Since this filter pack was not sampled downstream of a denuder and the target nitrophenols are found to be predominantly (80 - 90 % on average for all target nitrophenols) in the gas phase, it was expected that the majority of the mass would be found on the second filter in the filter pack, a

XAD-4™ coated SIF. The results observed matched these expectations with approximately 80 % of the target nitrophenols on average found on the first XAD-4™ coated SIF downstream of the uncoated quartz filter. For all target nitrophenols on average there was approximately 20 % of the total mass found on the uncoated quartz filter in the filter pack line filter pack, which was virtually identical to the average percentage expected to be in the particle phase from studies both in this work and in work performed by Busca (2010). There was a small percentage of the total mass found on the second XAD-4™ coated SIF downstream of both the uncoated quartz filter and XAD-4™ coated SIF in the filter pack which gave percentages quite similar to the percentages obtained from XAD-4™ coated SIF efficiency tests.

Comparison of the low volume filter efficiency determined by this work to high volume filter efficiency work performed by Saccon et al. (2013) for both uncoated quartz filters and XAD-4™ coated SIFs are illustrated in Figs. 5.2 and 5.3, respectively.

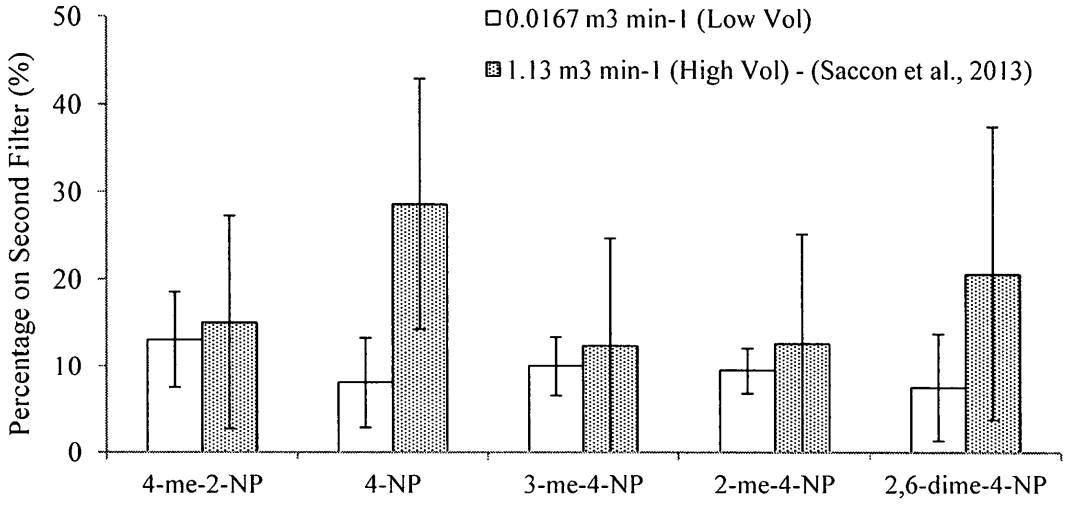

Figure 5.2. Comparison of the efficiency of second uncoated quartz fibre filters when collected in series conducted in this work for low volume filters with work by Saccon (private communication) using high volume air samplers.

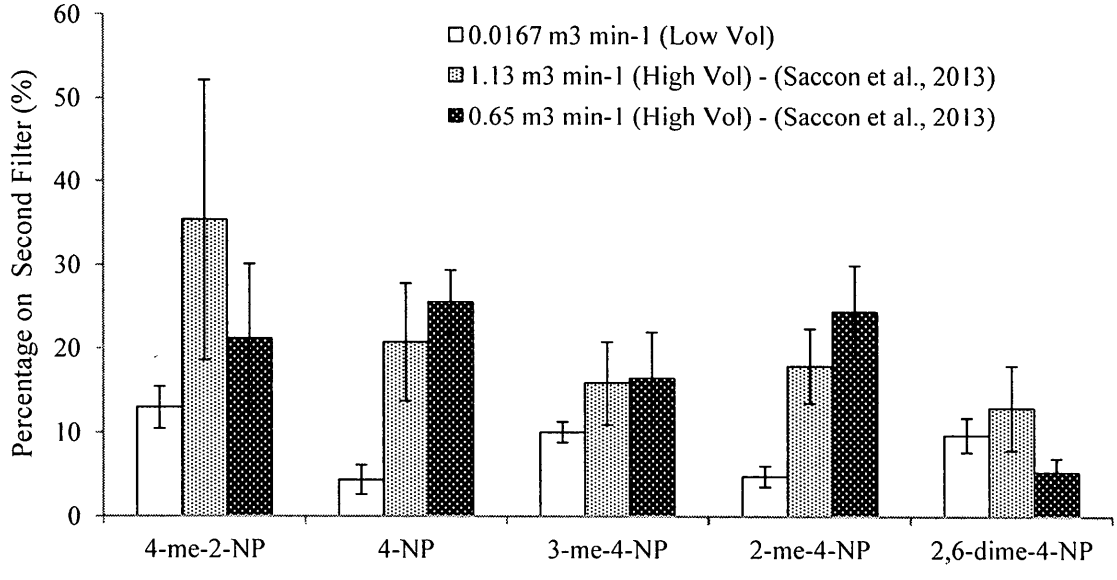

Figure 5.3. Comparison of the efficiency of second XAD-4^{TM} coated SIFs when collected in series conducted in this work for low volume filters with work by Saccon (private communication) using high volume air samplers.

The collection efficiency for both uncoated high volume quartz filters and XAD-4^{TM} coated high volume filters showed slightly more uncertainty in measurements compared to the low volume filter efficiency results. The high volume uncoated quartz filter efficiency was found to be 82 % on average for the target nitrophenols, while the high volume XAD-4^{TM} coated filter efficiency was found to be 81 % on average for the target nitrophenols. Due to the fact that the filter material for both the low volume and high volume uncoated quartz filters and XAD-4^{TM} coated SIFs were identical and both types of SIFs were coated with the same sorbent following similar procedures, the discrepancy observed was thought to only be attributed to differences in the face velocities of the two sampling methods. The high volume filters, which are sampled at a flow rate of 1.13 m^3 min^{-1}, have a calculated face velocity of 40 cm^2 s^{-1} whereas the low volume filters, which are sampled at a flow rate of 0.0167 m^3 min^{-1}, have a calculated face velocity of 20 cm^2 s^{-1}. Face velocity is the velocity of air at the face of the filter just prior to when the air enters the filters and it has been well established that the collection efficiency of filters tends to decrease with increasing face velocity (McDow and Huntzicker, 1990). Therefore the inefficiency of the high volume filters compared to the low volume filters that was observed in Figs. 5.2 and 5.3 was to be expected. However, Saccon et al. (2013) also performed in series XAD-4^{TM} coated SIF tests where the flow was altered to 0.65 m^3 min^{-1} in order to decrease the face velocity to 20 cm^2 s^{-1}, as is also shown in Fig. 5.3. The results from this test were quite surprising since the filter efficiency was found to be approximately 19 % on average for the target nitrophenols which was more comparable to the results from other high volume filter

tests than the low volume filter test which used the same face velocity. Therefore face velocity could not be causing this discrepancy in filter efficiency observed. The only other major difference between the two methods was that the low volume filter tests were performed in a commercial filter pack holder which is designed for in series filter sampling, whereas the high volume filters were sampled in series with a piece of metal mesh placed between the two filters. The sampling set-up for the high volume filters is most likely preventing the filter holder from fastening the edge of the top filter to the sampler, therefore there could be some air which bypasses the first filter completely and travels around the sides of the first filter allowing species to then become captured on the second filter, which may likely be causing the increased amount of mass observed on the secondary filter.

5.5. Ambient Measurements

In this work, 32 ambient samples were collected using the IOGAPS instrumentation between June 25, 2012 and May 2, 2013. High volume filter samples were collected in parallel on 25 of these dates, nine of which were uncoated quartz filters samples, five of which were XAD-4^{TM} coated SIF samples, ten of which were samples where an uncoated quartz filter was run in parallel to an XAD-4^{TM} coated SIF on two high volume air samplers and finally, one of which was two XAD-4^{TM} coated SIFs run in parallel on two high volume air samplers. The average daily temperatures calculated for each of the 24 hour sampling periods from hourly measurements taken by Environment

Canada at the North York, Toronto site, are shown in Fig. 5.4. This plot illustrates that there was good seasonal and temporal variability obtained with the data set. As observed, there is a lack of data acquired at temperatures below 0°C due to denuder cracking when denuders were used for sampling at these low temperatures.

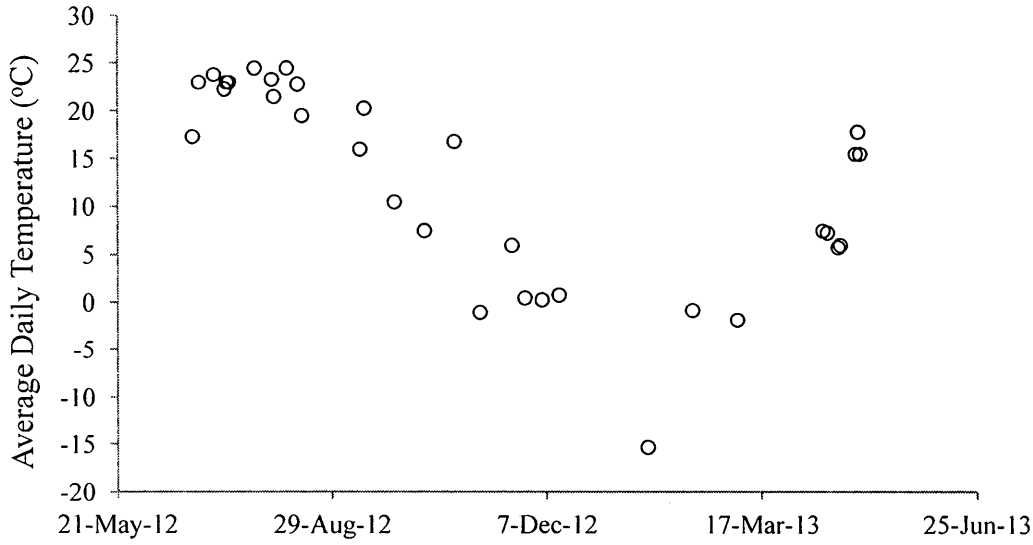

Figure 5.4. Average daily temperatures for dates on which ambient samples were collected.

5.5.1. Ambient Concentration Results

Ambient concentration results for gas phase, PM and total (gas phase + PM) obtained from the IOGAPS instrumentation are summarized in Table 4.10. Three of the five target nitrophenols, 4-nitrophenol, 2-methyl-4-nitrophenol and 2,6-dimethyl-4-nitrophenol, were detected in almost all of the 32 ambient samplings. The most abundant nitrophenol of the five target nitrophenols was 4-nitrophenol with average

gas and PM concentrations found to be 11.32 ng m^{-3} and 0.86 ng m^{-3}, respectively. Table 4.10 also showed the concentration results obtained after outlier removal from results of z-tests performed on the data. In most cases, only one or two outliers were found in the 32 total data points for each of the nitrophenols, and removing these outliers significantly improved error of the mean values. The nitrophenol with the largest number of outlier points determined was 4-nitrophenol, with 15 % of the data points found to be outliers. Since this percentage was lower than 20 % the results from 4-nitrophenol were still considered, but much uncertainty still lies in the results for this compound.

The ambient concentration measurements made by the IOGAPS system for gas phase and total (gas phase + PM) concentrations (Figs. 4.14 and 4.16) were found to generally increase with increasing temperature for most nitrophenols, which is similar to previous nitrophenol results obtained from high volume XAD-4^{TM} coated SIF samples at York University (Busca, 2010; Saccon, private communication). PM concentrations (Fig. 4.15) were found to not vary as much with temperature, but this is most likely a result of the average PM concentrations being so low (less than 0.2 ng m^{-3} for all nitrophenols other than 4-nitrophenol) that it is almost impossible to see any significant variations.

The average daytime and nighttime concentration values from day and night sampling conducted with the IOGAPS system over the course of three consecutive days in the Spring of 2013 which were presented in Table 4.11, showed that for all target nitrophenols, concentrations were found to be slightly higher in the daytime. The

significance of the difference of daytime and nighttime concentrations varied compound to compound, but in most cases, differences were found to be quite small. It was expected that daytime concentrations would be significantly higher since the formation of these nitrophenols by photooxidation of their precursors is almost completely driven by daytime chemistry. Also the daytime measurements made in this work (7:00 am to 7:00 pm) almost completely contained rush hour traffic hours therefore these events should increase the production of nitrophenol precursors therefore leading to increased concentrations of these secondary species. The very slight differences in day/night concentrations observed may be a consequence of traffic emission levels in afternoon rush hour bleeding through into the nighttime measurement. If there are very minimal loss processes expected for nitrophenols, these concentrations are expected to remain relatively consistent throughout a 24 hour period. As well the differences between daytime and nighttime average temperatures on the three days on which sampling occurred were found were found to be relatively small (2.6 ^{o}C on April 30th, 4.6 ^{o}C on May 1st and 5.0 ^{o}C on May 2), therefore significant differences due to temperature were not expected.

5.5.2. Comparison of Ambient Results from Different Sampling Lines

The comparison of concentration measurements determined from ambient samples for the three different lines sampled in parallel is a good way to determine how valid the results from the IOGAPS system were. Table 5.8 presents the outlier corrected

averages, standard deviations and error of the mean values for the ratios of total (gas phase + PM) concentrations from combinations of the three lines sampled, denuder line (sum of denuder + three filters in filter pack), filter pack line (sum of three filters in filter pack) and high volume filter line (determined solely from a single XAD-4^{TM} coated SIF).

Table 5.8. Averages and error of the mean values for total (gas phase + PM) concentration measurement ratios from the denuder line (DL), filter pack line (FPL) and high volume line (Hi-Vol). Error of the mean values are listed in parenthesis.

Compound	$\frac{Total\ Concentration\ (FPL)}{Total\ Concentration\ (DL)}$		$\frac{Total\ Concentration\ (Hi-Vol)}{Total\ Concentration\ (FPL)}$		$\frac{Total\ Concentration\ (Hi-Vol)}{Total\ Concentration\ (DL)}$	
	Ratio	Number of Samples	Ratio	Number of Samples	Ratio	Number of Samples
4-me-2-NP	0.82 ± 1.24 (0.24)	27	0.83 ± 0.82 (0.26)	10	0.97 ± 1.28 (0.43)	9
4-NP	0.72 ± 0.33 (0.07)	23	0.65 ± 0.42 (0.11)	14	0.40 ± 0.42 (0.11)	15
3-me-4-NP	1.01 ± 0.60 (0.11)	29	0.90 ± 0.78 (0.21)	14	1.02 ± 1.08 (0.27)	16
2-me-4-NP	0.89 ± 0.41 (0.08)	27	0.85 ± 0.67 (0.17)	15	0.71 ± 0.42 (0.11)	16
2,6-dime-4-NP	0.73 ± 0.42 (0.08)	26	1.04 ± 1.01 (0.26)	15	0.90 ± 1.12 (0.28)	16

Although the average ratios comparing the outlier corrected total concentration measurements from the three lines look relatively reasonable, large uncertainties due to the scattering of the data are present in almost every single measurement. Significantly fewer (approximately 50 %) high volume total concentration measurements were

performed in this work compared to low volume measurements due to the fact that there were no high volume XAD-4^{TM} coated SIFs available for sampling at the start of this work due to a malfunction with the planetary ball mill used for grinding the resin. Even though the sampling set is not completely consistent and has somewhat high uncertainty, some general comments can be made about the results obtained.

When analyzing the data comparing the total concentrations determined from the sum of the three filters in the filter pack line to total concentration determined from one high volume XAD-4^{TM} coated SIF, the results showed that there were larger total concentration values (approximately 15 %) determined from the filter pack line. This discrepancy observed is most likely attributed to the 15 – 20 % losses due to filter inefficiency, which have been determined from high volume SIF efficiency tests (Saccon et al., 2013). The inefficiency of the low volume filters is compensated for in the filter pack line since a second XAD-4^{TM} coated SIF is placed downstream of the first XAD-4^{TM} coated SIF to collect any possible breakthrough, so only small breakthrough losses (approximately 1% on average determined from a calculation for two filters in series based on the efficiency of one filter) are expected from the filter pack line total concentration measurement. Therefore, taking this sampling efficiency difference into account, the results obtained from these two techniques are within the expected range.

Similar ratios were observed when looking at the comparison of the high volume total concentrations to the denuder line total concentrations. Since the high volume filters results presented in Table 5.8 were not corrected for the inefficiency of high volume

SIFs, there is approximately a 10 % - 15 % loss than is unaccounted for. Once the inefficiency of the high volume SIFs is taken into account, the results obtained for the two lines become statistically similar for all compounds but 4-nitrophenol, whose difference may be attributed to the large low volume filter blank values associated with this compound.

When comparing the total concentration determined from the sum of the three filters in the filter pack line to the total concentration determined from the denuder and filters in the filters pack of the denuder line, the ratio differences observed compound to compound were found to not be highly significant (not more than three times the error of the mean less than one) except in the case of 4-nitrophenol. On average, however, all target nitrophenols except 3-methyl-4-nitrophenol, were found to have larger concentrations from the denuder line measurement which suggests that there may be a systematic bias from the denuder line.

The average PM concentrations obtained when the three lines were sampled in parallel are shown in Fig. 5.5. Two values for the denuder line are presented; one showing the PM concentration measurement determined only using the uncoated quartz filter in the filter pack (QA) and the other showing the PM concentration determined using the sum of the uncoated quartz filter and the two downstream XAD-4^{TM} coated SIFs (QA + XB + XC) which collect any breakthrough. When comparing the high volume filter line (uncoated quartz filter only) to the filter pack line (uncoated quartz filter only) both of which were not corrected for collection inefficiency, the results

showed the that these two lines were the most similar, with an average ratio of 1.32 determined for the five target nitrophenols. The PM concentration ratios determined from the denuder line (QA) in comparison to the filter pack line (uncoated quartz filter only), were found to be 0.53 on average for all five target nitrophenols. The fact that the single quartz filter gives significantly lower values compared to the other two sampling lines reiterates the fact that the depletion of the gas phase by the denuder in the denuder line indeed shifts the equilibrium of the remaining air stream, causing lower amounts of PM to be collected on the initial uncoated quartz filter. When comparing the ratio of the concentrations determined from the denuder line (QA + XB + XC) and the filter pack line (uncoated quartz filter only), the results showed that on average the denuder line gave values which were almost double the values determined from the filter pack line (1.78 on average for the five target nitrophenols). Since the denuder line values here are in theory corrected for filter inefficiency, this explains a certain portion of the higher values obtained. Also, due to the inefficiency of the denuder, there is some gas phase breakthrough which would be found in the results from the SIFs placed downstream of the uncoated quartz filter. Though this breakthrough was calculated to be only 3 %, as was shown in Table 5.7, this small breakthrough equates to approximately 40 % of the PM fraction on average, and therefore explains the rest of the discrepancy observed between these two lines.

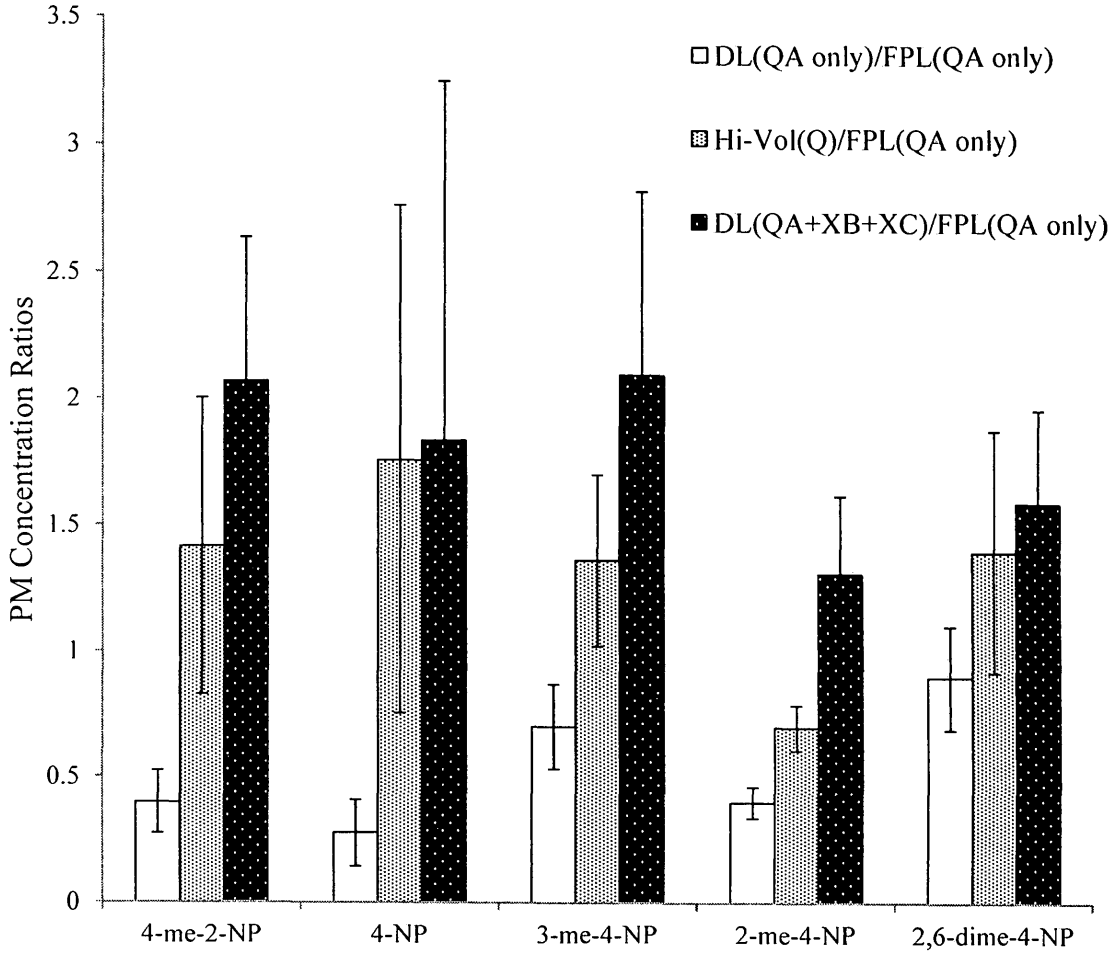

Figure 5.5. Average outlier corrected PM concentration ratios of denuder line (DL) and high volume (Hi-Vol) filter line samples compared to filter pack line (FPL) samples. DL(QA+XB+XC) contains the sum of the three filters in the filter pack to determine PM concentrations. Data was obtained from dates where all three lines were sampled in parallel. Single quartz filter samples were not corrected for filter inefficiency. Error bars are error of the mean values. Number of data points for each compound were as follows: 4-me-2-NP (8); 4-NP (4); 3-me-4-NP (11); 2-me-4-NP (14) and 2,6-dime-4-NP (12).

5.5.3. Comparison of Ambient Concentration Results to Other Studies

A summary of total (gas phase + PM) concentration measurements determined in this work from the denuder line, filter pack line and high volume filter line as well as total concentration measurements performed using XAD-4^{TM} coated SIFs with both high volume sampling obtained between February 2011 and August 2012 (Saccon, private communication) and low volume sampling obtained between August 2009 and March 2010 (Busca, 2010) are shown in Table 5.9.

In general, the results obtained in this work from the two IOGAPS system lines (denuder line and filter pack line) as well as the parallel high volume filter samples were found to be well within the same data ranges obtained in previous nitrophenol concentrations measurements made by other members of the Dr. Rudolph's group using high volume filter sampling at York University. The average concentration values obtained in this work were found in almost all cases to be consistently lower which was likely a consequence of significantly different sample set sizes and sampling dates. Since the results were taken over large periods of time over a variety of different years, it is difficult to directly compare the data, since many factors such as temperature, time of day, relative humidity and pollutants such as $PM_{2.5}$ and NO_2 concentrations, as well as many other factors can have significant effects on how ambient measurements can differ.

Table 5.9. Comparison of Total (gas phase + PM) concentrations determined in this work by denuder line (DL) and filter pack line (FPL) to both high volume and low volume SIF work performed. High volume results presented were not corrected for breakthrough.

Compound	Total (Gas Phase + PM) Concentration (ng m^{-3})									
	Low Volume DL[a]		Low Volume FPL[b]		High Volume SIF[c]		High Volume SIF[d]		Low Volume SIF[e]	
	Average	Range	Average	Range	Average	Range	Average	Range	Average	Range
4-me-2-NP	0.96	0.07 – 4.64	0.40	0.05 – 1.57	0.80	0.003 – 2.83	2.78	0.01 – 21.52	3.10	0.20 – 3.10
4-NP	12.36	2.25 – 26.62	8.69	2.25 – 26.62	3.43	0.78 – 7.64	6.88	0.61 – 18.57	10.38	0.30 – 16.00
3-me-4-NP	0.52	0.08 – 1.44	0.45	0.06 – 1.23	0.39	0.11 – 1.47	1.09	0.11 – 4.32	0.88	0.20 – 1.40
2-me-4-NP	2.64	0.33 – 10.37	1.59	0.14 – 4.50	0.91	0.21 – 2.88	3.22	0.19 – 8.51	2.38	0.10 – 6.00
2,6-dime-4-NP	1.01	0.23 – 3.78	0.65	0.03 – 2.369	0.44	0.06 – 1.26	1.06	0.05 – 5.44	1.77	0.10 – 3.40

[a] data based on 32 denuder line samples (this work)
[b] data based on 31 filter pack line samples (this work)
[c] data based on 16 high volume SIF samples (this work; Hassani (private communication))
[d] data based on 27 high volume SIF samples (Saccon, private communication)
[e] data based on 9 low volume SIF samples (Busca, 2010)

Additional comparisons were made between the measurements made in this work and other ambient studies regarding nitrophenols which were found in literature (Table 5.10). Big discrepancies were observed when comparing the separate gas phase and PM concentration measurements made by Nishioka and Lewtas (1992) in Boise, Idaho to concentration measurements found by Cecinato et al. (2005) in Rome, Italy, since the Cecinato study finds all but one of the target nitrophenols to be found predominantly in the PM fraction. The results from Nishioka and Lewtas (1992) are similar to the results found in this work, with the values from this work well within the concentration ranges observed by Nishioka and Lewtas (1992) for all target compounds except for the gas phase measurement of 4-nitrophenol which is found to be significantly higher in this work, most likely due to possible underestimations of denuder blank values. The results from Cecinato et al. (2005) which find almost all of the nitrophenols to be predominantly in PM could be due to larger PM levels or different PM composition in Rome compared to the North American locations. When comparing the total (gas phase + PM) concentrations from this work to work performed by Morville et al. (2004) and Delhomme et al. (2010) at urban, suburban and rural locations in France, the concentrations from this work showed good agreement with the results from both studies with extreme similarities observed with the values obtained at the urban site. From the comparison of the concentration results of nitrophenols from this work and from literature, it is clear that differences in concentration do indeed stem from differences between sampling locations.

Table 5.10. Average ambient nitrophenol concentrations reported in literature and in this work from denuder line values.

Compound	Concentration (ng m^{-3})								
	Nishioka and Lewtas (1992)		Morville et al. (2004)	Cecinato et al. (2005)		Delhomme et al. (2010)	Denuder Line Values (this work)		
	Boise, Idaho (Winter 1986/1987)		France	Rome, Italy (Spring 2003)		France (2002 – 2004)	Toronto, Ontario (June 2012 – May 2013)		
	Gas	PM	Total	Gas	PM	Total	Gas	PM	Total
4-me-2-NP	0.05-1.80	ND	0.58	6.9	2.9	1.6[a], 2.1[b], 2.7[c]	0.8	0.1	1.0
4-NP	<0.04-0.85	1.90-2.70	-	3.9	17.8	-	11.3	0.9	12.4
3-me-4-NP	<0.04-0.54	0.37-0.77	0.69	2.2	7.8	0.4[a], 0.3[b], 0.2[c]	0.5	0.1	0.5
2-me-4-NP	0.06-2.70	0.67-1.20	-	-	-	-	2.5	0.2	2.6
2,6-dime-4-NP	-	-	-	2.0	5.9	-	1.0	0.1	1.0

ND: not detected
-: not found in literature
[a] urban site
[b] suburban site
[c] rural site

5.5.4. Partitioning of Nitrophenols

Since the partitioning of nitrophenols determined from high volume samples showed no vapor pressure dependence (Busca, 2010), it was thought that a denuder-filter based technique would possibly produce different results since the these denuder-filter samples compensate for the sampling artifacts which could be biasing the high volume sample results. The percentage of the target nitrophenols found in the gas phase determined for 32 low volume denuder line samples from this work in comparison to the partitioning results for the percentage of the target nitrophenols found in the gas phase obtained from eight high volume samples conducted by Busca (2010) are shown in Fig. 5.6.

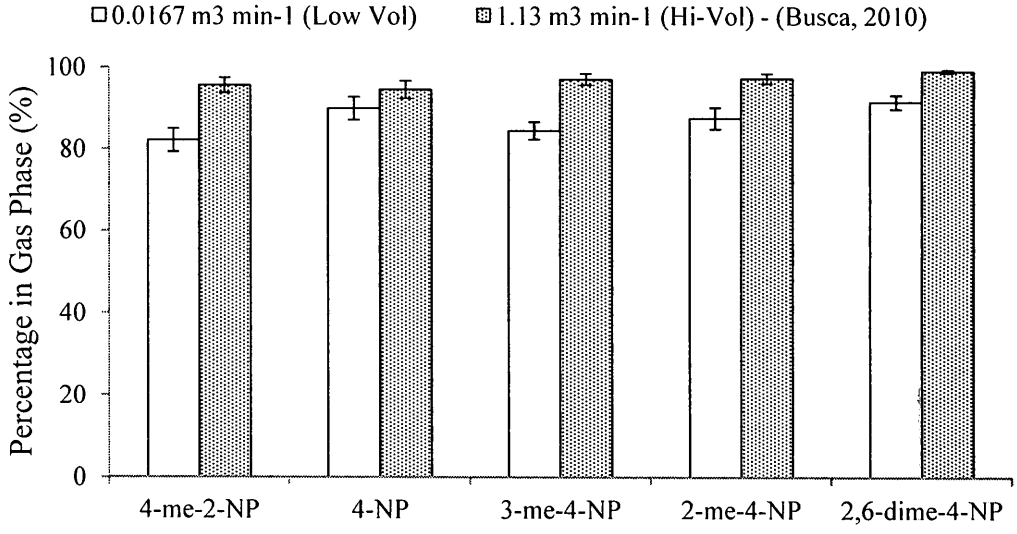

Figure 5.6. Average percentage of target nitrophenols found in the gas phase determined from low volume denuder line samples and from high volume filter parallel filter sampling. The error bars represent the error of the mean values.

The results from the denuder line show that significant fractions of nitrophenols were found to be in the gas phase, much like previous work by Busca (2010). The percentages of the target nitrophenols found in the gas phase from the denuder line measurements were slightly lower, but well above 80 % for all target nitrophenols. This result shows that once again no partitioning dependence on vapor pressure could be found, which is unexpected due to the fact that the range exhibited by the vapor pressures of the target nitrophenols is orders of magnitude (Table 2.1).

The overall average partitioning ratios for target nitrophenols from the three sampling lines employed in this work: denuder line, filter pack line and high volume filter line are shown in Fig. 5.7. While the values are seen to slightly vary, overall all three methods consistently show that all nitrophenols exist predominantly in the gas phase. The largest variability in these partitioning results was observed with the high volume filter line, but these values were not corrected for inefficiency of filter collection and there were approximately 30 % less of the high volume samples used to calculate these averages. Towards the end of this work it became apparent that there was a slight issue in the validity of the accuracy in parallel high volume air sampling both seen in this work, from the one parallel XAD-4^{TM} SIF sampling on April 15, 2013 and from work performed by Hassani (private communication) where XAD-4^{TM} coated SIFs were run in parallel and results were compared. Both studies showed that there were significant differences in the results obtained from the two samplers therefore the high volume

samples obtained may contain errors from the inaccurate flow calibrations of the high volume air samplers, since only one of these samplers is directly calibrated.

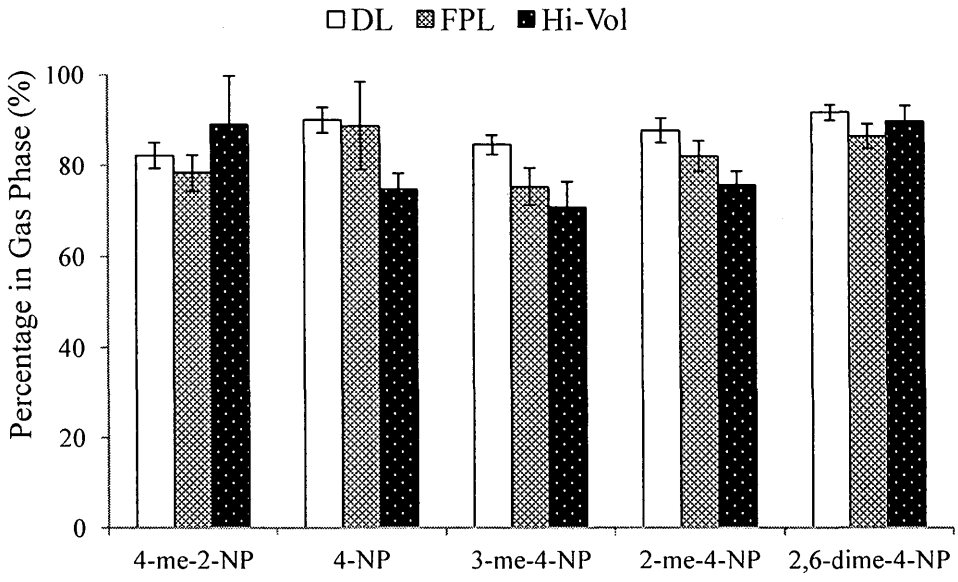

Figure 5.7. Comparison of all partitioning results obtained in this work from 32 denuder line (DL) samples, 31 filter pack line (FPL) samples and ten high volume filter line (Hi-Vol) samples. Error bars represent the error of the mean.

Comparisons were also performed, as illustrated in Fig. 5.8., on partitioning values from nine low volume denuder line samples and nine high volume filter samples which were run in parallel to each other. Once again, these results both showed that the nitrophenols do tend to favor the gas phase, but the lower partitioning values once again observed for the high volume air samplers may likely be attributed to the inaccuracy of the parallel high volume air samplers due to errors from flow calibrations. Another factor

that may be contributing to this difference is the fact that the denuder line results are not affected by sampling artifacts since downstream SIFs account for these artifacts, while the high volume samples may be. Positive artifacts may be occurring which would lead to an overestimation of the PM fraction and therefore a lower partitioning coefficient. This potentially may be the cause of the different findings observed for different substances, since the artifacts may well be compound specific.

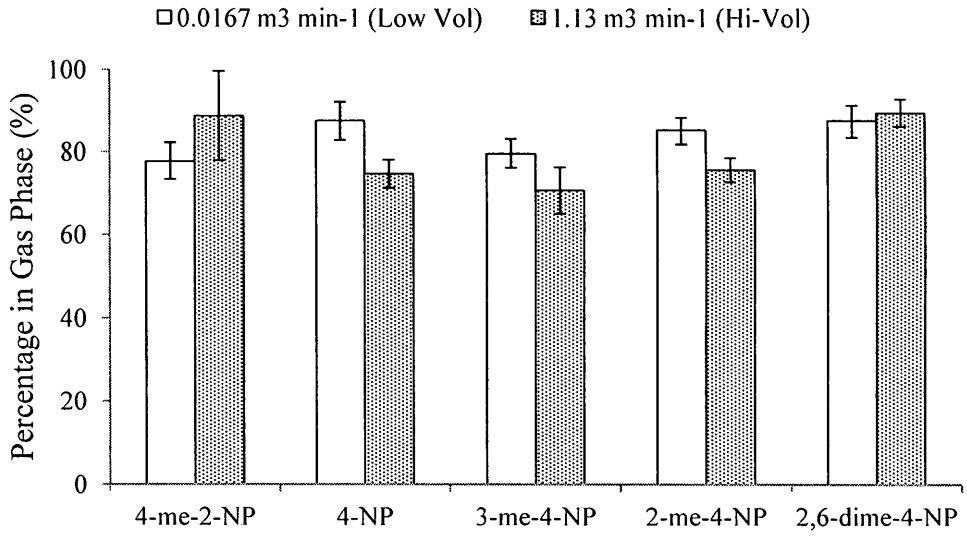

Figure 5.8. Comparison of partitioning results obtained in this work from nine low volume (Low Vol) denuder line samples run in parallel with high volume (Hi-Vol) filter samples. Error bars represent the error of the mean.

Since the partitioning of the target nitrophenols did not show any strong vapor pressure dependence, efforts then moved to determine whether there were any other factors influencing this partitioning. A number of factors were looked at in this work such

as temperature, relative humidity, NO_2 concentrations, $PM_{2.5}$ concentrations and day/night dependences. The only factor that showed a slight dependence with the partitioning for most of the nitrophenols was temperature as in observed in Fig. 5.9. It was found that for the majority of the nitrophenols the partitioning was found to increase with increasing temperature, which was expected since at higher temperatures, equilibrium tends to favor the gas phase.

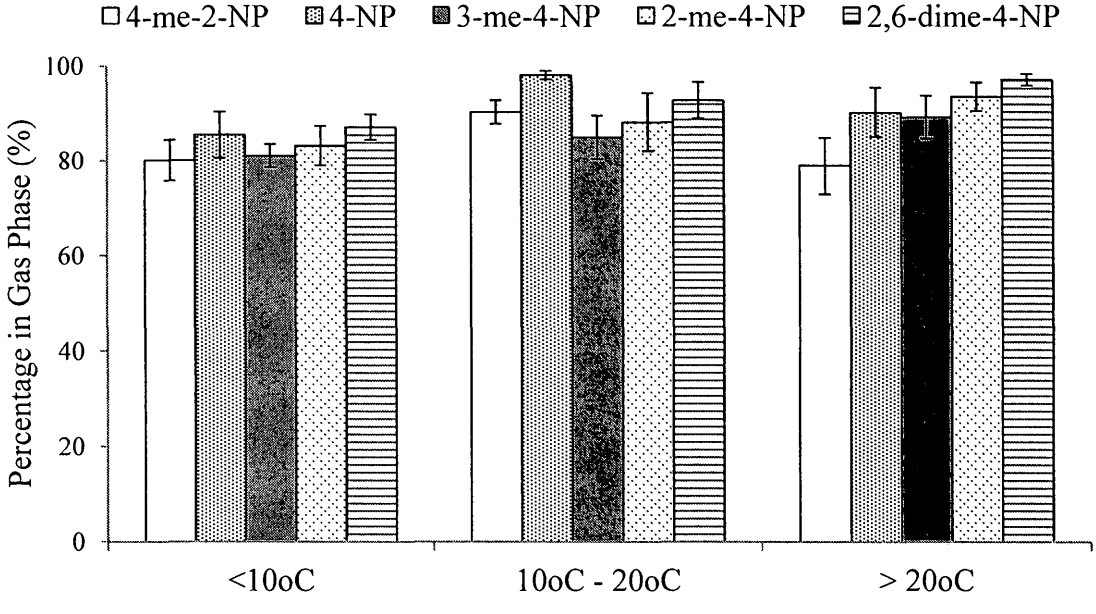

Figure 5.9. Low volume denuder line percentages in the gas phase for all target nitrophenols as functions of temperature. Error bars represent the error of the mean. The number of sampling dates in each bin are as follows: <10°C (13), 10°C-20°C (8), >20°C (11).

The partitioning dependences of these nitrophenols on relative humidity, NO_2 concentrations, $PM_{2.5}$ concentrations and time of day (day/night) are shown in Figs. 5.10 – 5.13. The comparisons of relative humidity, NO_2 concentrations and $PM_{2.5}$ concentrations were most likely limited by the low range of change covered by the measurements. The comparison of day and night partitioning results showed that even though concentrations during day and night were found to be marginally different, the ratio of the nitrophenols in the gas phase and in PM remained relatively consistent.

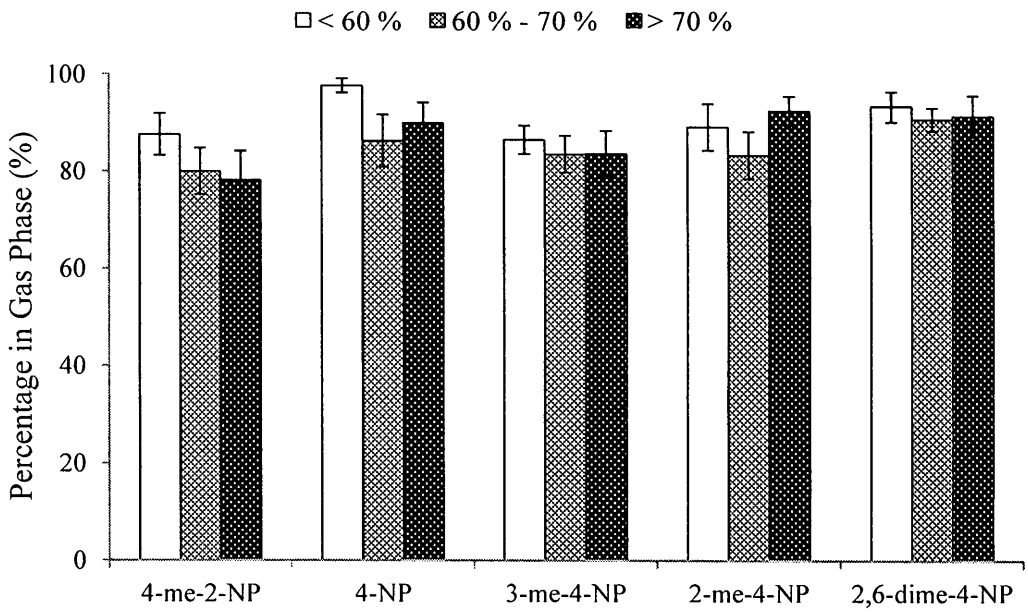

Figure 5.10. Low volume denuder line percentages in the gas phase for all target nitrophenols as functions of relative humidity. Error bars represent the error of the mean. The number of sampling dates in each bin are as follows: <60 % (11), 60 % - 70 % (12), >70 % (9).

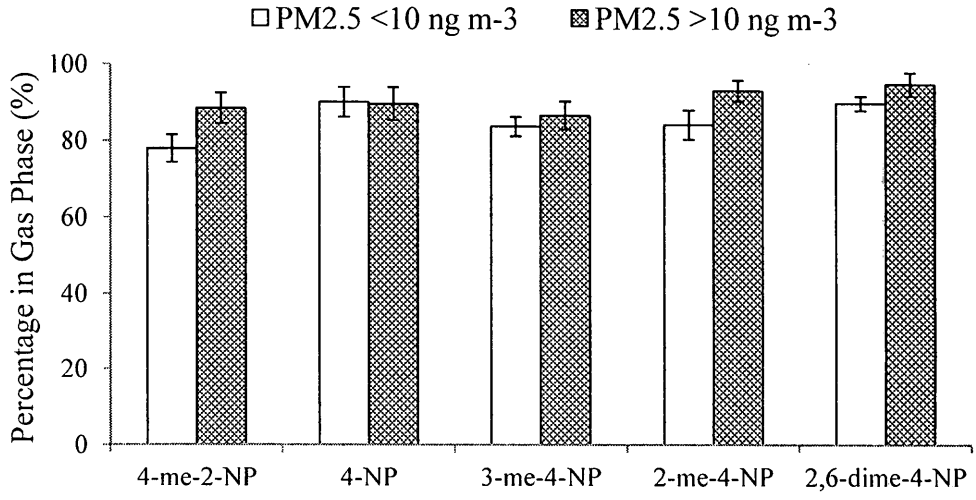

Figure 5.11. Low volume denuder line percentages in the gas phase for all target nitrophenols as functions of concentration of $PM_{2.5}$. Error bars represent the error of the mean. The number of sampling dates in each bin are as follows: <10 ng m^{-3} (18), >10 ng m^{-3} (13).

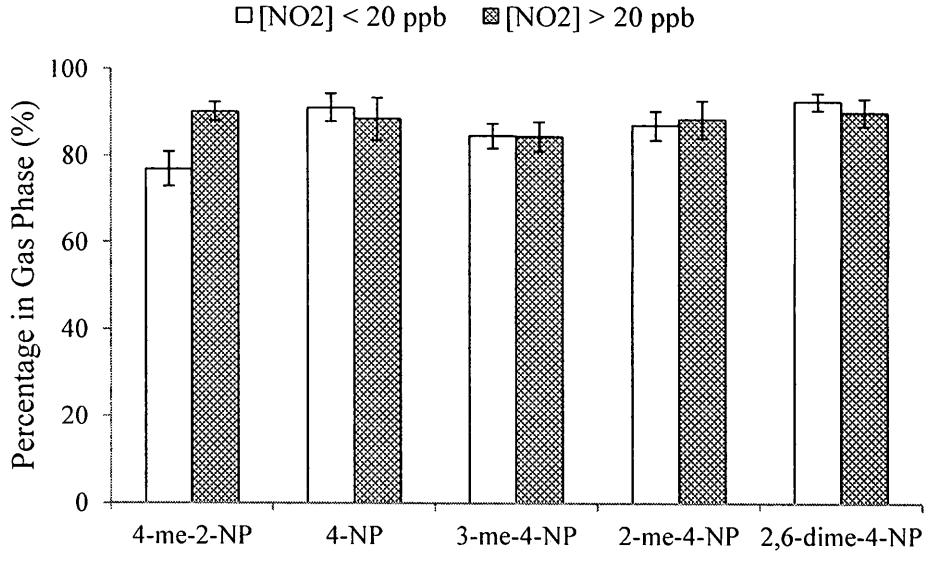

Figure 5.12. Low volume denuder line percentages in the gas phase for all target nitrophenols as functions of concentration of NO_2. Error bars represent the error of the mean. The number of sampling dates in each bin are as follows: <20 ppb (18), >20 ppb (13).

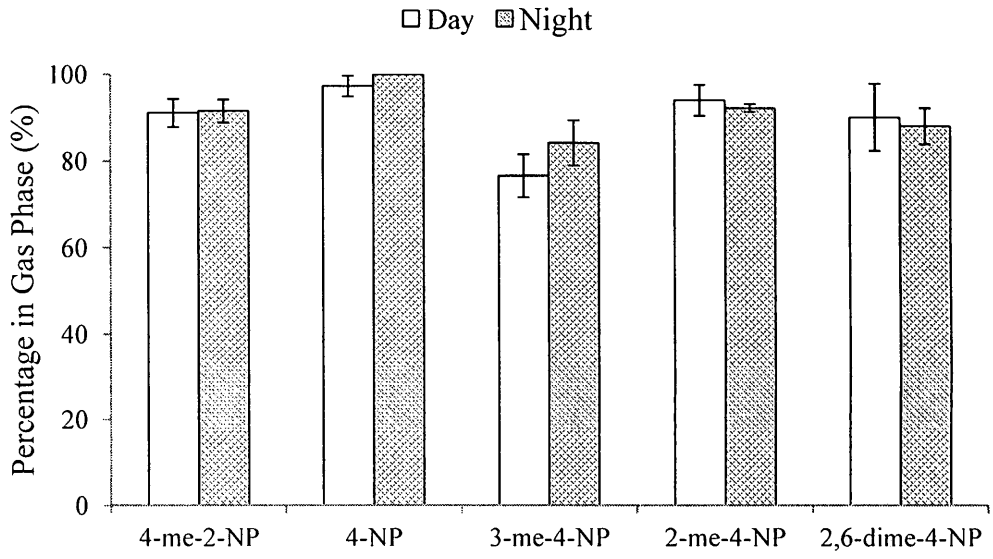

Figure 5.13. Low volume denuder line percentages in the gas phase for all target nitrophenols as functions day and night measurements from three day/night measurements. Error bars represent the error of the mean.

Partitioning coefficients presented in Table 4.12 were calculated in this work using IOGAPS denuder line results. The partitioning coefficients ranged in value from 0.022 m^3 μg^{-1} for 4-nitrophenol and 2,6-dimethyl-4-nitrophenol to 0.045 m^3 μg^{-1} for 4-methyl-2-nitrophenol. The results for the three isomers were very similar with the results for 4-methyl-2-nitrophenol and 2-methyl-4-nitrophenol found to be practically identical. The partitioning coefficients calculated for nine high volume samples and low volume samples run in parallel, as shown in Table 5.11, gave values which were an order of magnitude higher for all target nitrophenols except 2,6-dimethyl-4-nitrophenol which was found to give similar results from both techniques. The variation observed again is most likely due to the fact that the high volume concentration values were significantly

biased by the inaccuracy of parallel sampling on the high volume air samplers. Also, the presence of positive artifacts exhibited by the high volume filters which leads to an overestimation of the PM fraction and therefore a decrease in the partitioning coefficient may indeed be compound specific and therefore could be causing the compound specific variations observed.

Table 5.11. Partitioning coefficients calculated for nine low volume denuder line (DL) samples run in parallel to high volume (Hi-Vol) samples.

Compound	Partitioning Coefficient (m^3 μg^{-1})	
	Low Vol	Hi-Vol
4-me-2-NP	0.078	0.213
4-NP	0.032	0.112
3-me-4-NP	0.055	0.196
2-me-4-NP	0.038	0.117
2,6-dime-4-NP	0.030	0.035

6. Conclusions

In this work, a denuder-filter based technique called the IOGAPS system was developed to allow for the separation, sampling and analysis of nitrophenols in the gas phase and in PM. Atmospheric detection limit values for the XAD-4^{TM} coated denuders and both 47 mm uncoated quartz filters and XAD-4^{TM} coated SIFs employed in the IOGAPS set-up were found to be in the sub to low ng m^{-3} region, which, in all but the case of 4-nitrophenol for uncoated quartz filters, was found to be lower than the average ambient concentrations observed in work performed at York University by various members of Dr. Rudolph's group.

Method modifications regarding target nitrophenol selection and extraction procedures for all filter and denuder samples were performed in this work. The five nitrophenol compounds detected in almost all IOGAPS samples were 3-methyl-4-nitrophenol, 4-nitrophenol, 3-methyl-4-nitrophenol, 2-methyl-4-nitrophenol and 2,6-dimethyl-4-nitrophenol. A phenol species previously included as a target compound in work by Busca (2010) and Saccon (private communication), 4-methylphenol, was eliminated from this study due to the discovery of a contamination of 2-methyl-4-nitrophenol which was observed from the internal standard (2-methylphenol) previously used in high volume filter extractions to correct for the recovery of this target compound species. The extraction procedures for both 47 mm uncoated quartz filters and XAD-4^{TM} coated SIFs in addition to XAD-4^{TM} coated

denuders were significantly simplified from the typical extraction procedure used for high volume filter samples, by eliminating the HPLC and SPE clean-up steps. This shortened procedure still allowed for good separation of the target nitrophenol peaks in low volume filter and denuder samples and therefore was found to be effective in significantly reducing the time required to extract the denuder and six low volume filters which were required for each IOGAPS sample.

Work was performed in this thesis to develop the techniques involving the XAD-4^{TM} coated denuders. Acetonitrile was found to be the most effective extraction solvent for the nitrophenols due to both the high recovery (> 90 %) of internal standards and the ability to do multiple extractions (> 40) with this solvent before recoating of the denuder was necessary. The performance of the denuder itself was extensively monitored in this work, with almost 100 % of the target nitrophenols removed from the sorbent on the denuder within four denuder extractions and the denuder itself was found to be at least 97 % efficient for all target nitrophenols.

In series and parallel filter tests were also conducted in in this work. The breakthrough observed in this low volume sampling was found to be less (11 % in uncoated quartz filters and 9 % in XAD-4^{TM} coated SIFs) than the 15 – 20 % breakthrough typically observed in high volume filter sampling (Saccon et al., 2013). This result was most likely a consequence of the ineffective filter separation technique employed in high volume in series sampling compared to the three-stage filter packs used

for the low volume in series samples, which are specifically designed to separate the filters.

Ambient concentration measurements were conducted over the course of a year, and the results were found to be similar to previously obtained nitrophenol measurements made at York University, with the majority of the target nitrophenols found to be present in the gas phase. The comparisons of the ambient concentration data obtained from the three sampling lines used in this work: low volume denuder line, low volume filter pack line and high volume filter line, showed that all three measurement techniques gave similar results, but since all three measurements exhibited large variability, no conclusions regarding the performance of one technique compared to the others could be performed. Overall, there appeared to be a tendency for the results from the denuder line to give slightly higher gas phase concentration measurements, which most likely suggests that there is an underestimation of the blank values from the denuder. Also, the PM concentration results from the denuder line were consistently found to be lower than concentration results from uncoated quartz fibre filters, even when back-up SIFs were placed downstream in the denuder line to correct for the negative bias. Since uncoated quartz fibre filter in series testing showed that the very little gas phase was collected on the last filter, a positive artifact is therefore not likely. A more likely possibility is that there is a depletion of PM during the time the air stream passes through the denuder.

Partitioning results from the denuder line concentration values showed that nitrophenols were found to be predominantly in the gas phase (> 80 % for all

nitrophenols). The partitioning values determined in this work were found to be slightly less than the partitioning values obtained from Busca (2010), but the same lack of dependence of the partitioning on vapor pressure was observed. Therefore, the thought that sampling artifacts were biasing previous high volume filter partitioning results was found to not be the case, since the IOGAPS system, which compensates for the sampling artifacts observed in high volume filter sampling, gave almost identical results. Partitioning results also obtained from the low volume filter pack line and the high volume filter line, were found to be relatively similar, with all nitrophenols found to be 75 % or more in the gas phase from all methods. When looking at other possible dependences of the partitioning of the nitrophenols, it was found that only temperature showed a weak influence, with partitioning into the gas phase increasing with increasing temperature for three of the five target nitrophenols.

In summary, this work effectively developed a denuder-filter based technique for the sampling and analysis of nitrophenols. While the results obtained were not able to provide definite conclusions in regard to the effectiveness of this method in comparison to other low volume and high volume filter based methods, important results regarding filter and denuder efficiency were obtained. It was found that for three target compounds (3-methyl-4-nitrophenol, 2-methyl-4-nitrophenol and 2,6-dimethyl-4-nitrophenol) the concentration results obtained from the three sampling lines (denuder line, filter pack line and high volume filter line), showed good agreement. This work has confirmed that the XAD-4^{TM} coated SIFs are a good technique to determine total (gas phase + PM) concentrations since their efficiency was found consistently to be approximately 90 %.

Therefore sampling two XAD-4^{TM} coated SIFs in series will allow for the almost complete collection of the target nitrophenols, within a few percent. As well, the different methods used in this work to attempt to separate the gas phase from PM all provided the same conclusion, that nitrophenols are predominantly found in the gas phase and that the dependence of the partitioning of these nitrophenols on vapor pressure is much less than expected. Therefore this suggests that the SVOC limits defined by Junge (1977) do not necessarily reflect ambient conditions.

In order to further develop this method, a better understanding of the presence and evolution of denuder blank values over time is required, since the results obtained in this work suggest that the blank values presented here may be largely underestimated. The use of XAD-4^{TM} coated SIFs with both high volume and low volume sampling, should be tested to determine and compare total (gas phase + PM) concentration measurements for other SVOC such as n-alkanes and polycyclic aromatic hydrocarbons (PAHs) here at York University. As well, further measurements of other SVOC in both gas phase and PM will provide insight regarding the possibility of the partitioning of these compounds showing a similarly low dependence on vapor pressure.

References

Allen, S. K. and Allen, C. W. Phenol concentrations in air and rain water samples collected near a wood preserving facility. Bull. Environ. Contam. Toxicol.: 1997, 59: 702-707.

Andino, J. M., Smith, J. N., Flagan, R. C., Goddard III, W. A. and Seinfeld, J. H. Mechanism of atmospheric photooxidation of aromatics: a theoretical study. J. Phys. Chem.: 1996, 100: 10967-10980.

Atkinson, R. Gas-phase tropospheric chemistry of organic compounds. J. Phys. Chem. Ref. Data: 1994, Monogr. No. 2.

Atkinson, R., Aschmann, S. and Arey, J. Reactions of OH and NO_3 radicals with phenols, cresols and 2-nitrophenol at 296 $\pm$ 2 K. Environ. Sci. Technol.: 1992, 26: 1397-1403.

Bidleman, T. F. Atmospheric processes: wet and dry deposition of organic compounds are controlled by their vapor-particle partitioning. Environ. Sci. Technol.: 1988, 22(4): 361-367.

Bidleman, T. F., Billings, W. N. and Foreman, W. T. Vapor-particle partitioning of semivolatile organic compounds: estimates from field collections. Environ. Sci. Technol.: 1986, 20(10): 1038-1043.

Bolzacchini, E., Bruschi, M., Hjorth, J., Meinardi, S., Orlandi, M., Rindone, B. and Rosenbohm, E. Gas-phase reaction of phenol with NO_3. Environ. Sci. Technol.: 2001, 35: 1791-1797.

Busca, R. S. Method development for the sampling and analysis of atmospheric nitrophenols. MSc Thesis. York University, 2010.

Calvert, J. G., Atkinson, R., Becker, K. H., Kamens, R. M., Seinfeld, J. H., Wallington, T. J. and Yarwood, G. The mechanisms of atmospheric oxidation of aromatic hydrocarbons. New York: Oxford University Press, 2002.

Cecinato, A., Di Palo, V., Pomata, D., Scianò, M. C. T. and Possanzini, M. Measurement of phase-distributed nitrophenols in Rome ambient air. Chemosphere: 2005, 59: 679-683.

Chow, J. C. Measurement methods to determine compliance with ambient air quality standards for suspended particles. J. Air & Waste Manage. Assoc.: 1995, 45: 320-382.

Cofer, W. R., III, Collins, V. G. and Talbot, R. W. Improved aqueous scrubber for collection of soluble atmospheric trace gases. Environ. Sci. Technol.: 1985, 19: 557-560.

CRC Handbook of Chemistry and Physics. 93rd ed. CRC Press: Boca Raton, Florida, 2012-2013.

Delhomme, O., Morville, S. and Millet, M. Seasonal and diurnal variations of atmospheric concentrations of phenols and nitrophenols measured in the Strasboug area, France. Atmos. Pollut. R.: 2010, 1: 16-22.

Durham, J. L., Ellestad, T. G., Stockburger, L., Knapp, K. T. and Spiller, L. L. A transition-flow reactor tube for measuring trace gas concentrations. JAPCA J. Air Waste Man.: 1986, 36(11): 1228-1232.

Eaton, W. C. Standard operating procedure for coating annular denuders with XAD-4 resin. Revision No. 2. Method Document, North Carolina, 2003.

Environment Canada: Historical Weather Data, Toronto North York Site, http://climate.weather.gc.ca, Accessed May 2, 2013.

Fan, X., Lee, P. K. H., Brook, J. R. and Mabury, S. A. Improved measurement of seasonal and diurnal differences in the carbonaceous components of urban particulate matter using a denuder-based air sampler. Aerosol Sci. Tech.: 2004, 38(S2): 63-69.

Finlayson-Pitts, B. J. & Pitts, J. N., Jr. Chemistry of the upper and lower atmosphere: theory, experiments and applications. San Diego: Academic Press, 2000.

Fitz, D. R. Reduction of the positive organic artifact on quartz filters. Aerosol Sci. Tech.: 1990, 12(1): 142-148.

Forstner, H. J. L., Flagan, R. C. and Seinfeld, J. H. Secondary organic aerosol from photooxidation of aromatic hydrocarbons: molecular composition. Environ. Sci.Technol.: 1997, 31: 1345-1358.

Fuller, E. N., Schettler, P. D. and Giddings, J. C. A new method for prediction of binary gas-phase diffusion coefficients. Ind. Eng. Chem.: 1966, 58: 19-27.

Galarneau, E., Harner, T., Shoeib, M., Kozma, M. and Lane, D. A preliminary investigation of sorbent-impregnated filters (SIFs) as an alternative to polyurethane foam (PUF) for sampling gas-phase semivolatile organic compounds in air. Atmos. Environ.: 2006, 40: 5734-5740.

Gong, X. Private Communication.

Gundel, L. and Hering, S. V. Absorbing filter media for denuder-filter sampling of total organic carbon in airborne particles. Record of Invention WIB 1457, Lawrence Berkeley National Laboratory (USA), 1998.

Gundel, L. A., Lee, V. C., Mahanama, K. R. R., Stevens, R. K. and Daisey, J. M. Direct determination of the phase distributions of semi-volatile hydrocarbons using annular denuders. Atmos. Environ.: 1995, 29(14): 1719-1733.

Gundel, L., Daisey, J. M. and Stevens, R. K. Quantitative Organic Vapor-Particle Sampler. U.S. Patent 5,763,360, June 9, 1998.

Hassani, Y. Private Communication.

Herterich, R. and Herrmann, R. Comparing the distribution of nitrated phenols in the atmosphere of two German hill sites. Environ. Technol.: 1990, 11: 961-972.

Hinds, W. C. Aerosol Technology: Properties, behavior, and measurement of airborne particles. 2nd ed. John Wiley & Sons: New York, 1999.

Junge, C. E. Basic considerations about trace constituents in the atmosphere as related to the fate of global pollutants. Adv. Environ. Sci. Technol.: 1977, 8(1): 7-25.

Kennedy, D. C. Macroreticular polymeric adsorbents. Ind. Eng. Chem. Prod. Res. Develop.: 1973, 12(1): 56-61.

Kleindienst, T. E., Conver, T. S., McIver, C. D. and Edney, E. O. Determination of secondary organic aerosol products from the photooxidation of toluene and their implications in ambient $PM_{2.5}$. J. Atmos. Chem.: 2004, 47: 79-100.

Knapp, D. R. Handbook of analytical derivatization reactions. New York: John Wiley & Sons, 1979.

Lane, D. A. Private Communication.

Lane, D. A. Gas and particle phase measurements of atmospheric organic compounds. Amsterdam: Gordon and Breach Science Publishers, 1999.

Lane, D. A., Johnson, N. D., Barton, S. C., Thomas, H. S. and Schroeder, W. H. Development and evaluation of a novel gas and particles sampler for semi-volatile chlorinated organic compounds in ambient air. Environ. Sci. Technol.: 1988, 22: 941-947.

McDow, S. R. and Huntzicker, S. R. Vapor adsorption artifact in the sampling of organic aerosol: face velocity effects. Atmos. Environ.: 1990, 24A(10): 2563-2571.

Morville, S., Scheyer, A., Mirabel, P. and Millet, M. A multiresidue method for the analysis of phenols and nitrophenols in the atmosphere. J. Environ. Monitor.: 2004, 6: 963-966.

Moukhtar, S., Saccon, M., Kornilova, A., Irei, S., Huang, L. and Rudolph, J. Method for determination of stable carbon isotope ratio of methylnitrophenols in atmospheric particulate matter. Atmos. Meas. Tech.: 2011, 4: 2453-2464.

Nishioka, M. G. and Lewtas, J. Quantification of nitro- and hydroxylated nitro-aromatic/polycyclic aromatic hydrocarbons in selected ambient air daytime winter samples. Atmos. Environ.: 1992, 26A(11): 2077-2087.

Ontario Ministry of the Environment: Historical Pollutant Data, Toronto North Site, http://www.airqualityontario.com/history/station.php?stationid=34020, Accessed May 2, 2013.

Pankow, J. F. Review and comparative analysis of the theories on partitioning between the gas and aerosol particulate phases in the atmosphere. Atmos. Environ.: 1987, 21(11): 2275-2283.

Pankow, J. F. An absorption model of gas/particle partitioning of organic compounds in the atmosphere. Atmos. Environ.: 1994, 28(2): 185-188.

Pankow, J. F. and Bidleman, T. F. Effects of temperature, TSP and per cent non-exchangeable material in determining the gas-particle partitioning of organic compounds. Atmos. Environ.: 1991, 25A(10): 2241-2249.

Peters, A. J., Lane, D. A., Gundel, L. A., Northcott, G. L. and Jones, K. C. A comparison of high volume and diffusion denuder samplers for measuring semivolatile organic compounds in the atmosphere. Environ. Sci. Technol.: 2000, 34: 5001-5006.

Possanzini, M., Febo, A. and Liberti, A. Design of a high-performance denuder for sampling of atmospheric pollutants. Atmos. Environ.: 1983, 17(12): 2605-2610.

Saccon, M. Private Communication.

Saccon, M., Busca, R., Facca, C., Huang, L., Irei, S., Kornilova, A., Lane, D., and Rudolph, J. Method for the determination of concentrations and stable carbon isotope ratios of atmospheric phenols. Atmos. Meas. Tech. Discuss.: 2013, 6: 4705-4733.

Skoog, D. A., Holler, F. J. and Crouch, S. R. Principles of Instrumental Analysis 6th Edition. California: Thomson Brooks/Cole, 2007.

Shäfer, W. E. and Schönherr, J. Accumulation and transport of phenol, 2-nitrophenol and 4-nitrophenol in plant cuticles. Ecotox. Environ. Safety: 1985, 10(2): 239-252.

Sickles, J. E., II, Perrino, C., Allegrini, I., Febo, A., Possanzini, M. and Paur, R. J. Sampling and analysis of ambient air near Los Angeles using an annular denuder system. Atmos. Environ.: 1988, 22(8): 1619-1625.

Sigma-Aldrich Co. Amberlite XAD polymeric resins. Product Information, Missouri, United States of America, 1998.

Temime, B., Healy, R. M. and Wenger, J. C. A denuder-filter sampling technique for the detection of gas and particle phase carbonyl compounds. Environ. Sci. Technol.: 2007, 41: 6514-6520.

Tisch Environmental, Inc. Operations manual TE-6070-BL PM_{10} particulate matter 10 microns and less MFC brushless high volume air sampler.

Turpin, B. J., Liu, S., Podoiske, K. S., Gomes, M. S. P., Elsenreich, S. J. and McMurry, P. H. Design and evaluation of a novel diffusion separator for measuring gas/particle distributions of semivolatile organic compounds. Environ. Sci. Technol.: 1993, 27: 2441-2449.

Volkens, J. and Leith, D. Effects of sampling bias on gas-particle partitioning of semi-volatile compounds. Atmos. Environ.: 2003, 37: 3385-3393.

Waters Corporation. Oasis Sample Extraction Products. Product Information, Massachusetts, United States of America, 2008.

Zhao, J., Zhang, R., Misawa, K. and Shibuya, K. Experimental product study of the OH-initiated oxidation of *m*-xylene. Photochem. Photobiol.: 2005, 176: 199-207.

Appendix A. Ambient Sampling Dates and Times, Sample Descriptions and Sampling Volumes

Sampling Dates/Times					Samples Obtained		Sample Volumes (m^3)		
Sample Name / Start Date	Start Time	End Date	End Time	Denuder Number	Regular Low Volume IOGAPS Set-Up	High Volume Set-Up[a]	Denuder Line	Filter Pack Line	Hi-Vol Sampler A and/or B
25-Jun-12	10:25 AM	25-Jun-12	10:30 AM	78	yes	Q(A)	24.131	24.131	1632.9
28-Jun-12	10:45 AM	28-Jun-12	10:50 AM	98	yes	Q(A)	27.739	27.301	1627.2
05-Jul-12	10:00 AM	05-Jul-12	10:00 AM	78	yes	Q(A)	27.350	26.875	1627.2
10-Jul-12	10:30 AM	10-Jul-12	10:30 AM	78	yes	Q(A)	27.087	25.445	1627.2
11-Jul-12	10:45 AM	11-Jul-12	10:45 AM	98	yes	Q(A)	27.042	26.905	1627.2
12-Jul-12	10:45 AM	12-Jul-12	10:45 AM	78	yes	Q(A)	27.406	26.652	1627.2
24-Jul-12	9:35 AM	24-Jul-12	9:35 AM	78	yes	Q(A)	27.137	28.146	1627.2
01-Aug-12	8:45 AM	01-Aug-12	10:45 AM	78 & 98	yes	N/A	29.596	28.572	N/A
02-Aug-12	11:00 AM	02-Aug-12	9:30 AM	64	yes	X(A); Q(B)	25.469	25.261	1525.5
08-Aug-12	9:15 AM	08-Aug-12	9:30 AM	64	yes	N/A	27.661	26.982	N/A
13-Aug-12	9:40 AM	13-Aug-12	9:35 AM	78 & 98	yes	Q(A)	27.278	26.470	1621.6
15-Aug-12	9:30 AM	15-Aug-12	10:35 AM	78 & 98	yes	Q(A)	28.522	27.811	1700.4
11-Sep-12	8:35 AM	11-Sep-12	8:35 AM	64	yes	X(A)	26.690	25.220	1627.2
13-Sep-12	9:15 AM	13-Sep-12	8:40 AM	98	yes	X(A)	26.280	25.577	1587.7
27-Sep-12	9:05 AM	27-Sep-12	9:00 AM	98	yes	X(A)	26.153	25.311	1621.6
11-Oct-12	9:25 AM	11-Oct-12	9:55 AM	98	yes	X(A); Q(B)	25.769	26.170	1661.1
25-Oct-12	9:50 AM	25-Oct-12	10:00 AM	64	yes	X(A); Q(B)	26.476	25.91	1615.9
06-Nov-12	9:30 AM	06-Nov-12	9:35 AM	64	yes	X(A); Q(B)	24.307	25.27	1632.9
21-Nov-12	9:10 AM	21-Nov-12	9:15 AM	64	yes	X(A); Q(B)	25.408	25.149	1632.9
27-Nov-12	9:45 AM	27-Nov-12	11:45 AM	64	yes	X(A); Q(B)	26.022	27.001	1762.8
05-Dec-12	8:45 AM	05-Dec-12	8:45 AM	64	yes (3Q on FPL[b])	X(A); Q(B)	23.695	24.879	1627.2

Sampling Dates/Times				Denuder Number	Samples Obtained		Sample Volumes (m^3)		
Sample Name / Start Date	Start Time	End Date	End Time		Regular Low Volume IOGAPS Set-Up	High Volume Set-Up[a]	Denuder Line	Filter Pack Line	Hi-Vol Sampler A and/or B
13-Dec-12	11:10 AM	13-Dec-12	9:35 AM	98	yes	X(A); Q(B)	22.852	23.363	1519.9
23-Jan-13	10:20 AM	23-Jan-13	11:14 AM	64	yes	X(B)	24.134	25.968	1688.2
13-Feb-13	11:25 AM	13-Feb-13	10:25 AM	64	yes	X(A); Q(B)	22.845	23.889	1559.4
06-Mar-13	9:30 AM	06-Mar-13	10:45 AM	64	yes	X(A)	26.535	26.693	1678.1
15-Apr-13	9:35 AM	15-Apr-13	9:35 AM	64	yes	X(A); X(B)	26.866	25.572	1627.2
17-Apr-13	9:20 AM	17-Apr-13	10:10 AM	78	yes	X(A); Q(B)	27.452	26.078	1683.7(A); 1423.8(B)
22-Apr-13	9:55 AM	22-Apr-13	8:45 AM	78	yes	N/A	25.531	24.215	N/A
23-Apr-13	9:00 AM	23-Apr-13	9:00 AM	99	yes	N/A	27.899	25.837	N/A
30-Apr-13	7:15 AM	30-Apr-13	7:15 PM	78	yes	N/A	14.237	13.062	N/A
30-Apr-13	7:15 PM	01-May-13	7:15 AM	99	yes	N/A	13.509	12.638	N/A
01-May-13	7:15 AM	01-May-13	7:15 PM	78	yes	N/A	13.593	12.830	N/A
01-May-13	7:15 PM	02-May-13	7:15 AM	99	yes	N/A	14.053	13.095	N/A
02-May-13	7:15 AM	02-May-13	7:15 PM	78	yes	N/A	13.889	13.135	N/A
02-May-13	7:15 PM	03-May-13	7:15 AM	99	yes	N/A	13.823	13.016	N/A

[a] High Volume Set-Up Notation is as follows:
Q: uncoated quartz filter
X: XAD-4™ coated SIF
(A): filter was placed on sampler A
(B): filter was placed on sampler B
N/A: filter not sampled

[b] FPL: filter pack line

Appendix B. Ambient Sampling Dates and Meteorological Data

Date	Average Temperature[a] (°C)	Maximum Temperature[a] (°C)	Minimum Temperature[a] (°C)	Total Precipitation[a] (mm)	Total Snow[a] (mm)	Total Rain[a] (mm)	Average $PM_{2.5}$[b] ($\mu g\ m^{-3}$)	Average NO_2[b] (ppb)	Average Relative Humidity[a] (%)
25-Jun-12	17.3	20.5	14.0	0.0	0.0	0.0	1.74	3.32	53.92
28-Jun-12	23.0	31.5	14.5	0.0	0.0	0.0	11.13	17.92	56.21
05-Jul-12	23.8	29.0	18.5	0.0	0.0	0.0	13.04	21.13	63.58
10-Jul-12	22.3	28.5	16.0	0.0	0.0	0.0	6.58	7.40	48.56
11-Jul-12	23.0	31.0	15.0	0.0	0.0	0.0	11.38	16.15	48.58
12-Jul-12	23.0	32.5	13.5	0.0	0.0	0.0	15.50	21.50	49.21
24-Jul-12	24.5	27.5	21.5	0.0	0.0	0.0	4.96	5.48	57.29
01-Aug-12	23.3	28.0	18.5	0.0	0.0	0.0	8.65	10.30	62.50
02-Aug-12	21.5	28.0	15.0	0.0	0.0	0.0	18.38	11.74	67.65
08-Aug-12	24.5	30.5	18.5	trace	0.0	trace	10.16	10.09	71.80
13-Aug-12	22.8	27.0	18.5	1.4	0.0	1.4	8.92	10.76	73.75
15-Aug-12	19.5	25.5	13.5	0.6	0.0	0.6	12.54	21.23	71.42
11-Sep-12	16.0	25.0	7.0	0.0	0.0	0.0	11.71	16.12	64.25
13-Sep-12	20.3	28.5	12.0	0.0	0.0	0.0	14.38	12.84	64.75
27-Sep-12	10.5	17.5	3.5	0.0	0.0	0.0	3.08	16.48	62.88
11-Oct-12	7.5	12.5	2.5	0.2	0.0	0.2	3.08	9.32	66.24
25-Oct-12	16.8	23.0	10.5	0.0	0.0	0.0	15.96	19.40	82.63
06-Nov-12	-1.0	2.5	-4.5	0.0	0.0	0.0	4.12	18.64	63.32
21-Nov-12	6.0	11.0	1.0	0.0	0.0	0.0	18.79	33.96	89.08
27-Nov-12	0.5	2.5	-1.5	0.0	0.0	0.0	3.96	16.39	59.56
05-Dec-12	0.3	2.0	-1.5	0.2	0.2	0.0	3.60	19.20	62.42
13-Dec-12	0.8	6.5	-5.0	0.0	0.0	0.0	6.83	21.27	65.74

Date	Average Temperature[a] (°C)	Maximum Temperature[a] (°C)	Minimum Temperature[a] (°C)	Total Precipitation[a] (mm)	Total Snow[a] (mm)	Total Rain[a] (mm)	Average $PM_{2.5}$[b] (µg m-3)	Average NO_2[b] (ppb)	Average Relative Humidity[a] (%)
23-Jan-13	-15.3	-9.5	-21.0	0.0	0.0	0.0	9.27	25.35	66.20
13-Feb-13	-0.8	1.0	-2.5	0.0	0.0	0.0	16.79	23.76	74.75
06-Mar-13	-1.8	7.0	-10.5	trace	trace	0.0	6.69	20.04	76.23
15-Apr-13	7.5	13.5	1.5	trace	0.0	trace	9.68	16.88	66.71
17-Apr-13	7.3	13.5	1.0	5.0	0.0	5.0	4.12	13.15	61.23
22-Apr-13	5.8	12.5	-1.0	0.0	0.0	0.0	8.33	21.08	49.78
23-Apr-13	6.0	12.0	0.0	0.0	0.0	0.0	9.74	21.13	58.88
30-Apr-13	15.5	21.0	10.0	0.0	0.0	0.0	7.96	20.52	80.46
30-Apr-13[c]	16.2	19.1	11.5	0.0	0.0	0.0	10.67	21.62	80.92
30-Apr-13[d]	13.6	16.0	12.6	0.0	0.0	0.0	5.25	19.04	80.00
01-May-13	17.8	23.5	12.0	0.0	0.0	0.0	7.63	21.00	56.04
01-May-13[c]	19.4	21.6	16.0	0.0	0.0	0.0	7.23	18.08	64.50
01-Day-13[d]	14.8	19.0	10.9	0.0	0.0	0.0	8.33	23.08	47.58
02-May-13	15.5	23.0	8.0	0.0	0.0	0.0	10.00	21.88	43.67
02-May-13[c]	19.9	22.4	16.3	0.0	0.0	0.0	12.33	21.38	41.17
02-May-13[d]	14.9	18.4	11.5	0.0	0.0	0.0	7.67	23.24	46.17

[a] measurement from Environment Canada's North York, Toronto site
[b] measurement from Ontario's Ministry of the Environment Toronto North site
[c] daytime measurement
[d] nighttime measurement

Appendix C. Ambient Sample Masses

Sampling Date	Sample[a]	Mass (ng)				
		4-me-2-NP	4-NP	3-me-4-NP	2-me-4-NP	2,6-dime-4-NP
25-Jun-12	LV-D78-E1	3.471	165.471	6.185	11.904	3.225
	LV-D78-E2	0.340	< LDL	1.682	2.130	0.458
	LV-D78-E3	0.167	< LDL	0.339	0.709	0.361
	LV-D78-E4	< LDL	< LDL	0.146	< LDL	0.107
	Total D78 Mass	**3.979**	**165.471**	**8.353**	**14.744**	**4.150**
	LV-DFP-QA	0.196	< LDL	< LDL	0.502	< LDL
	LV-DFP-XB	11.062	75.372	0.479	11.415	0.616
	LV-DFP-XC	8.458	6.881	0.551	4.117	1.067
	Total DFP Mass	**19.716**	**82.252**	**1.030**	**16.035**	**1.683**
	LV-FPL-QA	2.810	7.208	1.146	4.365	0.587
	LV-FPL-XB	4.063	196.896	3.593	14.678	1.915
	LV-FPL-XC	13.628	50.923	1.278	8.808	3.072
	Total FPL Mass	**20.501**	**255.027**	**6.018**	**27.851**	**5.574**
	HV-QA	4.899	306.985	22.861	48.987	6.532
28-Jun-12	LV-D98-E1	29.299	4694.937	29.600	250.761	74.536
	LV-D98-E2	6.766	958.483	7.151	8.435	2.208
	LV-D98-E3	2.455	415.721	0.722	2.056	0.641
	LV-D98-E4	< LDL	< LDL	< LDL	< LDL	< LDL
	Total D98 Mass	**38.520**	**6069.141**	**37.474**	**261.253**	**77.385**
	LV-DFP-QA	0.854	14.122	0.590	1.156	0.150
	LV-DFP-XB	3.390	48.725	1.046	2.426	0.119
	LV-DFP-XC	0.891	42.978	0.812	1.246	< LDL
	Total DFP Mass	**5.135**	**105.825**	**2.449**	**4.828**	**0.270**
	LV-FPL-QA	1.064	< LDL	0.366	2.420	0.172
	LV-FPL-XB	0.341	1199.963	32.233	315.614	75.686
	LV-FPL-XC	< LDL	24.288	0.909	11.212	3.085
	Total FPL Mass	**1.405**	**1224.251**	**33.508**	**329.247**	**78.942**
	HV-QA	11.926	593.086	24.213	94.854	7.591

Sampling Date	Sample[a]	Mass (ng)				
		4-me-2-NP	4-NP	3-me-4-NP	2-me-4-NP	2,6-dime-4-NP
05-Jul-12	LV-D78-E1	3.945	589.906	31.141	267.210	125.412
	LV-D78-E2	2.702	< LDL	1.152	6.757	2.965
	LV-D78-E3	1.273	< LDL	0.567	2.410	0.500
	LV-D78-E4	0.140	< LDL	0.286	0.752	0.216
	Total D78 Mass	**< LDL**	**589.906**	**33.146**	**277.130**	**129.093**
	LV-DFP-QA	0.071	3.816	< LDL	2.949	0.205
	LV-DFP-XB	0.591	11.357	< LDL	2.380	0.660
	LV-DFP-XC	< LDL	22.151	< LDL	1.172	0.104
	Total DFP Mass	**0.663**	**37.324**	**< LDL**	**6.501**	**0.968**
	LV-FPL-QA	0.297	1.501	0.373	2.869	0.282
	LV-FPL-XB	< LDL	882.832	29.971	243.493	53.619
	LV-FPL-XC	< LDL	88.164	0.197	6.442	9.756
	Total FPL Mass	**0.297**	**972.497**	**30.540**	**252.804**	**63.657**
	HV-QA	4.882	1745.986	42.307	133.430	11.390
10-Jul-12	LV-D78-E1	5.705	829.201	6.926	39.015	16.976
	LV-D78-E2	1.499	457.466	0.746	3.363	0.544
	LV-D78-E3	0.024	106.072	0.136	1.711	0.143
	LV-D78-E4	< LDL	23.482	< LDL	0.258	< LDL
	Total D78 Mass	**7.227**	**1416.221**	**7.808**	**44.347**	**17.663**
	LV-DFP-QA	0.647	< LDL	0.160	1.181	0.120
	LV-DFP-XB	1.946	31.702	0.472	2.225	< LDL
	LV-DFP-XC	< LDL	12.261	< LDL	0.369	0.138
	Total DFP Mass	**2.593**	**43.962**	**0.632**	**3.774**	**0.259**
	LV-FPL-QA	0.437	< LDL	< LDL	1.799	0.102
	LV-FPL-XB	2.656	135.230	2.051	15.045	3.509
	LV-FPL-XC	0.643	20.193	0.858	3.081	1.366
	Total FPL Mass	**3.736**	**155.423**	**2.909**	**19.924**	**4.977**
	HV-QA	5.344	400.746	23.691	78.800	7.754

Sampling Date	Sample[a]	Mass (ng)				
		4-me-2-NP	4-NP	3-me-4-NP	2-me-4-NP	2,6-dime-4-NP
11-Jul-12	LV-D98-E1	4.035	1046.419	0.408	12.772	8.812
	LV-D98-E2	2.001	402.596	0.084	12.200	0.134
	LV-D98-E3	1.226	< LDL	0.002	1.490	0.632
	LV-D98-E4	< LDL	< LDL	< LDL	0.904	< LDL
	Total D98 Mass	**7.262**	**1449.014**	**0.494**	**27.366**	**9.578**
	LV-DFP-QA	0.063	< LDL	0.782	0.716	0.088
	LV-DFP-XB	0.178	38.155	2.580	6.539	1.633
	LV-DFP-XC	< LDL	33.977	< LDL	1.775	1.037
	Total DFP Mass	**0.241**	**72.131**	**3.362**	**9.029**	**2.758**
	LV-FPL-QA	0.063	1.734	0.542	2.678	0.071
	LV-FPL-XB	3.139	527.019	16.441	83.493	22.105
	LV-FPL-XC	< LDL	36.771	0.457	3.506	2.983
	Total FPL Mass	**3.202**	**565.524**	**17.440**	**89.677**	**25.159**
	HV-QA	11.390	870.552	55.325	120.413	21.154
12-Jul-12	LV-D78-E1	20.870	1191.444	31.221	234.502	98.974
	LV-D78-E2	0.807	74.204	2.155	18.766	4.355
	LV-D78-E3	< LDL	43.595	0.520	0.544	0.144
	LV-D78-E4	< LDL	< LDL	< LDL	< LDL	< LDL
	Total D78 Mass	**21.677**	**1309.243**	**33.897**	**253.812**	**103.473**
	LV-DFP-QA	0.566	< LDL	0.160	1.374	0.159
	LV-DFP-XB	< LDL	30.917	0.214	0.660	< LDL
	LV-DFP-XC	< LDL	20.135	0.348	0.004	< LDL
	Total DFP Mass	**0.566**	**51.052**	**0.722**	**2.039**	**0.159**
	LV-FPL-QA	< LDL	6.066	0.271	4.236	0.277
	LV-FPL-XB	< LDL	645.611	16.900	111.334	23.838
	LV-FPL-XC	< LDL	42.796	1.401	4.386	4.099
	Total FPL Mass	**< LDL**	**694.473**	**18.571**	**119.955**	**28.214**
	HV-QA	14.645	888.451	53.698	157.838	30.917

Sampling Date	Sample[a]	Mass (ng)				
		4-me-2-NP	4-NP	3-me-4-NP	2-me-4-NP	2,6-dime-4-NP
24-Jul-12	LV-D78-E1	1.882	192.081	0.733	14.260	8.102
	LV-D78-E2	0.243	< LDL	0.617	1.394	0.195
	LV-D78-E3	< LDL	< LDL	0.328	0.690	0.290
	LV-D78-E4	< LDL	< LDL	< LDL	< LDL	0.083
	Total D78 Mass	**< LDL**	**192.081**	**< LDL**	**16.345**	**8.670**
	LV-DFP-QA	0.015	< LDL	0.231	0.942	0.058
	LV-DFP-XB	1.546	15.506	0.314	1.000	< LDL
	LV-DFP-XC	< LDL	< LDL	0.030	< LDL	< LDL
	Total DFP Mass	**1.561**	**15.506**	**0.575**	**1.942**	**0.058**
	LV-FPL-QA	0.638	< LDL	0.155	1.718	1.321
	LV-FPL-XB	0.026	165.727	7.516	26.866	5.369
	LV-FPL-XC	< LDL	23.223	0.424	0.817	< LDL
	Total FPL Mass	**0.664**	**188.951**	**8.095**	**29.401**	**6.689**
	HV-QA	6.509	395.410	29.290	60.206	8.136
01-Aug-12	LV-D78-E1	7.462	631.186	20.888	61.145	26.537
	LV-D78-E4	2.163	3.951	0.079	0.499	0.000
	Total D78 Mass	**9.625**	**635.136**	**20.967**	**61.644**	**26.537**
	LV-D98-E1	0.467	38.075	0.145	< LDL	< LDL
	LV-D98-E4	< LDL	< LDL	< LDL	< LDL	< LDL
	Total D98 Mass	**0.467**	**38.075**	**0.145**	**<LDL**	**<LDL**
	Total D78 + D98 Mass	**10.092**	**673.212**	**21.112**	**61.644**	**26.537**
	LV-DFP-QA	2.037	< LDL	0.157	1.281	0.121
	LV-DFP-XB	5.523	314.382	10.073	30.050	3.145
	LV-DFP-XC	7.062	73.256	1.998	6.983	0.162
	Total DFP Mass	**14.622**	**387.638**	**12.228**	**38.313**	**3.428**
	LV-FPL-QA	2.395	0.789	0.086	1.203	< LDL
	LV-FPL-XB	5.376	137.915	0.620	10.673	< LDL
	LV-FPL-XC	< LDL	27.166	0.135	0.828	< LDL
	Total FPL Mass	**7.771**	**165.870**	**0.841**	**12.705**	**< LDL**

Sampling Date	Sample[a]	Mass (ng)				
		4-me-2-NP	4-NP	3-me-4-NP	2-me-4-NP	2,6-dime-4-NP
02-Aug-12	LV-D64-E1-E3	10.981	75.897	6.471	45.392	8.230
	LV-D64-E4	< LDL	< LDL	< LDL	< LDL	< LDL
	Total D64 Mass	**10.981**	**75.897**	**6.471**	**45.392**	**8.230**
	LV-DFP-QA	1.241	< LDL	1.079	2.422	0.013
	LV-DFP-XB	4.149	37.937	3.180	15.668	0.297
	LV-DFP-XC	0.409	3.529	< LDL	< LDL	< LDL
	Total DFP Mass	**5.799**	**41.466**	**4.259**	**18.091**	**0.310**
	LV-FPL-QA	0.282	12.027	0.025	0.231	0.271
	LV-FPL-XB	1.684	101.027	0.973	54.365	5.361
	LV-FPL-XC	< LDL	7.915	< LDL	4.402	< LDL
	Total FPL Mass	**1.966**	**120.970**	**0.998**	**58.998**	**5.631**
	HV-XA	515.619	24247.823	1228.028	4394.966	1398.884
08-Aug-12	LV-D64-E1-E3	1.055	337.555	8.167	100.821	39.464
	LV-D64-E4	< LDL	< LDL	< LDL	< LDL	< LDL
	Total D64 Mass	**< LDL**	**337.555**	**8.167**	**100.821**	**39.464**
	LV-DFP-QA	0.319	< LDL	0.430	1.599	0.494
	LV-DFP-XB	0.676	13.319	0.720	1.473	0.665
	LV-DFP-XC	0.050	1.928	0.174	0.299	0.110
	Total DFP Mass	**1.045**	**15.247**	**1.324**	**3.371**	**1.270**
	LV-FPL-QA	0.537	1.513	1.210	3.196	0.513
	LV-FPL-XB	0.544	309.327	11.972	89.215	25.331
	LV-FPL-XC	0.293	21.777	< LDL	0.776	< LDL
	Total FPL Mass	**1.375**	**332.617**	**13.182**	**93.187**	**25.844**

Sampling Date	Sample[a]	Mass (ng)				
		4-me-2-NP	4-NP	3-me-4-NP	2-me-4-NP	2,6-dime-4-NP
13-Aug-12	LV-D78-E1-E3	3.344	466.813	15.022	66.662	32.079
	LV-D78-E4	< LDL	< LDL	0.106	2.204	< LDL
	Total D78 Mass	**3.344**	**466.813**	**15.128**	**68.866**	**32.079**
	LV-D98-E1	0.163	< LDL	< LDL	1.370	0.102
	LV-D98-E4	< LDL	< LDL	< LDL	< LDL	< LDL
	Total D98 Mass	**0.163**	**< LDL**	**< LDL**	**1.370**	**0.102**
	Total D78 + D98 Mass	**3.507**	**466.813**	**15.128**	**70.236**	**32.181**
	LV-DFP-QA	0.496	< LDL	0.248	1.224	1.690
	LV-DFP-XB	0.697	6.617	0.057	0.905	0.671
	LV-DFP-XC	0.736	< LDL	< LDL	0.180	< LDL
	Total DFP Mass	**1.929**	**6.617**	**0.305**	**2.310**	**2.361**
	LV-FPL-QA	0.622	5.932	1.096	2.966	1.739
	LV-FPL-XB	1.041	297.401	7.895	47.774	8.865
	LV-FPL-XC	< LDL	20.579	0.686	5.020	0.214
	Total FPL Mass	**1.663**	**323.913**	**9.677**	**55.760**	**10.818**
	HV- QA	13.457	378.613	33.231	41.790	7.103

Sampling Date	Sample[a]	Mass (ng)				
		4-me-2-NP	4-NP	3-me-4-NP	2-me-4-NP	2,6-dime-4-NP
15-Aug-12	LV-D78-E1	6.828	525.042	16.188	177.480	17.105
	LV-D78-E4	< LDL	0.279	< LDL	< LDL	0.908
	Total D78 Mass	**6.828**	**525.322**	**16.188**	**177.480**	**18.013**
	LV-D98-E1	< LDL	0.212	1.149	< LDL	< LDL
	LV-D98-E4	< LDL	< LDL	< LDL	< LDL	< LDL
	Total D98 Mass	**< LDL**	**0.212**	**1.149**	**< LDL**	**< LDL**
	Total D78 + D98 Mass	**6.828**	**525.533**	**17.337**	**177.480**	**18.013**
	LV-DFP-QA	0.248	< LDL	0.486	2.093	0.985
	LV-DFP-XB	0.293	6.957	0.816	1.308	0.728
	LV-DFP-XC	< LDL	< LDL	0.158	0.730	0.436
	Total DFP Mass	**0.541**	**6.957**	**1.459**	**4.131**	**2.148**
	LV-FPL-QA	0.208	2.358	0.906	3.015	0.866
	LV-FPL-XB	0.339	406.983	17.211	109.202	0.525
	LV-FPL-XC	< LDL	68.536	0.516	4.857	< LDL
	Total FPL Mass	**0.547**	**477.877**	**18.634**	**117.074**	**1.391**
	HV- QA	0.339	406.983	8.685	54.966	0.481
11-Sep-12	LV-D64-E1-E3	85.186	699.910	3.309	50.288	30.818
	LV-D64-E4	1.365	6.048	< LDL	0.821	0.341
	Total D64 Mass	**86.551**	**705.958**	**3.309**	**51.109**	**31.159**
	LV-DFP-QA	1.291	< LDL	0.466	0.795	0.188
	LV-DFP-XB	2.185	4.487	< LDL	0.938	0.228
	LV-DFP-XC	0.553	< LDL	0.108	0.253	0.017
	Total DFP Mass	**4.030**	**4.487**	**0.573**	**1.987**	**0.433**
	LV-FPL-QA	1.249	18.032	1.382	5.202	1.288
	LV-FPL-XB	1.447	169.639	4.096	19.369	6.613
	LV-FPL-XC	1.054	5.050	0.153	1.900	1.162
	Total FPL Mass	**3.750**	**192.721**	**5.631**	**26.470**	**9.063**
	HV-XA	226.911	7634.857	413.264	1454.302	672.281

Sampling Date	Sample[a]	Mass (ng)				
		4-me-2-NP	4-NP	3-me-4-NP	2-me-4-NP	2,6-dime-4-NP
13-Sep-12	LV-D98-E1-E3	121.334	593.913	13.810	108.482	56.948
	LV-D98-E4	0.311	< LDL	< LDL	0.530	< LDL
	Total D98 Mass	**121.644**	**593.913**	**13.810**	**109.012**	**56.948**
	LV-DFP-QA	0.081	13.686	0.240	0.401	0.140
	LV-DFP-XB	0.188	13.733	< LDL	0.951	0.156
	LV-DFP-XC	< LDL	4.970	< LDL	0.530	0.044
	Total DFP Mass	**0.269**	**32.389**	**0.240**	**1.881**	**0.340**
	LV-FPL-QA	1.236	5.698	1.158	3.026	0.846
	LV-FPL-XB	0.797	279.312	12.497	42.369	25.605
	LV-FPL-XC	< LDL	6.347	1.187	3.614	4.876
	Total FPL Mass	**2.033**	**291.356**	**14.843**	**49.009**	**31.328**
	HV-XA	122.040	8435.405	480.024	1451.462	585.792
27-Sep-12	LV-D98-E1-E3	3.381	325.045	4.420	18.181	18.533
	LV-D98-E4	1.713	< LDL	0.484	< LDL	< LDL
	Total D98 Mass	**5.094**	**325.045**	**4.904**	**18.181**	**18.533**
	LV-DFP-QA	< LDL	4.738	< LDL	3.697	< LDL
	LV-DFP-XB	0.016	12.818	0.123	0.400	0.110
	LV-DFP-XC	< LDL	2.915	< LDL	0.044	0.097
	Total DFP Mass	**0.016**	**20.472**	**0.123**	**4.141**	**0.207**
	LV-FPL-QA	2.356	4.726	2.373	3.912	1.214
	LV-FPL-XB	1.607	59.459	2.895	9.089	5.862
	LV-FPL-XC	0.445	0.697	0.602	2.288	2.405
	Total FPL Mass	**4.407**	**64.882**	**5.870**	**15.289**	**9.481**
	HV-XA	631.913	6131.352	493.121	1108.705	845.816

Sampling Date	Sample[a]	Mass (ng)				
		4-me-2-NP	4-NP	3-me-4-NP	2-me-4-NP	2,6-dime-4-NP
11-Oct-12	LV-D98-E1-E3	1.371	330.374	4.348	5.000	4.747
	LV-D98-E4	1.071	7.083	< LDL	2.029	< LDL
	Total D98 Mass	**2.443**	**337.457**	**4.348**	**7.029**	**4.747**
	LV-DFP-QA	0.164	< LDL	0.991	0.800	0.827
	LV-DFP-XB	0.316	8.636	0.044	0.462	0.224
	LV-DFP-XC	0.650	2.308	< LDL	0.221	0.034
	Total DFP Mass	**1.129**	**10.945**	**1.035**	**1.483**	**1.085**
	LV-FPL-QA	1.243	6.807	3.065	5.779	0.941
	LV-FPL-XB	6.872	29.431	2.019	5.984	3.422
	LV-FPL-XC	1.738	< LDL	0.621	1.137	0.920
	Total FPL Mass	**9.853**	**36.238**	**5.704**	**12.900**	**5.284**
	HV-XA	2480.022	2498.294	176.077	544.841	219.265
	HV-QB	< LDL	724.240	69.766	142.855	< LDL
25-Oct-12	LV-D64-E1-E3	27.507	476.859	26.939	140.833	68.573
	LV-D64-E4	0.468	< LDL	0.391	0.485	0.510
	Total D64 Mass	**27.975**	**476.859**	**27.330**	**141.318**	**69.083**
	LV-DFP-QA	1.743	< LDL	0.762	1.652	0.973
	LV-DFP-XB	1.992	4.544	0.743	1.675	0.305
	LV-DFP-XC	< LDL	< LDL	0.056	0.369	0.135
	Total DFP Mass	**3.734**	**4.544**	**1.561**	**3.696**	**1.413**
	LV-FPL-QA	0.774	14.293	2.160	4.528	1.352
	LV-FPL-XB	28.173	309.109	14.446	75.565	41.739
	LV-FPL-XC	11.765	16.890	1.779	10.788	1.051
	Total FPL Mass	**40.713**	**340.293**	**18.384**	**90.880**	**44.142**
	HV-XA	845.935	8593.678	489.613	1478.687	596.277
	HV-QB	126.123	410.552	39.731	218.519	26.487

Sampling Date	Sample[a]	Mass (ng)				
		4-me-2-NP	4-NP	3-me-4-NP	2-me-4-NP	2,6-dime-4-NP
06-Nov-12	LV-D64-E1-E3	7.980	123.952	7.529	15.417	7.182
	LV-D64-E4	< LDL	< LDL	< LDL	< LDL	< LDL
	Total D64 Mass	**7.980**	**123.952**	**7.529**	**15.417**	**7.182**
	LV-DFP-QA	0.863	< LDL	1.014	2.455	0.500
	LV-DFP-XB	2.259	31.569	0.541	0.812	0.113
	LV-DFP-XC	0.609	46.067	0.280	0.166	0.048
	Total DFP Mass	**3.731**	**77.636**	**1.834**	**3.433**	**0.661**
	LV-FPL-QA	1.018	39.000	6.739	11.662	1.687
	LV-FPL-XB	12.291	93.369	4.480	10.289	3.182
	LV-FPL-XC	1.530	32.282	0.556	0.950	0.112
	Total FPL Mass	**14.839**	**164.651**	**11.774**	**22.901**	**4.981**
	HV-XA	328.203	2050.860	240.029	502.918	243.295
	HV-QB	< LDL	811.526	156.754	202.473	17.961
21-Nov-12	LV-D64-E1-E3	23.764	195.198	14.298	40.063	42.146
	LV-D64-E4	< LDL	< LDL	< LDL	< LDL	< LDL
	Total D64 Mass	**23.764**	**195.198**	**14.298**	**40.063**	**42.146**
	LV-DFP-QA	1.874	13.831	2.452	4.397	0.811
	LV-DFP-XB	0.033	44.681	0.514	1.993	0.057
	LV-DFP-XC	< LDL	39.323	< LDL	0.509	< LDL
	Total DFP Mass	**1.908**	**97.834**	**2.966**	**6.899**	**0.869**
	LV-FPL-QA	1.593	88.672	1.157	8.253	2.778
	LV-FPL-XB	21.963	225.954	9.804	36.896	46.567
	LV-FPL-XC	1.543	38.946	6.238	22.009	0.369
	Total FPL Mass	**25.099**	**353.571**	**17.199**	**67.158**	**49.714**
	HV-XA	< LDL	6235.854	502.918	1748.782	1538.145
	HV-QB	< LDL	1399.352	< LDL	251.459	24.493

Sampling Date	Sample[a]	Mass (ng)				
		4-me-2-NP	4-NP	3-me-4-NP	2-me-4-NP	2,6-dime-4-NP
27-Nov-12	LV-D64-E1-E3	9.146	333.049	8.223	15.733	6.373
	LV-D64-E4	0.113	2.148	0.908	0.542	0.330
	Total D64 Mass	**9.259**	**335.197**	**9.131**	**16.274**	**6.703**
	LV-DFP-QA	1.124	7.579	1.045	1.119	0.290
	LV-DFP-XB	< LDL	15.073	0.318	0.429	0.122
	LV-DFP-XC	< LDL	1.893	0.004	0.236	0.097
	Total DFP Mass	**1.124**	**24.545**	**1.367**	**1.783**	**0.509**
	LV-FPL-QA	0.039	12.023	2.023	3.263	0.293
	LV-FPL-XB	3.946	60.771	1.943	9.043	3.362
	LV-FPL-XC	0.713	33.507	0.354	2.150	0.173
	Total FPL Mass	**4.698**	**106.301**	**4.321**	**14.456**	**3.828**
	HV-XA	248.713	3744.707	301.258	458.893	173.399
	HV-QB	< LDL	1849.584	296.004	294.252	36.782
05-Dec-12	LV-D64-E1-E3	5.546	46.867	5.584	7.708	2.021
	LV-D64-E4	0.120	0.411	< LDL	0.155	< LDL
	Total D64 Mass	**5.665**	**47.277**	**5.584**	**7.863**	**2.021**
	LV-DFP-QA	2.454	4.474	3.217	3.674	0.462
	LV-DFP-XB	0.230	1.434	0.195	0.083	0.174
	LV-DFP-XC	< LDL	< LDL	0.140	< LDL	0.033
	Total DFP Mass	**2.683**	**5.908**	**3.552**	**3.757**	**0.669**
	LV-FPL-QA	0.175	0.922	0.195	0.119	0.174
	LV-FPL-XB	2.674	53.453	6.043	11.036	4.101
	LV-FPL-XC	< LDL	< LDL	< LDL	< LDL	< LDL
	Total FPL Mass	**2.849**	**54.375**	**6.238**	**11.155**	**4.275**
	HV-XA	488.569	2050.272	606.946	688.306	101.099
	HV-QB	< LDL	1276.522	243.791	346.382	52.070

Sampling Date	Sample[a]	Mass (ng)				
		4-me-2-NP	4-NP	3-me-4-NP	2-me-4-NP	2,6-dime-4-NP
13-Dec-12	LV-D98-E1-E3	< LDL	176.816	8.673	21.618	6.193
	LV-D98-E4	< LDL	< LDL	0.354	< LDL	0.059
	Total D98 Mass	**< LDL**	**176.816**	**9.027**	**21.618**	**6.252**
	LV-DFP-QA	2.036	2.159	1.294	1.741	0.588
	LV-DFP-XB	0.040	0.897	0.228	0.234	0.042
	LV-DFP-XC	< LDL	< LDL	< LDL	< LDL	< LDL
	Total DFP Mass	**2.076**	**3.056**	**1.522**	**1.975**	**0.631**
	LV-FPL-QA	1.496	42.933	9.250	10.184	1.645
	LV-FPL-QB	0.020	11.600	0.313	1.828	0.652
	LV-FPL-QC	< LDL	< LDL	0.059	0.215	0.066
	Total FPL Mass	**1.515**	**54.533**	**9.622**	**12.227**	**2.363**
	HV-XA	2814.762	4200.865	510.670	943.827	439.237
	HV-QB	< LDL	1387.623	224.938	246.216	28.877
23-Jan-13	LV-D64-E1-E3	1.578	45.580	6.958	10.566	5.535
	LV-D64-E4	< LDL	< LDL	0.768	1.810	< LDL
	Total D64 Mass	**1.578**	**45.580**	**7.726**	**12.376**	**5.535**
	LV-DFP-QA	0.064	17.746	0.091	17.558	1.207
	LV-DFP-XB	0.121	38.109	0.397	0.410	0.078
	LV-DFP-XC	< LDL	< LDL	< LDL	< LDL	< LDL
	Total DFP Mass	**0.185**	**55.855**	**0.488**	**17.968**	**1.284**
	LV-FPL-QA	7.825	98.949	3.688	32.944	5.231
	LV-FPL-XB	3.051	32.674	8.378	29.468	8.389
	LV-FPL-XC	< LDL	< LDL	< LDL	< LDL	< LDL
	Total FPL Mass	**10.877**	**131.623**	**12.066**	**62.412**	**13.621**
	HV-XB	4777.480	12899.993	2485.820	2709.064	2125.786

Sampling Date	Sample[a]	Mass (ng)				
		4-me-2-NP	4-NP	3-me-4-NP	2-me-4-NP	2,6-dime-4-NP
13-Feb-13	LV-D64-E1-E3	< LDL	106.859	8.813	16.054	7.644
	LV-D64-E4	< LDL	2.516	< LDL	< LDL	0.052
	Total D64 Mass	**< LDL**	**109.374**	**8.813**	**16.054**	**7.695**
	LV-DFP-QA	0.643	7.256	3.664	4.143	3.686
	LV-DFP-XB	< LDL	15.316	0.472	1.286	0.859
	LV-DFP-XC	< LDL	< LDL	0.197	0.152	< LDL
	Total DFP Mass	**0.643**	**22.572**	**4.333**	**5.582**	**4.545**
	LV-FPL-QA	1.818	59.212	9.336	13.665	4.832
	LV-FPL-XB	3.730	47.319	4.065	10.008	7.217
	LV-FPL-XC	< LDL	13.621	2.072	5.882	1.103
	Total FPL Mass	**5.548**	**120.152**	**15.472**	**29.555**	**13.152**
	HV-XA	2386.701	11168.197	1751.291	2482.169	771.570
	HV-QB	< LDL	3247.479	729.313	868.603	78.253
06-Mar-13	LV-D64-E1-E3	9.082	188.716	11.625	26.595	11.254
	LV-D64-E4	< LDL	< LDL	0.082	0.051	< LDL
	Total D64 Mass	**9.082**	**188.716**	**11.707**	**26.646**	**11.254**
	LV-DFP-QA	0.810	< LDL	1.043	0.996	< LDL
	LV-DFP-XB	1.392	22.236	0.427	0.479	0.419
	LV-DFP-XC	0.633	19.472	0.229	0.293	0.125
	Total DFP Mass	**2.834**	**41.708**	**1.700**	**1.769**	**0.544**
	LV-FPL-QA	0.239	48.399	8.771	12.685	1.191
	LV-FPL-XB	8.656	161.695	2.825	17.307	12.334
	LV-FPL-XC	3.556	29.454	0.332	0.753	0.118
	Total FPL Mass	**12.451**	**239.548**	**11.928**	**30.744**	**13.643**
	HV-XA	2966.538	7633.911	492.014	1448.396	303.563

Sampling Date	Sample[a]	Mass (ng)				
		4-me-2-NP	4-NP	3-me-4-NP	2-me-4-NP	2,6-dime-4-NP
15-Apr-13	LV-D64-E1-E3	16.651	369.466	18.114	43.698	26.049
	LV-D64-E4	< LDL	3.535	0.698	0.472	0.984
	Total D64 Mass	**16.651**	**373.001**	**18.813**	**44.171**	**27.034**
	LV-DFP-QA	1.975	< LDL	2.197	0.949	2.263
	LV-DFP-XB	2.365	13.315	1.385	1.265	1.554
	LV-DFP-XC	0.914	3.790	0.949	0.800	< LDL
	Total DFP Mass	**5.254**	**17.105**	**4.532**	**3.013**	**3.817**
	LV-FPL-QA	3.332	17.980	4.399	4.980	1.425
	LV-FPL-XB	10.216	118.095	6.562	16.578	11.224
	LV-FPL-XC	2.488	6.494	2.158	3.028	0.868
	Total FPL Mass	**16.036**	**142.569**	**13.119**	**24.587**	**13.516**
	HV-XA	1437.663	12670.114	753.501	1225.094	964.536
	HV-XB	989.512	4711.167	181.934	504.950	434.606
17-Apr-13	LV-D78-E1-E3	1.695	108.005	5.458	14.492	11.026
	LV-D78-E4	< LDL	< LDL	0.226	< LDL	< LDL
	Total D78 Mass	**1.695**	**108.005**	**5.684**	**14.492**	**11.026**
	LV-DFP-QA	0.151	< LDL	1.423	0.852	< LDL
	LV-DFP-XB	0.583	< LDL	0.266	< LDL	0.506
	LV-DFP-XC	< LDL	< LDL	< LDL	< LDL	< LDL
	Total DFP Mass	**0.733**	**< LDL**	**1.689**	**0.852**	**0.506**
	LV-FPL-QA	0.619	< LDL	2.294	3.044	1.548
	LV-FPL-XB	1.409	108.131	1.982	2.104	5.167
	LV-FPL-XC	< LDL	< LDL	< LDL	< LDL	< LDL
	Total FPL Mass	**2.029**	**108.131**	**4.276**	**5.147**	**6.715**
	HV-XA	560.940	4130.332	137.816	847.358	270.983
	HV-QB	12.199	2353.535	118.338	239.991	42.160

Sampling Date	Sample[a]	Mass (ng)				
		4-me-2-NP	4-NP	3-me-4-NP	2-me-4-NP	2,6-dime-4-NP
22-Apr-13	LV-D78-E1-E3	15.940	107.900	3.724	15.561	7.700
	LV-D78-E4	< LDL	0.817	1.805	< LDL	< LDL
	Total D78 Mass	**15.940**	**108.717**	**5.529**	**15.561**	**7.700**
	LV-DFP-QA	< LDL	< LDL	0.933	1.374	0.711
	LV-DFP-XB	0.539	< LDL	0.570	0.012	0.449
	LV-DFP-XC	< LDL	< LDL	< LDL	< LDL	< LDL
	Total DFP Mass	**0.539**	**< LDL**	**1.503**	**1.387**	**1.160**
	LV-FPL-QA	1.576	< LDL	2.265	2.232	1.060
	LV-FPL-XB	9.610	114.420	3.763	16.381	8.733
	LV-FPL-XC	1.324	< LDL	0.633	0.648	1.232
	Total FPL Mass	**12.510**	**114.420**	**6.661**	**19.261**	**11.026**
23-Apr-13	LV-D99-E1-E3	20.609	206.113	6.252	15.103	11.426
	LV-D99-E4	< LDL	0.765	1.253	< LDL	< LDL
	Total D99 Mass	**20.609**	**206.878**	**7.505**	**15.103**	**11.426**
	LV-DFP-QA	< LDL	< LDL	0.690	1.019	0.588
	LV-DFP-XB	< LDL	< LDL	0.126	0.240	0.419
	LV-DFP-XC	< LDL	< LDL	< LDL	< LDL	< LDL
	Total DFP Mass	**< LDL**	**< LDL**	**0.816**	**1.258**	**1.007**
	LV-FPL-QA	< LDL	< LDL	1.665	1.553	1.002
	LV-FPL-XB	3.079	186.916	5.132	14.382	8.543
	LV-FPL-XC	3.441	< LDL	0.407	1.010	0.866
	Total FPL Mass	**6.520**	**186.916**	**7.204**	**16.945**	**10.411**

Sampling Date	Sample[a]	Mass (ng)				
		4-me-2-NP	4-NP	3-me-4-NP	2-me-4-NP	2,6-dime-4-NP
30-Apr-13 - DAY	LV-D78-E1-E3	24.553	184.497	2.275	15.362	22.597
	LV-D78-E4	0.597	4.383	< LDL	0.604	0.940
	Total D78 Mass	**25.150**	**188.880**	**2.275**	**15.966**	**23.537**
	Total DFP Mass	**1.287**	**15.339**	**0.965**	**0.612**	**0.724**
	LV-FPL-QA	0.595	< LDL	1.590	1.416	1.092
	LV-FPL-XB	2.748	107.146	3.180	8.516	8.901
	LV-FPL-XC	< LDL	< LDL	< LDL	< LDL	< LDL
	Total FPL Mass	**3.344**	**107.146**	**4.770**	**9.932**	**9.993**
30-Apr-13 - NIGHT	LV-D99-E1-E3	26.943	66.290	3.819	13.410	13.014
	LV-D99-E4	< LDL	11.771	0.324	0.583	0.770
	Total D99 Mass	**26.943**	**78.061**	**4.142**	**13.993**	**13.784**
	Total DFP Mass	**3.528**	**< LDL**	**1.229**	**0.902**	**1.221**
	LV-FPL-QA	0.902	< LDL	3.100	1.743	2.003
	LV-FPL-XB	9.292	19.478	2.961	12.188	12.858
	LV-FPL-XC	< LDL	< LDL	< LDL	< LDL	< LDL
	Total FPL Mass	**10.194**	**19.478**	**6.061**	**13.931**	**14.861**
30-Apr-13	**Overall Denuder**	**52.093**	**266.941**	**6.417**	**29.960**	**37.321**
	Overall DFP	**4.816**	**15.339**	**2.194**	**1.514**	**1.944**
	Overall FPL	**13.538**	**126.624**	**10.831**	**23.863**	**24.854**

Sampling Date	Sample[a]	Mass (ng)				
		4-me-2-NP	4-NP	3-me-4-NP	2-me-4-NP	2,6-dime-4-NP
01-May-13 - DAY	LV-D78-E1-E3	30.906	326.806	6.123	46.915	42.027
	LV-D78-E4	< LDL	< LDL	< LDL	< LDL	< LDL
	Total D78 Mass	**30.906**	**326.806**	**6.123**	**46.915**	**42.027**
	Total DFP Mass	**5.575**	**2.255**	**0.967**	**7.002**	**14.197**
	LV-FPL-QA	5.338	< LDL	5.534	5.933	7.320
	LV-FPL-XB	7.619	39.298	5.520	8.763	14.904
	LV-FPL-XC	< LDL	< LDL	< LDL	< LDL	< LDL
	Total FPL Mass	**12.956**	**39.298**	**11.054**	**14.696**	**22.224**
01-May-13 - NIGHT	LV-D99-E1-E3	19.046	208.962	3.106	18.943	12.359
	LV-D99-E4	0.745	< LDL	< LDL	< LDL	< LDL
	Total D99 Mass	**19.790**	**208.962**	**3.106**	**18.943**	**12.359**
	Total DFP Mass	**0.665**	**< LDL**	**0.186**	**1.732**	**0.999**
	LV-FPL-QA	1.674	< LDL	1.713	2.740	0.655
	LV-FPL-XB	15.514	147.202	4.173	16.281	17.016
	LV-FPL-XC	< LDL	< LDL	< LDL	< LDL	< LDL
	Total FPL Mass	**17.188**	**147.202**	**5.886**	**19.020**	**17.672**
01-May-13	**Overall Denuder**	**50.696**	**535.768**	**9.229**	**65.857**	**54.387**
	Overall DFP	**6.240**	**2.255**	**1.153**	**8.734**	**15.196**
	Overall FPL	**30.145**	**186.500**	**16.940**	**33.716**	**39.896**

Sampling Date	Sample[a]	Mass (ng)				
		4-me-2-NP	4-NP	3-me-4-NP	2-me-4-NP	2,6-dime-4-NP
02-May-13 - DAY	LV-D78-E1-E3	24.381	322.721	5.429	62.432	51.564
	LV-D78-E4	0.824	3.188	< LDL	< LDL	< LDL
	Total D78 Mass	**25.205**	**325.909**	**5.429**	**62.432**	**51.564**
	Total DFP Mass	**1.777**	**0.081**	**1.975**	**0.926**	**0.771**
	LV-FPL-QA	0.443	< LDL	0.939	1.247	1.466
	LV-FPL-XB	15.741	107.247	5.298	13.498	14.080
	LV-FPL-XC	< LDL	< LDL	< LDL	< LDL	< LDL
	Total FPL Mass	**16.184**	**107.247**	**6.237**	**14.745**	**15.546**
02-May-13 - NIGHT	LV-D99-E1-E3	4.614	204.982	3.803	8.350	3.287
	LV-D99-E4	< LDL	< LDL	< LDL	< LDL	< LDL
	Total D99 Mass	**4.614**	**204.982**	**3.803**	**8.350**	**3.287**
	Total DFP Mass	**0.546**	**< LDL**	**0.883**	**0.816**	**0.835**
	LV-FPL-QA	0.184	< LDL	1.348	1.073	1.111
	LV-FPL-XB	5.175	249.156	4.251	6.870	3.759
	LV-FPL-XC	< LDL	< LDL	< LDL	< LDL	< LDL
	Total FPL Mass	**5.359**	**249.156**	**5.598**	**7.943**	**4.870**
02-May-13	**Overall Denuder**	**29.819**	**530.891**	**9.232**	**70.781**	**54.851**
	Overall DFP	**2.323**	**0.081**	**2.858**	**1.742**	**1.606**
	Overall FPL	**21.543**	**356.404**	**11.835**	**22.688**	**20.416**

[a] Sample Notation is XX-YYY-ZZ as follows:
XX: either low volume (LV) or high volume (HV)
YYY: either denuder number (D64, D78, D99) or denuder line (DL) or filter pack line (FPL)
ZZ: either denuder extraction number (E1-E3, E4) or filter type (Q or X) with position of filter (A,B or C)

Appendix D. Ambient Sample Concentrations

Sampling Date	Sample[a]	Concentration (ng m^{-3})				
		4-me-2-NP	4-NP	3-me-4-NP	2-me-4-NP	2,6-dime-4-NP
25-Jun-12	Gas Phase (DL)	0.165	6.857	0.346	0.611	0.172
	PM (DL)	**0.817**	**3.409**	0.043	0.664	0.070
	Total (DL)	**0.982**	**10.266**	0.389	1.275	0.242
	Total (FPL)	0.850	10.568	0.249	1.154	0.231
	PM (HV-A)	0.003	0.188	0.014	0.030	0.004
28-Jun-12	Gas Phase (DL)	1.389	**218.795**	1.351	9.418	2.790
	PM (DL)	0.185	**3.815**	0.088	0.174	0.010
	Total (DL)	1.574	**222.610**	1.439	9.592	2.799
	Total (FPL)	0.051	**44.843**	1.227	**12.060**	**2.892**
	PM (HV-A)	0.007	0.364	0.015	0.058	0.005
5-Jul-12	Gas Phase (DL)	< LDL	21.569	1.212	10.133	**4.720**
	PM (DL)	0.024	1.365	< LDL	0.238	0.035
	Total (DL)	0.024	22.933	1.212	10.370	**4.755**
	Total (FPL)	0.011	**36.186**	1.136	**9.407**	2.369
	PM - HV-A	0.003	1.073	0.026	0.082	0.007
10-Jul-12	Gas Phase (DL)	0.267	**52.284**	0.288	1.637	0.652
	PM (DL)	0.096	1.623	0.023	0.139	0.010
	Total (DL)	0.363	**53.907**	0.312	1.777	0.662
	Total (FPL)	0.147	6.108	0.114	0.783	0.196
	PM (HV-A)	0.003	0.246	0.015	0.048	0.005

Sampling Date	Sample[a]	Concentration (ng m^{-3})				
		4-me-2-NP	4-NP	3-me-4-NP	2-me-4-NP	2,6-dime-4-NP
11-Jul-12	Gas Phase (DL)	0.269	**53.584**	**0.018**	**1.012**	**0.354**
	PM (DL)	0.009	2.667	0.124	0.334	0.102
	Total (DL)	0.277	**56.251**	**0.143**	**1.346**	**0.456**
	Total (FPL)	0.119	21.019	0.648	3.333	0.935
	PM (HV-A)	0.007	0.535	0.034	0.074	0.013
12-Jul-12	Gas Phase (DL)	0.791	**47.772**	1.237	9.261	3.776
	PM (DL)	0.021	1.863	0.026	0.074	0.006
	Total (DL)	0.812	**49.635**	1.263	9.336	3.781
	Total (FPL)	< LDL	26.057	0.697	4.501	1.059
	PM (HV-A)	0.009	0.546	0.033	0.097	0.019
24-Jul-12	Gas Phase (DL)	< LDL	7.078	< LDL	0.602	0.319
	PM (DL)	0.058	0.571	0.021	0.072	0.002
	Total (DL)	0.058	7.650	0.021	0.674	0.322
	Total (FPL)	0.024	6.713	0.288	1.045	0.238
	PM (HV-A)	0.004	0.243	0.018	0.037	0.005
1-Aug-12	Gas Phase (DL)	0.341	**22.747**	0.713	2.083	0.897
	PM (DL)	**0.494**	**13.098**	**0.413**	**1.295**	0.116
	Total (DL)	**0.835**	**35.844**	**1.127**	**3.377**	1.012
	Total (FPL)	0.272	5.805	0.029	0.445	< LDL
2-Aug-12	Gas Phase (DL)	0.431	2.980	0.254	1.782	0.323
	PM (DL)	0.228	1.628	0.167	0.710	0.012
	Total (DL)	0.659	4.608	0.421	2.493	0.335
	Total (FPL)	0.078	4.789	0.040	2.336	0.223
	PM (HV-A)	0.338	15.895	0.805	2.881	0.917

Sampling Date	Sample[a]	Concentration (ng m^{-3})				
		4-me-2-NP	4-NP	3-me-4-NP	2-me-4-NP	2,6-dime-4-NP
8-Aug-12	Gas Phase (DL)	< LDL	12.203	0.295	3.645	1.427
	PM (DL)	0.038	0.551	0.048	0.122	0.046
	Total (DL)	0.038	12.754	0.343	3.767	1.473
	Total (FPL)	0.051	12.327	0.489	3.454	0.958
13-Aug-12	Gas Phase (DL)	0.129	17.113	0.555	2.575	1.180
	PM (DL)	0.071	0.243	0.011	0.085	0.087
	Total (DL)	0.199	17.356	0.566	2.659	1.266
	Total (FPL)	0.063	12.237	0.366	2.107	0.409
	PM (HV-A)	0.008	0.233	0.020	0.026	0.004
15-Aug-12	Gas Phase (DL)	0.239	18.426	0.608	6.223	0.632
	PM (DL)	0.019	0.244	0.051	0.145	0.075
	Total (DL)	0.258	18.669	0.659	6.367	0.707
	Total (FPL)	0.020	17.183	0.670	4.210	0.050
	PM (HV-A)	0.0002	0.239	0.005	0.032	0.0003
11-Sep-12	Gas Phase (DL)	3.243	26.450	0.124	1.915	1.167
	PM (DL)	0.151	0.168	0.021	0.074	0.016
	Total (DL)	3.394	26.618	0.145	1.989	1.184
	Total (FPL)	0.149	7.642	0.223	1.050	0.359
	Total (HV-A)	0.139	4.692	0.254	0.894	0.413
13-Sep-12	Gas Phase (DL)	4.629	22.599	0.525	4.148	2.167
	PM (DL)	0.010	1.232	0.009	0.072	0.013
	Total (DL)	4.639	23.832	0.535	4.220	2.180
	Total (FPL)	0.068	11.391	0.580	1.916	1.225
	Total (HV-A)	0.077	5.313	0.302	0.914	0.369

Sampling Date	Sample[a]	Concentration (ng m^{-3})				
		4-me-2-NP	4-NP	3-me-4-NP	2-me-4-NP	2,6-dime-4-NP
27-Sep-12	Gas Phase (DL)	0.195	12.429	0.188	0.695	0.709
	PM (DL)	0.001	0.783	0.005	0.158	0.008
	Total (DL)	0.195	13.211	0.192	0.854	0.717
	Total (FPL)	0.174	2.563	0.232	0.604	0.375
	Total (HV-A)	0.390	3.781	0.304	0.684	0.522
11-Oct-12	Gas Phase (DL)	0.095	13.095	0.169	0.273	0.184
	PM (DL)	0.044	0.425	0.040	0.058	0.042
	Total (DL)	0.139	13.520	0.209	0.330	0.226
	Total (FPL)	0.376	1.385	0.218	0.493	0.202
	Total (HV-A)	1.493	1.504	0.106	0.328	0.132
	PM (HV-B)	< LDL	0.436	0.042	0.086	< LDL
25-Oct-12	Gas Phase (DL)	1.057	18.011	1.032	5.338	2.609
	PM (DL)	0.141	0.172	0.059	0.140	0.053
	Total (DL)	1.198	18.183	1.091	5.477	2.663
	Total (FPL)	1.571	13.134	0.710	3.508	1.704
	Total (HV-A)	0.078	5.318	0.303	0.915	0.369
	PM (HV-B)	0.524	0.254	0.025	0.135	0.016
6-Nov-12	Gas Phase (DL)	0.328	5.099	0.310	0.634	0.295
	PM (DL)	0.153	3.194	0.075	0.141	0.027
	Total (DL)	0.482	8.293	0.385	0.775	0.323
	Total (FPL)	0.587	6.516	0.466	0.906	0.197
	Total (HV-A)	0.201	1.256	0.147	0.308	0.149
	PM (HV-B)	< LDL	0.497	0.096	0.124	0.011

Sampling Date	Sample[a]	Concentration (ng m^{-3})				
		4-me-2-NP	4-NP	3-me-4-NP	2-me-4-NP	2,6-dime-4-NP
21-Nov-12	Gas Phase (DL)	0.935	7.683	0.563	1.577	1.659
	PM (DL)	0.075	**3.851**	0.117	0.272	0.034
	Total (DL)	1.010	**11.533**	0.679	1.848	1.693
	Total (FPL)	0.998	14.059	0.684	2.670	1.977
	Total (HV-A)	< LDL	3.819	0.308	1.071	0.942
	PM (HV-B)	< LDL	0.857	< LDL	0.154	0.015
27-Nov-12	Gas Phase (DL)	0.356	12.881	0.351	0.625	0.258
	PM (DL)	0.043	0.943	0.053	0.069	0.020
	Total (DL)	0.399	13.825	0.403	0.694	0.277
	Total (FPL)	0.174	3.937	0.160	0.535	0.142
	Total (HV-A)	0.141	2.124	0.171	0.260	0.098
	PM (HV-B)	< LDL	1.049	0.168	0.167	0.021
5-Dec-12	Gas Phase (DL)	0.239	1.995	0.236	0.332	0.085
	PM (DL)	0.113	0.249	0.150	0.159	0.028
	Total (DL)	0.352	2.245	0.386	0.490	0.114
	Total (FPL)	0.114	2.186	0.251	0.448	0.172
	Total (HV-A)	0.300	1.260	0.373	0.423	0.062
	PM (HV-B)	< LDL	0.784	0.150	0.213	0.032
13-Dec-12	Gas Phase (DL)	< LDL	7.737	0.395	0.946	0.274
	PM (DL)	0.091	0.134	0.067	0.086	0.028
	Total (DL)	0.091	7.871	0.462	1.032	0.301
	Total (FPL)	0.065	2.334	0.412	0.523	0.101
	Total (HV-A)	1.852	2.764	0.336	0.621	0.289
	PM (HV-B)	< LDL	0.913	0.148	0.162	0.019

Sampling Date	Sample[a]	Concentration (ng m^{-3})				
		4-me-2-NP	4-NP	3-me-4-NP	2-me-4-NP	2,6-dime-4-NP
23-Jan-13	Gas Phase (DL)	0.065	1.889	0.320	0.513	0.229
	PM (DL)	0.008	2.314	0.020	0.744	0.053
	Total (DL)	0.073	4.203	0.340	1.257	0.283
	Total (FPL)	0.419	5.069	0.465	2.403	0.525
	Total (HV-B)	2.830	7.641	1.472	1.605	1.259
13-Feb-13	Gas Phase (DL)	< LDL	4.788	0.386	0.703	0.337
	PM (DL)	0.028	0.988	0.190	0.244	0.199
	Total (DL)	0.028	5.776	0.575	0.947	0.536
	Total (FPL)	0.232	5.030	0.648	1.237	0.551
	Total (HV-A)	1.531	7.162	1.123	1.592	0.495
	PM (HV-B)	< LDL	2.083	0.468	0.557	0.050
6-Mar-13	Gas Phase (DL)	0.342	7.112	0.441	1.004	0.424
	PM (DL)	0.107	1.572	0.064	0.067	0.021
	Total (DL)	0.449	8.684	0.505	1.071	0.445
	Total (FPL)	0.466	8.974	0.447	1.152	0.511
	Total (HV-A)	1.768	4.549	0.293	0.863	0.181
15-Apr-13	Gas Phase (DL)	0.620	13.884	0.700	1.644	1.006
	PM (DL)	0.196	0.637	0.169	0.112	0.142
	Total (DL)	0.815	14.520	0.869	1.756	1.148
	Total (FPL)	0.627	5.575	0.513	0.961	0.529
	Total (HV-A)	0.884	7.786	0.463	0.753	0.593
	Total (HV-B)	0.608	2.895	0.112	0.310	0.267

Sampling Date	Sample[a]	Concentration (ng m^{-3})				
		4-me-2-NP	4-NP	3-me-4-NP	2-me-4-NP	2,6-dime-4-NP
17-Apr-13	Gas Phase (DL)	0.062	3.934	0.207	0.528	0.402
	PM (DL)	0.027	< LDL	0.062	0.031	0.018
	Total (DL)	0.088	3.934	0.269	0.559	0.420
	Total (FPL)	0.078	4.146	0.164	0.197	0.257
	Total (HV-A)	0.333	2.453	0.082	0.503	0.161
	PM (HV-B)	0.009	1.653	0.083	0.169	0.030
22-Apr-13	Gas Phase (DL)	0.624	4.258	0.217	0.610	0.302
	PM (DL)	0.021	< LDL	0.059	0.054	0.045
	Total (DL)	0.645	4.258	0.275	0.664	0.347
	Total (FPL)	0.517	4.725	0.275	0.795	0.455
23-Apr-13	Gas Phase (DL)	0.739	7.415	0.269	0.541	0.410
	PM (DL)	< LDL	< LDL	0.029	0.045	0.036
	Total (DL)	0.739	7.415	7.535	15.148	11.462
	Total (FPL)	0.252	7.234	0.279	0.656	0.403

Sampling Date	Sample[a]	Concentration (ng m^{-3})				
		4-me-2-NP	4-NP	3-me-4-NP	2-me-4-NP	2,6-dime-4-NP
30-Apr-13	Day - Gas Phase (DL)	1.767	13.267	0.160	1.121	1.653
	Day - PM (DL)	0.090	1.077	0.068	0.043	0.051
	Day - Total (DL)	1.857	14.344	0.228	1.164	1.704
	Day - Total (FPL)	0.256	8.203	0.365	0.760	0.765
	Night - Gas Phase (DL)	1.994	5.778	0.307	1.036	1.020
	Night - PM (DL)	0.261	< LDL	0.091	0.067	0.090
	Night - Total (DL)	2.256	5.778	0.398	1.103	1.111
	Night - Total (FPL)	0.807	1.541	0.480	1.102	1.176
	Overall - Gas Phase (DL)	1.878	9.621	0.231	1.080	1.345
	Overall - PM (DL)	0.174	0.553	0.079	0.055	0.070
	Overall - Total (DL)	2.051	10.174	0.310	1.134	1.415
	Overall - Total (FPL)	0.527	4.927	0.421	0.929	0.967
1-May-13	Day - Gas Phase (DL)	2.274	24.042	0.450	3.451	3.092
	Day - PM (DL)	0.410	0.166	0.071	0.515	1.044
	Day - Total (DL)	2.684	24.208	0.522	3.966	4.136
	Day - Total (FPL)	1.010	3.063	0.862	1.145	1.732
	Night - Gas Phase (DL)	1.408	14.870	0.221	1.348	0.879
	Night - PM (DL)	0.047	< LDL	0.013	0.123	0.071
	Night - Total (DL)	1.456	14.870	0.234	1.471	0.951
	Night - Total (FPL)	1.313	11.241	0.449	1.452	1.350
	Overall - Gas Phase (DL)	1.834	19.380	0.334	2.382	1.967
	Overall - PM (DL)	0.226	0.082	0.042	0.316	**0.550**
	Overall - Total (DL)	2.059	19.461	0.375	2.698	**2.517**
	Overall - Total (FPL)	1.163	7.194	0.653	1.301	1.539

Sampling Date	Sample[a]	Concentration (ng m^{-3})				
		4-me-2-NP	4-NP	3-me-4-NP	2-me-4-NP	2,6-dime-4-NP
2-May-13	Day - Gas Phase (DL)	1.815	23.465	0.391	4.495	3.713
	Day - PM (DL)	0.128	0.006	0.142	0.067	0.056
	Day - Total (DL)	1.943	23.471	0.533	4.562	3.768
	Day - Total (FPL)	1.232	8.165	0.475	1.123	1.184
	Night - Gas Phase (DL)	0.334	14.829	0.275	0.604	0.238
	Night - PM (DL)	0.040	< LDL	0.064	0.059	0.060
	Night - Total (DL)	0.373	14.829	0.339	0.663	0.298
	Night - Total (FPL)	0.412	19.142	0.430	0.610	0.374
	Overall - Gas Phase (DL)	1.076	19.157	0.333	2.554	1.979
	Overall - PM (DL)	0.084	0.003	0.103	0.063	0.058
	Overall - Total (DL)	1.160	19.160	0.436	2.617	2.037
	Overall - Total (FPL)	0.824	13.629	0.453	0.868	0.781

Outlier data points are bolded

[a] Sample Notation is as follows:

DL: denuder line

FPL: filter pack line

Appendix E. Ambient Partitioning Data from Denuder Line and High Volume Filter Line

Sampling Date		4-me-2-NP	4-NP	3-me-4-NP	2-me-4-NP	2,6-dime-4-NP
25-Jun-12	LV-Gas Phase (%)	**16.791**	**66.797**	89.025	47.903	71.152
	LV-Partitioning Coefficient (m^3 μg^{-1})	**2.848**	**0.286**	0.071	0.625	0.233
28-Jun-12	LV-Gas Phase (%)	88.237	**98.286**	93.866	98.186	99.653
	LV-Partitioning Coefficient (m^3 μg^{-1})	0.012	**0.010**	0.038	0.011	0.002
5-Jul-12	LV-Gas Phase (%)	N/A	94.049	100.000	97.708	**99.255**
	LV-Partitioning Coefficient (m^3 μg^{-1})	N/A	0.005	N/A	0.002	**0.001**
10-Jul-12	LV-Gas Phase (%)	73.598	**96.989**	92.507	92.156	98.557
	LV-Partitioning Coefficient (m^3 μg^{-1})	0.055	**0.005**	0.012	0.013	0.002
11-Jul-12	LV-Gas Phase (%)	96.793	**95.258**	**12.816**	**75.192**	**77.643**
	LV-Partitioning Coefficient (m^3 μg^{-1})	0.0029	**0.008**	**1.034**	**0.050**	**0.044**
12-Jul-12	LV-Gas Phase (%)	97.456	**96.247**	97.914	99.203	99.847
	LV-Partitioning Coefficient (m^3 μg^{-1})	0.002	**0.003**	0.001	0.001	0.0001
24-Jul-12	LV-Gas Phase (%)	N/A	92.530	N/A	89.380	99.333
	LV-Partitioning Coefficient (m^3 μg^{-1})	N/A	0.016	N/A	0.024	0.0014
1-Aug-12	LV-Gas Phase (%)	40.834	63.460	63.323	61.670	88.559
	LV-Partitioning Coefficient (m^3 μg^{-1})	0.168	0.067	0.067	0.072	0.015
2-Aug-12	LV-Gas Phase (%)	65.441	64.669	60.306	71.503	96.374
	LV-Partitioning Coefficient (m^3 μg^{-1})	0.029	0.030	0.036	0.022	0.002
8-Aug-12	LV-Gas Phase (%)	N/A	95.678	86.049	96.765	96.882
	LV-Partitioning Coefficient (m^3 μg^{-1})	N/A	0.004	0.016	0.003	0.003
13-Aug-12	LV-Gas Phase (%)	64.514	98.602	98.022	96.816	93.166
	LV-Partitioning Coefficient (m^3 μg^{-1})	0.062	0.002	0.002	0.004	0.008
15-Aug-12	LV-Gas Phase (%)	92.661	98.694	92.238	97.725	89.344
	LV-Partitioning Coefficient (m^3 μg^{-1})	0.006	0.001	0.007	0.002	0.010

Sampling Date		4-me-2-NP	4-NP	3-me-4-NP	2-me-4-NP	2,6-dime-4-NP
11-Sep-12	LV-Gas Phase (%)	95.551	99.368	85.228	96.259	98.630
	LV-Partitioning Coefficient (m^3 μg^{-1})	0.004	0.001	0.015	0.003	0.001
13-Sep-12	LV-Gas Phase (%)	99.779	94.828	98.293	98.303	99.407
	LV-Partitioning Coefficient (m^3 μg^{-1})	0.0002	0.004	0.001	0.001	0.0004
27-Sep-12	LV-Gas Phase (%)	99.684	94.075	97.554	81.451	98.898
	LV-Partitioning Coefficient (m^3 μg^{-1})	0.001	0.020	0.008	0.074	0.004
11-Oct-12	LV-Gas Phase (%)	68.384	96.859	80.774	82.577	81.398
	LV-Partitioning Coefficient (m^3 μg^{-1})	0.150	0.011	0.077	0.069	0.074
	HV-Gas Phase (%)	100.000	77.526	71.622	79.227	100.000
	HV-Partitioning Coefficient (m^3 μg^{-1})	N/A	0.094	0.129	0.085	N/A
25-Oct-12	LV-Gas Phase (%)	88.223	99.056	94.596	97.451	97.996
	LV-Partitioning Coefficient (m^3 μg^{-1})	0.008	0.001	0.004	0.002	0.001
	HV-Gas Phase (%)	12.975	95.440	92.494	87.125	95.747
	HV-Partitioning Coefficient (m^3 μg^{-1})	0.420	0.003	0.005	0.009	0.003
6-Nov-12	LV-Gas Phase (%)	68.142	61.488	80.410	81.789	91.571
	LV-Partitioning Coefficient (m^3 μg^{-1})	0.113	0.152	0.059	0.054	0.022
	HV-Gas Phase (%)	100.000	71.649	60.494	71.296	93.125
	HV-Partitioning Coefficient (m^3 μg^{-1})	N/A	0.096	0.159	0.098	0.018
21-Nov-12	LV-Gas Phase (%)	92.569	**66.613**	82.821	85.310	97.980
	LV-Partitioning Coefficient (m^3 μg^{-1})	0.004	**0.027**	0.011	0.009	0.001
	HV-Gas Phase (%)	N/A	81.672	100.000	87.429	98.433
	HV-Partitioning Coefficient (m^3 μg^{-1})	N/A	0.012	N/A	0.008	0.001

Sampling Date		4-me-2-NP	4-NP	3-me-4-NP	2-me-4-NP	2,6-dime-4-NP
27-Nov-12	LV-Gas Phase (%)	89.176	93.177	86.981	90.124	92.939
	LV-Partitioning Coefficient (m^3 μg^{-1})	0.031	0.018	0.038	0.028	0.019
	HV-Gas Phase (%)	100.000	66.938	50.440	60.930	82.500
	HV-Partitioning Coefficient (m^3 μg^{-1})	N/A	0.125	0.248	0.162	0.054
5-Dec-12	LV-Gas Phase (%)	67.859	88.892	61.121	67.664	75.125
	LV-Partitioning Coefficient (m^3 μg^{-1})	0.132	0.035	0.177	0.133	0.092
	HV-Gas Phase (%)	100.000	66.629	71.344	66.523	66.005
	HV-Partitioning Coefficient (m^3 μg^{-1})	N/A	0.446	0.692	0.552	0.143
13-Dec-12	LV-Gas Phase (%)	N/A	98.301	85.573	91.628	90.835
	LV-Partitioning Coefficient (m^3 μg^{-1})	N/A	0.003	0.025	0.013	0.015
	HV-Gas Phase (%)	100.000	75.170	69.421	79.310	93.831
	HV-Partitioning Coefficient (m^3 μg^{-1})	N/A	0.048	0.064	0.038	0.010
23-Jan-13	LV-Gas Phase (%)	89.525	44.935	94.063	40.786	81.166
	LV-Partitioning Coefficient (m^3 μg^{-1})	0.013	0.132	0.007	0.157	0.025
13-Feb-13	LV-Gas Phase (%)	N/A	82.893	67.041	74.202	62.869
	LV-Partitioning Coefficient (m^3 μg^{-1})	N/A	0.012	0.029	0.021	0.035
	HV-Gas Phase (%)	100.000	77.473	70.599	74.078	90.792
	HV-Partitioning Coefficient (m^3 μg^{-1})	N/A	0.017	0.025	0.021	0.006
6-Mar-13	LV-Gas Phase (%)	76.213	81.899	87.322	93.775	95.386
	LV-Partitioning Coefficient (m^3 μg^{-1})	0.047	0.033	0.022	0.010	0.007
15-Apr-13	LV-Gas Phase (%)	76.016	95.615	80.588	93.614	87.627
	LV-Partitioning Coefficient (m^3 μg^{-1})	0.033	0.005	0.025	0.007	0.015
17-Apr-13	LV-Gas Phase (%)	69.799	100.000	77.096	94.449	95.610
	LV-Partitioning Coefficient (m^3 μg^{-1})	0.105	N/A	0.072	0.014	0.011
	HV-Gas Phase (%)	97.493	59.743	49.618	74.911	84.461
	HV-Partitioning Coefficient (m^3 μg^{-1})	0.006	0.164	0.246	0.081	0.045

Sampling Date		4-me-2-NP	4-NP	3-me-4-NP	2-me-4-NP	2,6-dime-4-NP
22-Apr-13	LV-Gas Phase (%)	96.726	100.000	78.627	91.819	86.905
	LV-Partitioning Coefficient (m^3 μg^{-1})	0.004	N/A	0.033	0.011	0.018
23-Apr-13	LV-Gas Phase (%)	100.000	100.000	3.570	3.574	3.573
	LV-Partitioning Coefficient (m^3 μg^{-1})	N/A	N/A	0.011	0.009	0.009
30-Apr-13	Day-LV-Gas Phase (%)	95.131	92.489	70.205	96.309	97.017
	Day-LV-Partitioning Coefficient (m^3 μg^{-1})	0.005	0.008	0.040	0.004	0.003
	Night-LV-Gas Phase (%)	88.420	100.000	77.125	93.942	91.863
	Night-LV-Partitioning Coefficient (m^3 μg^{-1})	0.025	N/A	0.056	0.012	0.017
	Overall-LV-Gas Phase (%)	91.538	94.566	74.521	95.189	95.048
	Overall-LV-Partitioning Coefficient (m^3 μg^{-1})	0.012	0.007	0.043	0.006	0.007
1-May-13	Day-LV-Gas Phase (%)	84.719	99.315	86.366	87.014	74.750
	Day-LV-Partitioning Coefficient (m^3 μg^{-1})	0.025	0.001	0.022	0.021	0.047
	Night-LV-Gas Phase (%)	96.747	100.000	94.350	91.624	92.523
	Night-LV-Partitioning Coefficient (m^3 μg^{-1})	0.004	N/A	0.007	0.011	0.010
	Overall-LV-Gas Phase (%)	89.040	99.581	88.898	88.291	**78.162**
	Overall-LV-Partitioning Coefficient (m^3 μg^{-1})	0.016	0.001	0.016	0.017	**0.037**
2-May-13	Day-LV-Gas Phase (%)	93.415	99.975	73.324	98.538	98.527
	Day-LV-Partitioning Coefficient (m^3 μg^{-1})	0.006	0.00002	0.030	0.001	0.001
	Night-LV-Gas Phase (%)	89.412	100.000	81.157	91.100	79.742
	Night-LV-Partitioning Coefficient (m^3 μg^{-1})	0.015	N/A	0.030	0.013	0.033
	Overall-LV-Gas Phase (%)	92.773	99.985	76.360	97.598	97.155
	Overall-LV-Partitioning Coefficient (m^3 μg^{-1})	0.008	0.00002	0.031	0.002	0.003

Outlier data points are bolded

LV: low volume

HV: high volume